Adaptive Control Solutions for Advanced Unmanned Underwater Vehicle Applications

By
Charita Darshana Makavita, B.Sc. Eng. (Hons), M.Sc.
National Centre for Maritime Engineering and Hydrodynamics
Australian Maritime College

Submitted in fulfilment of the requirements for the degree of Doctor of Philosophy
University of Tasmania

May 2018

[Page intentionally left blank]

Declarations

Declaration of Originality and Authority of Access

This thesis contains no material which has been accepted for a degree or diploma by the University or any other institution, except by way of background information and duly acknowledged in the thesis, and to the best of my knowledge and belief no material previously published or written by another person except where due acknowledgement is made in the text of the thesis, nor does the thesis contain any material that infringes copyright.

This thesis may be made available for loan and limited copying and communication in accordance with the Copyright Act 1968.

Charita Darshana Makavita (30/08/2017)

Statement of Published Work Contained in Thesis

The publishers of the papers comprising Chapters 2, 3, 5-part A and Appendix I hold the copyright for that content, and access to the material should be sought from the respective journals and conference proceedings. The remaining non published content of the thesis may be made available for loan and limited copying and communication in accordance with the Copyright Act 1968.

Statement of Co-Authorship

The following people and institutions contributed to the publication of work undertaken as part of this thesis:

Mr. Charita Darshana Makavita, University of Tasmania (Candidate)

Dr. Hung Nguyen, University of Tasmania (Author 1)

Dr. Shantha Jayasinghe, University of Tasmania (Author 2)

Prof. Dev Ranmuthugala, University of Tasmania (Author 3)

Publication list and proportion of work details:

Chapter 2-part A (Paper 1) **"Composite Model Reference Adaptive Control for an Unmanned Underwater Vehicle"** Candidate was the primary author while Author1, Author 2 and Author 3 assisted with refinement and presentation. [Candidate: 80%, Author 1: 10%, Author 2: 5%, Author 3: 5%]
Chapter 2-part B (Paper 2) **"Predictor-Based Model Reference Adaptive Control of an Unmanned Underwater Vehicle"** Candidate was the primary author while Author1, Author 2 and Author 3 assisted with refinement and presentation. [Candidate: 80%, Author 1: 10%, Author 2: 5%, Author 3: 5%]
Chapter 3-part A (Paper 3)

"Command Governor Adaptive Control for an Unmanned Underwater Vehicle" Candidate was the primary author while Author1, Author 2 and Author 3 assisted with refinement and presentation. [Candidate: 80%, Author 1: 5%, Author 2: 5%, Author 3: 10%]
Chapter 3-part B (Paper 4) **"Command Governor Adaptive Control for Unmanned Underwater Vehicles with Measurement Noise and Actuator Dead-Zone"** Candidate was the primary author while Author1, Author 2 and Author 3 assisted with refinement and presentation. [Candidate: 80%, Author 1: 10%, Author 2: 5%, Author 3: 5%]
Chapter 4 (Paper 5) **"Experimental Comparison of Two Composite MRAC methods for UUV Operations under Low Adaptation Gains"** Candidate was the primary author while Author1, Author 2 and Author 3 assisted with refinement and presentation. Author 2 assisted on experimental validations. [Candidate: 80%, Author 1: 5%, Author 2: 10%, Author 3: 5%]
Chapter 5-part A (Paper 6) **"Experimental Study of Command Governor Adaptive Control for Unmanned Underwater Vehicles"** Candidate was the primary author while Author1, Author 2 and Author 3 assisted with refinement and presentation. Author 2 assisted on experimental validations. [Candidate: 80%, Author 1: 5%, Author 2: 10%, Author 3: 5%]
Chapter 5-part B (Paper 7) **"Experimental Study of a Command Governor Adaptive Depth Controller for an Unmanned Underwater Vehicle"** Candidate was the primary author and while Author1, Author 2 and Author 3 assisted with refinement and presentation. Author 2 assisted on experimental validations. [Candidate: 80%, Author 1: 5%, Author 2: 10%, Author 3: 5%]
Chapter 6 (Paper 8) **"Extended Command Governor Adaptive Control for Unmanned Underwater Vehicles"** Candidate was the primary author and while Author1, Author 2 and Author 3 assisted

with refinement and presentation. [Candidate: 80%, Author 1: 5%, Author 2: 5%, Author 3: 10%]
Appendix I (Paper 9) **"Fuzzy Gain Scheduling Based Optimally Tuned PID Controllers for an Unmanned Underwater Vehicle"** Candidate was the primary author and with Author 1 and Author 3 assisted with refinement and presentation. [Candidate: 80%, Author 1: 10%, Author 3: 10%]

We the undersigned agree with the above stated "proportion of work undertaken" for each of the above published (or submitted) peer-reviewed manuscripts contributing to this thesis

Signed:

----------	----------	----------
Dr. Hung Nguyen Primary Supervisor National Centre for Maritime Engineering and Hydrodynamics University of Tasmania	Dr. Shantha Jayasinghe Co-Supervisor National Centre for Ports and Shipping University of Tasmania	Prof. Dev Ranmuthugala Co-Supervisor National Centre for Maritime Engineering and Hydrodynamics University of Tasmania
Date: 30/08/2017	Date: 30/08/2017	Date:30/08/2017

Acknowledgements

The author sincerely acknowledges the following people without whom this work will not have been accomplished.

First and foremost I would like to express my deepest gratitude to my supervisory team of Dr. Hung Nguyen, Prof. Dev Ranmuthugala and Dr. Shantha Jayasinghe. They inducted me to the research culture and greatly supported me by providing facilities, funding and even hands on support to carry out experiments. Furthermore, they encouraged me through the invariable ups and downs of this long journey, emphasised the importance of academic publications, and provided valuable feedback on my writing that was instrumental in bringing greater clarity to the research articles and this thesis.

I would like to thank the graduate research coordinators, Dr. Jonathan Duffy, Dr. Walid Amin and Dr. Rouzbeh Abbassi, for arranging the confirmation of candidature and yearly reviews and for giving pertinent advice over the years; Confirmation of Candidature (COC) panel members, Assoc. Prof. Paul Brandner and Dr. Shinsuke Matsubara, for providing valuable feedback on the COC report and presentation; Dr. Khoa Duy Le for building the initial version of the AMC UUV used in experiments and providing essential guidance on how to use it for testing; Alpha Isaako for supporting me throughout the experiments carried out at the survival pool allowing me to use the pool on every possible free slot in a busy schedule and, Michael Underhill and Jock Ferguson, for providing technical support to make hardware changes to the UUV.

Furthermore I would like to thank Prof. N. Rajkumar of Colombo International Nautical and Engineering College (CINEC), for his initial effort to make this candidature a reality and continuous support over the course of the candidature; My cousins, Daninda and Tharinda Weerasinghe, for their support in starting this journey and all my friends and colleagues at both AMC/UTAS and CINEC who supported me in numerous ways.

Finally, I bow in respect to my parents, the sacrifices they have made not only throughout my life but specifically throughout these four years for my benefit is immense. Without their love and encouragement this thesis may not have happened. To them I dedicate this thesis.

[Page intentionally left blank]

Abstract

Unmanned Underwater Vehicles (UUVs) have evolved from rudimentary Remotely Operated Vehicles (ROVs) with operator control of the actuator outputs directly to sophisticated ROVs and Autonomous Underwater Vehicles (AUVs) with semi and fully autonomous control systems that require minimal to zero operator input. In addition, the rapid progress in technology has made UUVs to evolve from the mammoth work-class ROVs to mini and micro ROVs and AUVs. With these changes in UUVs there has been a parallel evolution of UUV applications culminating in advanced applications such as operating in cluttered environments in tandem with human divers and being launched and recovered by underwater docking platforms or naval submarines. Thus future UUV autonomous control systems must precisely manoeuvre UUVs that are more susceptible to parameter changes and disturbances while operating under conditions which require large parameter variations.

Adaptive control has been identified as a key enabling technology for all of the above applications. Although proven to be superior to fixed-gain controllers, adoption of adaptive control for UUV applications has been lacklustre in the past due to the lack of demanding applications that justify the added complexity and some inherent limitations. However, it has come to a point that it is no longer feasible to ignore the benefits of adaptive control for future high performance, safety critical UUV applications.

Therefore, this thesis is an effort to design and evaluate adaptive control systems for such future applications. It was identified that to ensure precise manoeuvres throughout the entire operation, the main focus should be on improving transient tracking without control signal oscillation or instability. Also, the controllers are required to show sufficient robustness against measurement noise and time-delay. To this end, three modifications to the standard Model Reference Adaptive Control (MRAC) architecture that improves transient performance without using high learning rates were developed for an existing small ROV/AUV. Composite MRAC (CMRAC) and Predictor MRAC (PMRAC) both use a prediction error in addition to the tracking error to improve transient performance. Command Governor Adaptive Control (CGAC) uses command signal modification to achieve the same end. The performance improvements of these architectures were all initially verified using simulations and then validated using

experiments. Simulations and experiments were carried out to investigate transient operations, actuator failures and external disturbances. The acquired data were subjected to a comprehensive analysis in both time domain and frequency domain to provide a compelling quantitative evaluation of the different methods.

The results indicated that significant improvements in transient tracking, fault tolerance and disturbance rejection can be obtained with the proposed solutions, compared to standard MRAC with minimal additional complexity. The transient tracking performance improvement was achieved while reducing the high frequencies in the control signal and with less control effort or less energy usage. It has also been shown that, under partial actuator failures, regulation and tracking task can still be carried out with negligible variations. In addition several forms of disturbances such as large impacts, wave disturbances and tether snags are simulated and tested and significant improvements were observed in reducing maximum deviation, settling time and oscillations at the output. Furthermore, it is shown that some proposed solutions are able to overcome the actuator dead-zone without using an additional dead-zone inverse. Also, introduced in this thesis is a novel adaptive control methodology named Extended CGAC (ECGAC) which increases the robustness to noise and time-delay while retaining the enhanced performance. In summary, the feasibility of designing adaptive controllers with transient performances equivalent to steady state performances while ensuring much better control signal is verified in this thesis.

[Page intentionally left blank]

Table of Contents

List of Figures

List of Tables

Nomenclature

$\boldsymbol{A} \in \mathbb{R}^{p \times p}$	System matrix
$\boldsymbol{A}_m \in \mathbb{R}^{p \times p}$	Reference system matrix
$\boldsymbol{A}_{prd} \in \mathbb{R}^{p \times p}$	State predictor system matrix
$\boldsymbol{B} \in \mathbb{R}^{p \times q}$	Control input matrix
$\boldsymbol{B}_m \in \mathbb{R}^{p \times q}$	Command input matrix
$\{B\} = \{O_b, X_b, Y_b, Z_b\}$	Reference frame fixed to body of vehicle
$\boldsymbol{c}(t) \in \mathbb{R}^q$	Command input
$\boldsymbol{C}_{RB}$	Coriolis and centripetal matrix
$\boldsymbol{C}_A$	Coriolis and centripetal added mass matrix
$\boldsymbol{D}(\boldsymbol{\nu})$	Damping matrix
$\boldsymbol{e}_m$	Tracking error
$\boldsymbol{e}_Y$	CMRAC prediction error
$\hat{\boldsymbol{e}}$	PMRAC prediction error
e_ψ	Heading error
$\boldsymbol{e}_r$	Heading rate error
e_d	Depth error
e_w	Depth rate error
$\{E\} = \{O_e, X_e, Y_e, Z_e\}$	Reference frame fixed to Earth
F_B	Buoyancy force on the vehicle
F_W	Weight of the vehicle
$\boldsymbol{f}(t)$	Command governor state vector
$\boldsymbol{g}(\boldsymbol{\eta})$	Weight and buoyancy matrix

$\boldsymbol{g}(t) \in \mathbb{R}^{p\times q}$	Command governor output
$\boldsymbol{g}_f(t) \in \mathbb{R}^{p\times q}$	Modified command governor output
$\boldsymbol{H} \in \mathbb{R}^{p\times q}$	Uncertainty input matrix
I_x, I_y, I_z	Moments of inertia
$I_{xy}, I_{yx}, I_{xz}, I_{zx}, I_{zy}, I_{yz}$	Products of inertia
$\boldsymbol{K}_x \in R^{p\times q}$	Ideal feedback gain
$\boldsymbol{K}_c \in R^{q\times q}$	Ideal feed forward gain
$\boldsymbol{K}_1 \in R^{p\times q}$	Nominal feedback gain
$\boldsymbol{K}_2 \in R^{q\times q}$	Nominal feedforward gain
$\hat{\boldsymbol{K}}_x \in R^{p\times q}$	Estimate of feedback gain
$\hat{\boldsymbol{K}}_c \in R^{q\times q}$	Estimate of feed forward gain
$m, \boldsymbol{M}_{RB}$	Mass and mass inertia matrix
$\boldsymbol{M}_A$	Inertia added mass matrix
$r_g^b = [x_g, y_g, z_g]$	Coordinates of centre of gravity in b-frame
$\boldsymbol{u}(t) \in \mathbb{R}^q$	Control input vector
$\boldsymbol{u}_n(t) \in \mathbb{R}^q$	Nominal feedback control law
$\boldsymbol{u}_a(t) \in \mathbb{R}^q$	Adaptive feedback control law
$\boldsymbol{W} \in \mathbb{R}^{s\times q}$	Unknown weight matrix
$\hat{\boldsymbol{W}} \in \mathbb{R}^{s\times q}$	Estimate of unknown weight matrix
$\hat{\boldsymbol{W}}_f(t) \in \mathbb{R}^{a\times b}$	Low-pass filtered weight estimate
$X_u, Y_v, Z_w, K_p, M_q, N_r$	Linear drag coefficients
$X_{u\|u\|}, Y_{v\|v\|}, Z_{w\|w\|}, K_{p\|p\|}, M_{q\|q\|}, N_{r\|r\|}$	Quadratic drag coefficients

$X_{\dot{u}}, Y_{\dot{v}}, Z_{\dot{w}}, K_{\dot{p}}, M_{\dot{q}}, N_{\dot{r}}$	Zero-frequency added mass coefficients
x_f, r_f, σ_f, u_f	Filtered x, r, σ, u
$\boldsymbol{x}(t) \in \mathbb{R}^p$	State vector
$\boldsymbol{x}_l(t) \in \mathbb{R}^p$	Ideal reference state vector
$\boldsymbol{x}_m(t) \in \mathbb{R}^p$	Reference state vector
$\hat{\boldsymbol{x}}(t) \in \mathbb{R}^p$	Predicted state vector
$\hat{Y}(t)$	Estimate of $Y(t)$
$(0 \quad 0 \quad z_b)$	Coordinates of centre of buoyancy in b-frame
$\tau_H = [X_H, Y_H, Z_H, K_H, M_H, N_H]$	Hydrostatic and hydrodynamic forces
$\tau = [\tau_u \quad \tau_v \quad \tau_w \quad \tau_p \quad \tau_q \quad \tau_r]$	Vector of inputs
$\boldsymbol{\delta}(x): \mathbb{R}^p \rightarrow \mathbb{R}^q$	System matched uncertainty
$\Lambda \in \mathbb{R}^{m \times m}$	Unknown control effectiveness matrix
$\boldsymbol{\kappa} = \mathbb{R}_+$	Command governor filter gain
$\sigma: R^n \rightarrow R^s$	Known regressor vector
$\boldsymbol{\Gamma}_x, \boldsymbol{\Gamma}_c, \boldsymbol{\Gamma}_\sigma, \boldsymbol{\Gamma}_{un}$	Learning rates
$\boldsymbol{\Gamma}_f \in \mathbb{R}^{a \times a}$	Filter gain matrix
λ_f	Filter inverse coefficient
$\lambda = \mathbb{R}_+$	Command governor gain

Abbreviations

ADRC	Active Disturbance Rejection Control
AMC	Australian Maritime College
AUV	Autonomous Underwater Vehicle
CB	Centre of Buoyancy
CFD	Computational Fluid Dynamics
CG	Centre of Gravity
CGAC	Command Governor Adaptive Control
CGAC-I	CGAC with Dead-zone Inverse
CGAC-NI	CGAC without Dead-zone Inverse
CLRM	Closed-Loop Reference Model
CMRAC	Composite Model Reference Adaptive Control
CPM	Control Plant Model
DOF	Degrees-Of-Freedom
ECGAC	Extended Command Governor Adaptive Control
GTM	Generic Transport Model
IMU	Inertial Measurement Unit
JHUROV	John Hopkins University Remotely Operated Vehicle
MIMO	Multiple Input Multiple Output
M-MRAC	Modified Model Reference Adaptive Control
MPC	Model Predictive Control
MRAC	Model Reference Adaptive Control
MRAC-HG	MRAC with High Gain
MRAC-LG	MRAC with Low Gain
NASA	National Aeronautics and Space Administration
NPS	Naval Postgraduate School
PD	Proportional-Derivative
PID	Proportional-Integral-Derivative
PO	Peak Overshoot

PPM	Process Plant Model
PMRAC	Predictor Model Reference Adaptive Control
RCGAC	Robust Command Governor Adaptive Control
RMS	Root Mean Square
ROV	Remotely Operated Vehicle
SMC	Sliding Mode Control
SNAME	Society of Naval Architects and Marine Engineers
T-S	Takagi-Sugeno
UAV	Unmanned Aerial Vehicle
UUV	Unmanned Underwater Vehicle
WCGAC	Weight-filtered Command Governor Adaptive Control
WHOI	Woods Hole Oceanographic Institution

[Page intentionally left blank]

Chapter 1:

Introduction

1.1 Background

Unmanned Underwater Vehicles (UUVs) are being increasingly used in underwater operations, replacing or supplementing divers, driven by the demand from the offshore oil industry, heightened maritime security concerns and the need for comprehensive ocean data collection and ocean floor mapping (Brun 2012). These vehicles are generally categorised into Remotely Operated Vehicles (ROVs) and Autonomous Underwater Vehicles (AUVs). The former is commanded by an operator from the surface through a wired (tether) or wireless (acoustic) link, while AUVs are fully autonomous with the ability to carry out pre-programmed missions. Although there are a number of tasks that can be carried out by either type of vehicle, in practice they are employed in applications that conform to the capabilities and strengths of each type. ROVs are used mostly for tasks that require station keeping and operator supervision such as oil pipeline inspection (Chen et al. 2014), ship hull inspection , dam inspection (Maalouf, Creuze & Chemori 2012b), aquaculture (Frost et al. 1996) and underwater construction (Kawaguchi et al. 2011). AUVs, on the other hand, are generally preferred for underwater surveys (Williams et al. 2009) and scientific measurements (Kukulya et al. 2010).

Generally, ROVs are operated by a human pilot. This is a challenging task due to the working environment and task complexity, which can lead to operator fatigue and stress, which in turn can result in operator error that lead to accidents and even loss of vehicle (Ho, Pavlovic & Arrabito 2011). Therefore, there is an interest in moving towards automating low-level tasks, freeing the pilot to concentrate on the high-level planning and control. This has led to the development of ROVs with low-level control systems, i.e. semi-autonomous ROVs (Proctor et al. 2015). While initial functionality was limited to auto heading and depth hold, further developments led to automated station keeping and tracking capabilities, with the first commercial implementation in 2001 (Whitworth & Cohan 2011). Although there has been progress, recent research by Dukan (2014) suggests that more work need to be done to reach the full potential of this type of vehicle. Another recent development is the hybrid ROV/AUV, which is a vehicle capable of fully autonomous operation or remote operation by the pilot, depending on the prevailing requirements (Meinecke, Ratmeyer & Renken 2011).

Overall, these developments have led to some form of autonomous control of many UUVs.

Such autonomous control is challenging, mainly due to model uncertainty, highly nonlinear and time varying hydrodynamic effects and non-deterministic external disturbances as described below.

1.1.1 UUV Control Challenges

To develop precise motion control systems, it is required to have an accurate mathematical model. These models are derived by applying equations of motion and determining the corresponding hydrostatics (e.g. mass, buoyancy) and hydrodynamic (e.g. added mass, drag) parameters. Hydrostatic parameters are somewhat easy to determine using simple measurements or theoretical calculations. The hydrodynamic parameters can be obtained through a number of methods ranging from analytical derivations, numerical simulation and/or experimental measurements. The experimental methods include the use of captive models in towing tanks, test basins and rotating arm facilities (Nomoto & Hattori 1986), and free running tests based system identification (Eng et al. 2016). Captive model tests include the use of Planar Motion Mechanisms (PMM) where the vehicle/model undergoes pre-determined motions with the facility to measure resulting forces and moments (Avila et al. 2011). While captive model test are successfully used to identify hydrodynamic parameters they can be quite expensive, time consuming and require specialised facilities (Avila, Donha & Adamowski 2013). On the other hand, although system identification is a relatively low cost option, the identification of the parameters is difficult and challenging due to several constraints including sensor limitations and measurement noise (Avila, Donha & Adamowski 2013).

Analytical derivations are generally restricted to a limited number of parameters and only provide reasonably accurate values for simple bodies (Eidsvik 2015). The simulation option uses Computational Fluid Dynamics (CFD) techniques to numerically solve the mathematical equations that govern the hydrodynamic interaction with the vehicle (Tyagi & Sen 2006). Although CFD can be a cheaper alternative with reasonable accuracy, it is yet to be successfully used for some situations e.g. unsteady

motion of complex-shaped ROVs at low-speed (Martin & Whitcomb 2014). Furthermore it can require extensive computational resources and some form of experimental validation.

Even when the parameters of a mathematical model have been determined and the controller is designed based on that model, parameter variations could occur during the operation resulting in performance degradation of the controller. For example, the change in buoyancy due to a change in pressure, temperature and salinity (Wu, Liu & Xu 2014); changes in mass and inertia parameters as the vehicle lifts and/or deposits payloads during underwater construction operations (Ippoliti, Longhi & Radicioni 2002); and change in added mass and drag coefficients when operating near the free surface and boundaries in comparison to a deeply submerged UUV (Sayer 1996). In addition, actuator failures also results in parametric uncertainty. In particular, partial thrust loss due to component failure or physical damage is reflected as a change in the control effectiveness.

Apart from model uncertainty and parametric variations, UUVs are constantly subjected to disturbances due to the harsh environmental conditions that have a severe effect on the operation and stability of UUVs. Disturbances can occur due to collisions with objects, ocean currents , waves (Willy 1994), and tether effects (McLain & Rock 1992).

Recent trends and new applications have further exacerbated the challenges enumerated above. These are briefly explained below.

1.1.2 New Trends and Applications

Until recently ROVs were dominated by large work-class ROVs operated by large private organization with vast resources such as the oil industry or large government organizations (e.g. Woods Hole Oceanographic Institution, WHOI). In contrast, recent studies show an increased use of under-actuated mini/micro ROVs in underwater inspections and less complex maintenance tasks (Brun 2012; Rubin 2013). This has given many researchers that had no access previously to such technology a new opportunity and consequently underwater operations of such vehicles has exponentially increased. For example these mini-ROVs are now used in diverse fields such as marine ecology (Jessup 2014) and marine archaeology (L'Hour & Creuze 2016). Even more

encouragingly, mini ROVs developed for hobbyist such as OpenROV (OpenROV 2016) had been utilized in serious research and conservation activities (Selbe 2014). This is mainly due to characteristics such as high manoeuvrability, minimal operating space, and lower costs in comparison to the larger traditional work class ROVs (Pacunski et al. 2008). Moreover, their greater portability allows quick deployment and the ability to operate from shore, small vessels, or other surface platform by a single individual with minimum support infrastructure.

However, for operator of these ROVs, hamstrung by low budgets and resources, finding accurate model parameters is a significant challenge. This is exemplified by Evers et al. (2009), where an attempt to determine the model parameters using system identification failed due to sensor failure. Furthermore, these vehicles are highly sensitive to any parameter variations due to their high power to weight ratio (Maalouf 2013) and are more prone to electrical or mechanical faults such as actuator failures (Pacunski et al. 2008), due to the use of low cost components. In addition, smaller mass makes them more susceptible to external disturbances. Thus, having a control system that can work with minimal knowledge of the initial parameter values and subsequent parameter variations is important for mini ROV operations. In this respect Maalouf (2013) concluded that adaptive control is the best alternative for designing a semi-autonomous control system for a mini ROV.

Another recent trend is the use of AUVs in advanced applications, for example, operating AUVs in tandem with a larger vessel such as a surface ship or a submarine. Rodgers et al. (2008) show that modern navies are interested in using AUVs in close proximity to submarines. More precisely they are interested in launching and recovering such AUVs from the submarine. This docking procedure is extremely complicated and has a low success rate thus erecting a barrier for widespread adoption. The main reason for this is, a large vessel like a submarine can create significant environmental variations surrounding the AUV, causing it to lose control and possibly collide (Leong et al. 2015). Leong (2014) in his work on hydrodynamic effects on AUVs in close proximity to large vessels concludes that an adaptive control mechanism is required to maintain acceptable trajectory under these conditions.

Another advanced application of AUVs is robotic diver assistance (DeMarco, West & Howard 2014). In this scenario, an AUV is operated in close proximity to divers to aide with tasks such as tool carrying, illumination and/or welding. This close quarter operation requires precise manoeuvres as there is the added responsibility of diver safety. It is challenging to conduct such precise manoeuvres due to parameter variations. Valladarez and Toit (2015) of Naval Postgraduate School (NPS), who have taken some pioneering steps in collaboration with National Aeronautics and Space Administration (NASA) in developing a robotic diver assistant (Stewart 2013), have identified adaptive control as a key enabling technology for such applications.

1.2 Problem Definition

The above mentioned trends, applications, and challenges do not occur in isolation, but as integrated developments that function together. On one hand, mini and inexpensive semi-autonomous ROVs and hybrid ROV/AUVs are being increasingly used in applications that were traditionally the domain of commercial UUVs. On the other hand, the use of mini UUVs is prevalent in advance applications that place greater demands on control systems than traditional applications. Not only does the control system have to adapt to changes, it also has to occur quickly without a transition region of poor tracking performance. This is required as any significant deviation from the required trajectory can result in accidents, loss of vehicle and in extreme cases injury to humans operating in the vicinity. Thus, all these applications demand some form of adaptive control that can allow the controller to learn the unknown parameters. At the same time it should have excellent tracking even under large parametric variations and various external disturbances.

The above requirement, although seemingly simple, is fraught with difficulty. Any adaptive controller requires some time to learn the parameter values once there is some change. This time duration is a transient period and depends on the rate of parameter learning. The latter depends on the value of the adaptation gains or learning rates, which are usually user defined constants (Ioannou & Fidan 2006). The performance of conventional adaptive controllers cannot be guaranteed during the transient phase (Cao & Hovakimyan 2006b). Thus, the behaviour of the vehicle could be far from ideal in that time period (Zang & Bitmead 1990). This general behaviour is illustrated in Fig.

1.1. As seen from Fig. 1.1(a) at low adaptive gains the output of the system deviates significantly from the intended reference signal in the transient time. The corresponding control signal is smooth with no high frequency oscillations as seen in in Fig. 1.1(b). This behaviour is well known even in UUV applications with Antonelli et al. (2001) stating that at the beginning of position tracking tasks, the vehicle does not track the desired depth because the adaptation requires a period of time to take effect. Similarly, Zhao and Yuh (2005) also allowed for an initial adaptation period to learn the parameters before beginning the trajectory tracking experiments using the ODIN III AUV. As seen above, the precise manoeuvring required in modern applications make any prolong period of transient undesirable in future control systems.

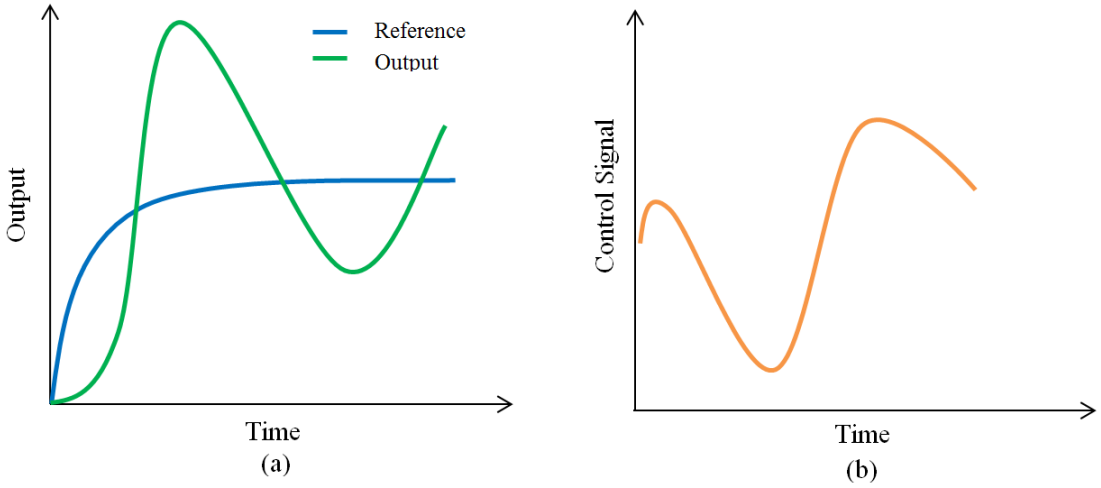

Figure 1. 1: The behaviour of a system using an adaptive controller with low gain a) response of the system in the transient period where the output is significantly different from the reference signal b) corresponding control signal is smooth and well behaved

The usual adaptive control solution has been to increase the adaptation gain, leading to fast learning, thus considerably shortening the period of learning. However, high adaptive gain values lead to high frequency oscillations in the control signal which is a result of parameter adaptation in a time varying and nonlinear manner (Jonathan & Anthony 2010). This general behaviour is illustrated in Fig. 1.2. As seen from Fig 1.2(a) at high adaptive gains the system output closely follow the intended reference signal in the transient time but the control signal has rapid oscillations in transient time as shown in Fig. 1.2(b). There are many studies reported on this phenomenon in general adaptive control applications (Anderson 2005; Georgiou & Smith 1997; Jonathan & Anthony 2010). In contrast, this has not been widely reported in UUV applications, probably

because the applications were not as demanding and did not require high adaptive gains. An indication is given in Smallwood and Whitcomb (2004) where two different sets of adaptive gains were tested for the same trajectory and results presented for tracking error and parameter estimates. Although the effect on the control signal has not been discussed by the authors, at high gains the parameter estimates oscillates wildly, which implies the same effect on the control signal. More recently, Valladarez (2015) has shown this oscillatory response of standard adaptive control in relation to a robotic diver assist application.

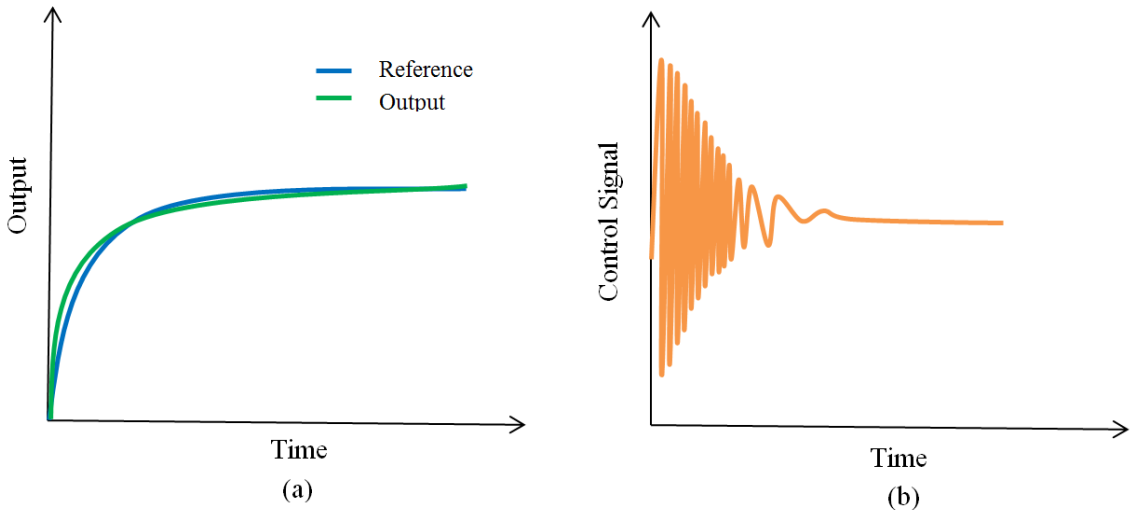

Figure 1. 2: The behaviour of a system using an adaptive controller with high gain a) response of the system in the transient period where the output of the system follows the reference signal b) corresponding control signal has high frequency oscillations

As the adaptive gain is increased the system becomes susceptible to unmodelled dynamics and input time-delay, that could lead to eventual instability (Nguyen, N & Summers 2011). In addition, these oscillations lead to wear, fatigue, and premature failure in motors and actuators (Stepanyan & Krishnakumar 2010). Therefore, in adaptive control there is a trade-off between performance (good reference tracking in transient time) and robustness (to maintain smooth control signal, and stability) (Hovakimyan & Cao 2010). This interplay is illustrated in Fig. 1.3, where the uncertainty suppression is increased with the increase of adaptive gains, whereas stability decreases. In other words, any successful application of adaptive control must solve the problem of this trade-off between performance and robustness.

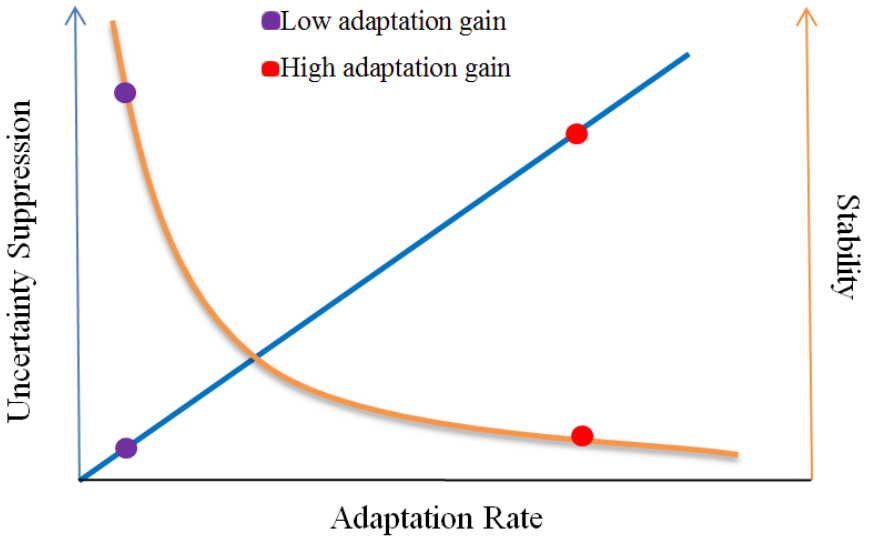

Figure 1. 3: Uncertainty suppression and stability vs adaptation rate

In recent times, driven mainly by aeronautical applications, several modifications to the standard adaptive control have been proposed as solutions to this problem. The predominant approach is to increase the adaptive gain to ensure fast learning and then use some form of direct or indirect filtering to suppress the high frequency content. While there are several methods based on this approach (Cao & Hovakimyan 2008; Stepanyan & Krishnakumar 2010; Yucelen, Torre & Johnson 2013) there have been only two previous studies that apply these methods to underwater vehicles as given below.

Maalouf (2013) did a study into improving the autonomous capability of low mass semi-autonomous ROVs using several control methods. A control method used in her study was the L1 adaptive control due to its ability to decouple performance from robustness. This is an adaptive control method that uses high gain adaptation and a properly designed low pass filter to subvert the high frequency effects (Cao & Hovakimyan 2008). This work was the first use of L1 adaptive control in an underwater vehicle application. Valladarez (2015) in his study of the precise motion control of robotic diver assistants also applied L1 adaptive control to an AUV. While not focused specifically on the trade-off problem, both these studies showed promising results for L1 adaptive control. Although there are numerous successful applications of the L1 adaptive control in the relevant literature, some reservations have been expressed by various researches. For example, the use of high adaptation gain could lead to numerical

instability (Campbell et al. 2010b; Ioannou et al. 2014) as well as adaptation freezing (Ortega & Panteley 2014), which effectively stops the stabilization or performance improvements due to adaptation. Another is the lack of an explicit reference model which makes it difficult to tune and evaluate the controller (Campbell et al. 2010b) and may prevent it from tracking a time-varying reference with acceptable error (Hsu, Battistel & Nunes 2014).

From the above mentioned problem definition it is clear that for demanding UUV applications using adaptive control, it is required to find solutions that trade-off between performance and robustness. However, the predominant method may create problems due to high adaptation gains. Therefore, it is justifiable to look at an alternate approach to solving this trade-off, where the adaptive gains are kept at low values thus guaranteeing smooth control signals and robustness to high frequency dynamical content, and then using either an additional modification or component that can improve the transient tracking performance. This leads to the following research question of this project.

1.3 Research Question

The aim of this project is to develop advanced low gain adaptive control algorithms for UUVs for precise manoeuvring subjected to initial model uncertainty and subsequent model parameter variations. These parametric variations could occur due to rapid changes in the environment, changes to the vehicle configuration or actuator failures. In particular, it requires good transient tracking with smooth control signals while rejecting external disturbances. This in turn allows the safe operation of UUVs in cluttered environments in close proximity to both humans and infrastructure under extreme conditions. Thus, the specific research question of this project is:

What modifications or additions to adaptive control systems provide good transient tracking with smooth control signals under model parameter variation and external disturbances at low adaptation gains for UUV applications?

1.4 Research Objectives

The research objectives required to be achieved to answer the above research question include:

1) To identify modifications or additions to adaptive control algorithms that enable good transient tracking without increasing the adaptive learning rates;
2) To determine the extent to which such algorithms enable good transient tracking without increasing the adaptive learning rates;
3) To examine the performance of such algorithms in UUV applications under model parameter variations and external disturbances;
4) To determine the best combination of these different algorithms for current and future UUV applications; and
5) To propose additional modifications to above mentioned best algorithms to improve the performance for UUV applications.

1.5 Methodology

To answer the research questions and to fulfil the research objectives the following steps were undertaken.

1) Identified the adaptive control algorithms that can be used to achieve good transient tracking response without using higher learning rates. For this end a literature review was conducted that looked at different methods available. It was identified that while there was only one major method that falls into this category, there are some methods that could be used with low learning rates based on their theoretical foundations and past results. The major method selected was Command Governor Adaptive Control (CGAC) by Yucelen and Johnson (2012a). In addition, two composite adaptive control methods called Composite Model Reference Adaptive Control (CMRAC) by Lavretsky (2009) and Predictor-Based Model Reference Adaptive Control (PMRAC) by Lavretsky, Gadient and Gregory (2010) were also selected.
2) Ran numerical simulation of the three methods using a full nonlinear model of an actual underwater vehicle in MATLAB/Simulink to test their viability under

model uncertainty, parameter variations and external disturbances. These simulations were carried out for both heading and depth control. To create maximum model uncertainty, the initial parameter values were set to zero, thus assuming no *a priori* knowledge of the parameter values. For CMRAC and PMRAC the simulations were carried out at different learning rates to determine the effect of the learning rate and to determine the base learning rate used for final comparison of the different methods. In addition, the comparison with MRAC provided an indication of the transient tracking performance and control signal behaviour. For CGAC, the simulations were run at the base learning rate and compared with MRAC at the same learning rate and at a much higher learning rate. This gave an indication of the effect on the control signal when MRAC is used with high learning rates compared with low gain methods. Then the simulations were extended towards investigating the detrimental effect of noise on CGAC as reported in literature and the viability of using input filtering and robustification[1] filter to overcome the noise effect. In addition to the effect of disturbances, the ability of CGAC to overcome and actuator dead-zone without any additional dead-zone inverse was tested using a simulated thruster dead-zone.

3) Conducted experimental validation of the simulation results for CMRAC, PMRAC and CGAC using the actual vehicle in a controlled environment. The experiments mirrored the simulations in testing for normal operations under initial model uncertainty, sudden parameter variations and external disturbances. In addition, CGAC was tested for ability to overcome dead-zone and the effect of noise and robustification filter. The experiments differed from simulations for depth control as the full state measurement was not available, thus requiring some estimation of the depth rate that would make the effect of noise more prominent.
4) Analysed the results from both simulations and experiments to provide a solid quantitative evaluation of the performance of each method under different conditions. These provided important information on the individual performance of these three methods. Determined, based on the evaluations at the base

[1] To make a system more robust, usually to noise

learning rate, the ability of the modifications to improve performance without scarifying robustness and the best method or combination of methods for the precise manoeuvring of UUVs.

5) Suggested additional modifications to the aforementioned control methods as required and validate the new modifications through experiments.

1.6 Novel Aspects

In this work two major novel contributions and three minor novel contributions were made.

1.6.1 Major novel contributions

1) This is a pioneering study to address the problem of achieving better transient tracking performance without inducing control oscillations and instability in underwater vehicles. Moreover, it is the first study in marine control to take the approach of setting adaptation gains to a low value to ensure robustness (stability and smooth control signals) while relying on modifications to the control system to improve the performance (transient tracking). In addition, this study is uniquely differentiated from the previous studies in considering not just one method but three methods that can address this trade-off.
2) This study is the first instance where these three methods (CMRAC, PMRAC and CGAC) are applied to an underwater vehicle and their performances are tested. In addition, this is one of the foremost studies where both PMRAC and CGAC have been comprehensively analysed using quantitative data in addition to qualitative data from both simulations and experiments in any type of application. This study is also uniquely differentiated from previous studies in specifically focusing on tracking capability improvements of CMRAC, PMRAC and CGAC at low adaptation gains.

1.6.2 Minor novel contributions

1) The introduction of an extension to CGAC that overcomes limitations of the robustification filter. It has been observed that:

a. while the filter improves robustness, when small low-pass filter gains are used, there was a significant degradation of tracking performance for a short initial period; and
b. while it removes noise from the command governor signal, under large measurement noise the control signal was still noisier than MRAC.

As a possible solution CGAC was combined with a weight filter that removes high frequencies from the control signal thus reducing noise and increasing robustness to time-delay; and prediction error was added using the state predictor to improve learning and counteract the loss of information due to the filter.

2) In CGAC, it is not required to use an actuator dead-zone inverse. It is well known that adaptive control is significantly affected by actuator nonlinearities including actuator dead-zone (Crespo, Matsutani & Annaswamy 2010). CGAC is shown to have an inherent disturbance rejection capability and thus does not require separate Active Disturbance Rejection Control (ADRC). The work shows that this allows CGAC to overcome actuator dead-zone without any additional dead-zone inverse or disturbance observer.

3) The emphasis placed on the thrust loss anomaly in UUVs. This is the condition when there is a loss of partial thrust as a whole due to either electrical or mechanical faults in the actuators. Thus, it is important that for underactuated UUVs the low level controller can effectively and efficiently overcome the thrust loss without any significant deviations from the reference.

1.7 Adaptive Control Overview

Closed-loop control systems usually consist of a plant that needs to be controlled and a controller that is driven by the feedback from the plant output measurements. In the early days of control design the controller parameters were fixed constants, thus these controllers were usually referred to as fixed-gain controllers. With the advent of more demanding applications it was realized that a fixed-gain controllers cannot provide acceptable plant behaviour in all situations (Ioannou & Fidan 2006). This is especially true for plants that have unknown or time-varying parameters. Therefore, this led to the development of adaptive control, i.e. "*Adaptive control is the combination of a*

parameter estimator, which generates parameter estimates online, with a control law in order to control classes of plants whose parameters are completely unknown and/or could change with time in an unpredictable manner" (Ioannou & Fidan 2006, pp.1). The difference between fixed-gain control and adaptive control is illustrated in the Fig. 1.4, where Fig. 1.4(a) shows that for fixed-gain control the performance can be improved (error decreases) only with the increase in the accuracy of the model, while Fig. 1.4(b) shows that adaptive control can improve performance even under low model accuracy as it can learn the parameter values over time.

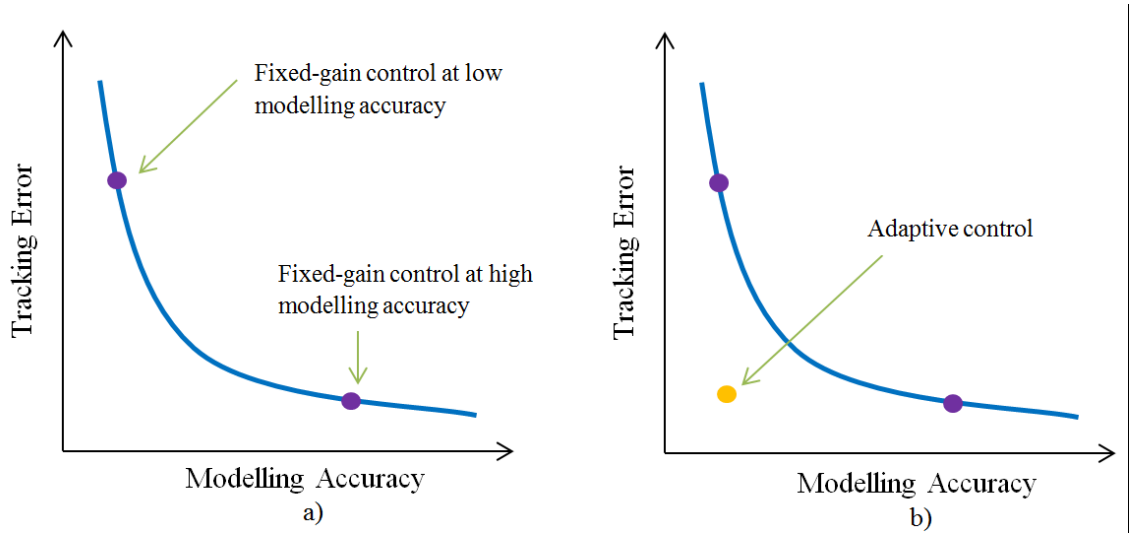

Figure 1. 4: Tracking error vs modelling accuracy for a) fixed-gain control b) adaptive control

Over the years, adaptive control has been further sub-divided according to different criteria. One such division is into direct and indirect adaptive control. In direct adaptive control the plant parameters are parameterized using the desired control parameters and then the control parameters are directly estimated. In indirect adaptive control the plant parameters are estimated first, using a model of the plant and then the control parameters are derived using those plant parameters.

Model Reference Adaptive Control (MRAC) is one sub category of adaptive systems in which the desired characteristics of the system are represented usually by a reference model. The parameters are adjusted such that the tracking error tends to zero. This tracking error is defined as the difference between the system output and reference model output. MRAC can also be categorized into direct and indirect MRAC according to the way the control parameters are estimated, either directly or indirectly. Thus for indirect MRAC, in addition to the reference model an identification model (a plant

model) is also used to calculate control parameters from the plant parameters. Direct and indirect MRAC architecture are illustrated in Figs. 1.5 and 1.6.

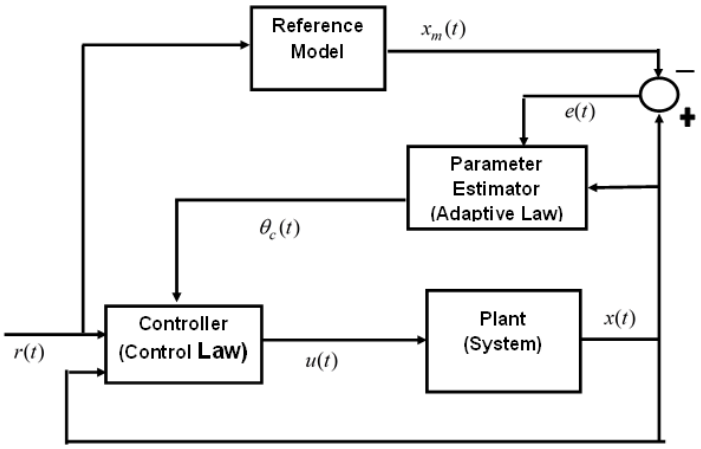

Figure 1. 5: Direct MRAC architecture

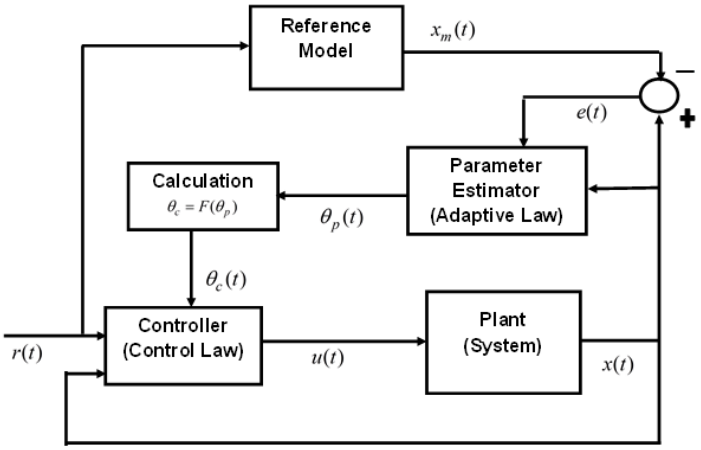

Figure 1. 6: Indirect MRAC architecture

There are also adaptive control architectures categorized under MRAC that does not use the reference model, instead replacing it with a state predictor. These can also fall under either direct or indirect MRAC, but differ from traditional MRAC in using the prediction error instead of the tracking error. This prediction error is defined as the difference between the state predictor and the system output. The prediction error is also used in general indirect adaptive control to refer to the difference between identification model output and system output. Most MRAC methods have traditionally used the reference model and the direct approach to parameter estimation. The direct MRAC with state predictor approach is interesting in that it was modified by Cao and Hovakimyan (2006b) to develop the L1 adaptive control approach that has become a

prominent adaptive control method in the last decade. Direct MRAC architecture with a state predictor is illustrated in Fig. 1.7.

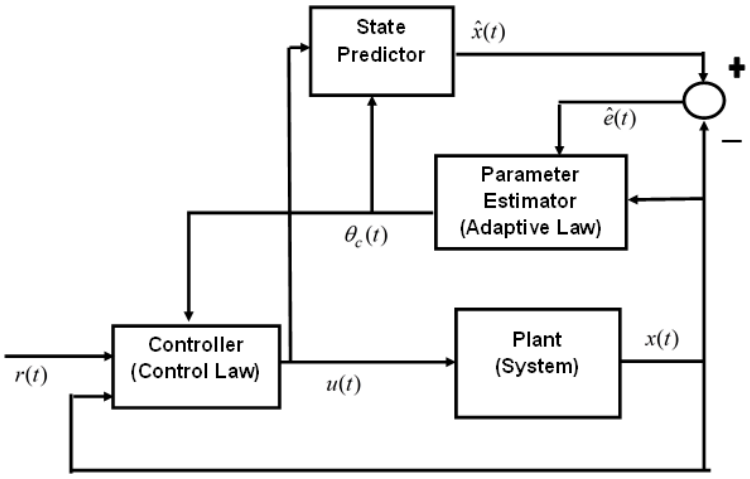

Figure 1. 7: Direct MRAC architecture with State Predictor

Two groups of researches, Duarte-Mermoud and Narendra (1989) and Slotine and Li (1989) independently developed a direct MRAC approach in which they combined both tracking error and prediction error to directly estimate the control parameters referred to as the Combined\Composite MRAC (CMRAC). The possible advantage of CMRAC is based on a conjecture usually referred to as the *CMRAC conjecture* which states; "*better (smoother than MRAC) transient characteristics can be obtained, when using prediction errors in addition to tracking errors, in formulating adaptive law dynamics*" (Lavretsky 2009, pp. 1). One possible scheme of CMRAC that uses a state predictor to generate the prediction error is illustrated in Fig. 1.8.

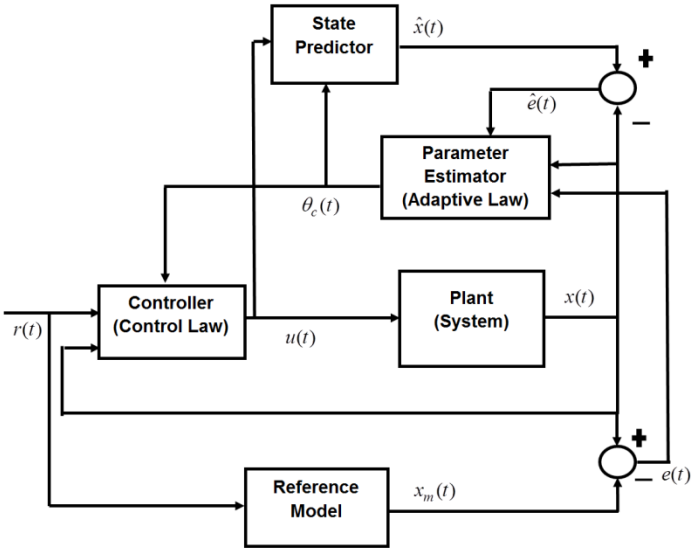

Figure 1. 8: Composite MRAC architecture using a reference model and state predictor

1.7.1 Low Gain Adaptive Control

There have been very few methods that take the approach of using low gains for robustness and using an additional modification for improved transient tracking. The first method that explicitly states this objective was CGAC. Although first proposed in Yucelen and Johnson (2012a, 2012b) there have been very few quantitative results and no experimental results of this method in literature. The first study provided only a simple simulation of wing rock aircraft dynamics to illustrate the concept, while a more detailed simulation of the same dynamics was provided in Yucelen and Johnson (2013). Although it demonstrated the transient tracking improvements and smooth control signal of CGAC, it only provided qualitative results in the form of graphical plots. In Magree, Yucelen and Johnson (2012) qualitative simulation results were provided for CGAC applied to a high-fidelity autonomous helicopter model. CGAC was extended to enable the handling of state constraints in Schatz, Yucelen and Johnson (2013) and illustrated using simulations of lateral and the longitudinal motion of an aircraft. Further simulations of this extension for a helicopter model and wing rock dynamics are given in Schatz et al. (2013).

Apart from these studies there have been others that were derived from or related to CGAC. They include:

1. A modified version of the command governor based on the work of Yucelen and Johnson (2012b) was combined with an adaptive backstepping controller in Sørensen, MEN and Breivik (2015). Although it was not an exact study on CGAC, it provides some quantitative data in the form of performance indices by using simulation of a marine surface vessel.
2. A command governor modification was developed without adaptive control as a form of robust control by De La Torre, Yucelen and Johnson (2016), with experimental results for fault tolerant control of a Hexarotor given in Falconí, Schatz and Holzapfel (2016). Although based on CGAC (De La Torre, Yucelen & Johnson 2016), it does not directly relate to the current study due to it being a non-adaptive control method.
3. Recently Na, Herrmann and Zhang (2017) proposed another modification for better transient performance without high adaptive gains using simulation results. A closer inspection of this method indicate that it is variant of CGAC, where the robustification filter that is separately added in CGAC has been incorporated into the command governor design.

Although not explicitly proposed for the purpose, another form of adaptive control that could be used to improve transient tracking at low gains is CMRAC. Although applied mainly as a modification that leads to smoother transient behaviour under high adaptation gain (Hovakimyan & Cao 2010), several studies show CMRAC improves tracking accuracy (Duarte-Mermoud, Rioseco & González 2005; Duarte-Mermoud, Rojo & Pérez 2002; Yu & Lloyd 1997), including one study that applied CMRAC to a UUV (Mrad & Majdalani 2003). In that work a variant named Bounded Gain Forgetting (BGF) CMRAC method was compared with standard adaptive control with only qualitative simulation results being provided. More recently, another variant of composite adaptive control was introduced by Lavretsky (2009). This method has several novel improvements over previous CMRAC methods including being applicable to a generic class of Multiple Input Multiple Output (MIMO) dynamical systems with matched nonlinear-in-state and linear-in-parameters uncertainties (Lavretsky 2009). Although it has shown promising results (Dydek, Annaswamy & Lavretsky 2013; Gregory, Gadient & Lavretsky 2011), it is mainly used with high learning rates to

provide smoother control input and has thus far not been quantitatively assessed for tracking improvements under low learning rates.

Another composite variant named PMRAC was first proposed in Lavretsky, Gadient and Gregory (2010) and has the advantage of being applicable to a generic class of MIMO dynamical systems with matched nonlinear-in-state and linear-in-parameters uncertainties similar to CMRAC. It differed from CMRAC in that the prediction error is generated by a state predictor with an error feedback. Thus, its prediction component has the structural formulation of indirect Modified-MRAC (M-MRAC) (Stepanyan & Krishnakumar 2012b) or Closed-Loop Reference Model (CLRM) architecture (Gibson, Annaswamy & Lavretsky 2013). Lavretsky, Gadient and Gregory (2010) tested it in simulations for an aircraft pitch control under high adaptive gains and observed that while the tracking performance was similar to MRAC the oscillations in the control signal was reduced. A more detailed simulation study of PMRAC for a generic aircraft was reported in Campbell and Kaneshige (2010). In this study, PMRAC was simulated using the NASA Generic Transport Model (GTM) in a full nonlinear simulation for a doublet manoeuvre. Only a few qualitative results were presented with similar conclusions. PMRAC was also used in a more extensive study that looked at simulation based sensitivity analysis of seven different controllers for the same NASA GTM in Campbell et al. (2010b). It was followed by a pilot handling study of the same controllers using a flight simulator (Campbell et al. 2010a). In addition, Khosravi, Lachini and Sarhadi (2015) applied PMRAC to an automotive vehicle lateral control in simulation with only qualitative results, similar to Lavretsky, Gadient and Gregory (2010), presented with very similar conclusions. A closer look at these studies showed that they gave very few specific quantitative details of PMRAC and no experimental results.

1.8 Thesis Structure

This thesis comprises a collation of published and submitted refereed journal and conference papers presented in chapters 2 to 6. The relevant publishing details are given at the beginning of each chapter. As the chapters consist of standalone publications, it is inevitable that some content will be repeated in a number of chapters although all effort has been taken to reduce such repetition. This is especially so with regard to the

introductions, modelling of the vehicle dynamics and the experimental setup. The structure of the thesis is outlined below.

***Chapter 1*:** The introductory chapter, which provides the relevant background and problem definition leading to the research question, objectives, methodology of the project, and the novel contributions including an introduction to general adaptive control and a brief description of the adaptive control modifications considered in this thesis.

***Chapter 2*:** This presents the design and simulation CMRAC and PMRAC for UUV applications using validated numerical models and compares its performance against the standard MRAC. The simulations are performed at three different learning rates for both heading and depth control. Several test scenarios were considered including normal operational conditions, external disturbance, and partial thruster failure. Simulations show promising results for both methods and form the basis of experimental work in chapter 4.

***Chapter 3*:** This presents the design and simulation of CGAC for a UUV and its comparison with MRAC. The vehicle dynamics are assumed to be decoupled thus allowing for the design of separate heading and depth controllers. Simulations are carried out at different learning rates to observe the transient performance and verify the disturbance rejection capability of the CGAC controller. Consideration is also given to practical issues such as noise and actuator dead-zones. Extensive simulations confirmed that the robust modification of CGAC (RCGAC) performed well without adding excessive noise to the control signal. It is also shown that RCGAC can operate satisfactorily with a large thruster dead-zone by compensating for the dead-zone nonlinearity. These simulation results form the basis for the experimental work in chapter 5.

***Chapter 4*:** This follows on from chapter 2 and presents experimental validation of CMRAC and PMRAC for underwater vehicle applications. The standard MRAC is used as the baseline for performance comparison. Several test scenarios were considered including initial operation, external disturbance, and thruster failure. The results are

analysed extensively using six performance indices at three learning rates. In addition, frequency domain of the control signals, noise level in control signals and time-delay effects are analysed. These results showed a significant advantage of PMRAC over CMRAC and MRAC under all conditions. Thus, these results motivated the use of the state predictor modification described in chapter 6.

Chapter 5: This chapter consists of the experimental validation of RCGAC in chapter 3 for underwater vehicle applications. The standard MRAC is used as the baseline for performance comparison. Experimental results show that RCGAC achieves a low frequency control signal through low gain values and improves transient performance through modifications to the command signal. In addition, the ability of RCGAC to overcome disturbances such as tether forces, tolerate faults such as partial thruster failure, and overcome a thruster dead-zone was confirmed. Furthermore, the effects of measurement noise, time-delay, and robustification filter were tested, which indicate the adverse effect of the robustification filter on tracking performance of RCGAC for a short initial duration, during the transient phase that inspired the modifications proposed in chapter 6.

***Chapter 6*:** This chapter is based on the results from chapter 5 and presents an explicit attempt to improve robustness of CGAC to measurement noise and time-delay without incurring the performance degradation of the robustification filter. The chapter also includes the experimental validation of the proposed extension to CGAC named ECGAC. The proposed extension includes replacing the robustification filter of RCGAC with a weight filter that reduces high frequencies and adds phase to the system. This yields significant reduction in control signal noise from the RCGAC without incurring the adverse effects of the robustification filter. Although, this increased robustness is accompanied by a slight reduction in overall tracking performance, it is counteracted by adding the prediction error using the closed-loop state predictor of PMRAC. Thus, this chapter culminates the work of this project by proposing a complete low gain MRAC solution that can be used in advanced UUV applications.

***Chapter 7*:** The concluding chapter provides an overall summary of the project, bringing together the findings of the individual chapters. It also concludes on the

findings and outcomes, as well as discussing the implications of the findings, limitations, recommendations and areas of future work.

***Appendices*: Appendix I** provide a preliminary approach to controlling UUVs under uncertainty using fuzzy gain scheduling of multiple PID controllers. **Appendix II** describes the simulation setup including Simulink models that were used to gather the simulation results. **Appendix III** is about the experimental set up used for obtaining experimental results for all controllers discussed in this thesis. **Appendix IV** provides the Lyapunov stability proof of the proposed Extended Command Governor Adaptive Control (ECGAC).

Chapter 2:

Simulation & Verification of Composite Model Reference Adaptive Controllers

This chapter consists of two subchapters:

Part A: Composite Model Reference Adaptive Control for an Unmanned Underwater Vehicle.

Part B: Predictor-Based Model Reference Adaptive Control for an Unmanned Underwater Vehicle.

In this chapter, Part A and Part B present performance analysis of Composite Model Reference Adaptive Control (CMRAC) and Predictor-Based Model Reference Adaptive Control (PMRAC) respectively, with numerical simulations carried out with a dynamic model of the UUV. The results provided the verification of the suitability of composite methods for UUV applications and formed the foundation for experimental validation in Chapter 4.

Chapter 2:

Part A –

Composite Model Reference Adaptive Control for an Unmanned Underwater Vehicle

This subchapter has been published in the Journal of "*Underwater Technology*". The citation for the research article is:

Makavita, CD and Nguyen, HD and Ranmuthugala, D and Jayasinghe, SG, Composite model reference adaptive control for an unmanned underwater vehicle, *Underwater Technology*, 33, (2) pp. 81-93. ISSN 1756-0543 (2015) [Refereed Article]

Abstract

The control of Unmanned Underwater Vehicles (UUVs) is challenging due to the non-linear and time varying nature of the hydrodynamic forces from the surrounding fluid. In addition, the presence of external disturbances makes the control even more difficult. Model Reference Adaptive Control (MRAC) is an adaptive control technique that performs well in such situations, while the improved Composite Model Reference Adaptive Control (CMRAC) is capable of better transient performance. However, the latter is yet to be used in UUV controls. Thus, this paper tests the suitability of CMRAC in UUV applications using validated simulation models and compares its performance against the standard MRAC. Several test scenarios have been considered including initial operation, external disturbance, and thruster failure. Simulation results show that CMRAC offers better tracking, faster disturbance rejection, and quick recovery from thruster failure compared to MRAC. In addition, CMRAC is more robust against parameter uncertainties and thus the control signal shows fewer oscillations which in turn reduce the probability of actuator damage.

Keywords: unmanned underwater vehicles (UUV), composite/combined model reference adaptive control, external disturbances, thruster failure, and remotely operated vehicle

2A.1 Introduction

Unmanned Underwater Vehicles (UUVs) are extensively used in industry, military, and academia to carry out various underwater operations such as inspection of subsea installations, gathering of marine and security data, and exploring marine and archaeological sites. In addition to these traditional large scale applications there is a growing trend in underwater exploration carried out by smaller UUVs offering affordable and flexible operations, mainly due to the continuous improvement in UUV technologies.

UUVs offer considerable challenges in autonomous control, mainly because of the coupled nonlinear and time varying hydrodynamic forces and moments that adversely affect the motion of the vehicle. In addition, they are subjected to various external disturbances such as ocean currents, ocean waves, and tether motion.

In literature, there are several control techniques proposed to deal with these problems. The most popular and simple control solution is the Proportional-Integral-Derivative (PID) controller (Miskovic et al. 2006), but it does not perform well in highly nonlinear systems. The sliding mode control (Healey & Lienard 1993; Yoerger et al. 1985) is another popular method that has been utilised over the past decades. It is more robust against disturbances and nonlinearities compared to the PID control, but suffer from chatter, which is high frequency oscillations of the control signal. As a solution to this issue, chatter free sliding mode controllers referred to as higher order sliding mode control, have been proposed for UUVs and experimentally tested with promising results (Garcia-Valdovinos, Salgado-Jiménez & Torres-Rodríguez 2009; Pisano & Usai 2004). Another robust approach is the H_∞ control that has been simulated and tested for an AUV (Roche et al. 2011).

Model Predictive Control (MPC) is a well-known control method originally proposed for process control systems (Qin & Badgwell 2003). Owing to the fast response, robust operation, and relatively low tuning effort MPC is gaining acceptance in other areas as well with varying success (Vazquez et al. 2014). MPC predicts the optimal future control profile using a mathematical model of the system and current states. It has been simulated (Budiyono 2011; Medagoda & Williams 2012) and experimentally tested (Steenson et al. 2014) for UUVs with promising results. The major disadvantage of

MPC is that if there is any modelling error or variation in model stability, then the performance is affected.

The intelligent control methods can be categorized into three groups namely: fuzzy control; reinforcement learning; and artificial intelligence. An example of the use of fuzzy control for heading control of an AUV is given in Chang, Chang and Liu (2003) while a fuzzy depth controller is given in Jun, Kim and Lee (2011). Reinforcement learning for high level control is simulated by Carreras, Yuh and Batlle (2002) while the same for cable tracking of an underwater vehicle is tested by El-Fakdi and Carreras (2008). A form of artificial intelligence called "language-centred intelligence" is applied to AUVs in Hallin et al. (2009).

Adaptive control is the emerging control trend that has been successfully implemented in several UUVs (Antonelli et al. 2003; Maalouf, Creuze & Chemori 2012a). While robust control methods such as sliding mode and H_∞ reduce the effect of uncertainty and nonlinearity, they do so at the expense of compromised performance. Adaptive control offers the advantage of being able to adjust the controller output even in the presence of parameter uncertainties and thereby ensures the possibility of achieving a much higher degree of robust performance. This is even more useful when it is difficult to get a good estimate of the model parameters due to the lack of hydrodynamic testing facilities.

The improved performance of adaptive control over Proportional-Derivative (PD) control has been demonstrated by various studies (Antonelli et al. 2003; Maalouf et al. 2013; Smallwood & Whitcomb 2004). Smallwood and Whitcomb (2002) show that while fixed model based controllers performed better in known conditions, adaptive control provides superior performance under unknown conditions and parameter variations. In Cavalletti, Ippoliti and Longhi (2011) large variations in mass and inertial parameters are considered, and comparisons are made between switching controller and adaptive controller. These studies have shown that when there is a lack of knowledge of vehicle configuration, the adaptive controller has better performance. However, a major disadvantage of adaptive control is that, as the gains are adapted in a time varying and nonlinear manner, it can lead to unacceptable transient response (Jonathan & Anthony 2010).

Model Reference Adaptive Control (MRAC) is one method where the system attempts to follow a reference signal generated by an ideal model (Åström & Wittenmark 1995). The control parameters are adapted according to the error between the reference and actual state. Slotine and Li (1989) and Duarte-Mermoud and Narendra (1989) improved the MRAC to develop the Composite/Combine Model Reference Adaptive Control (CMRAC) technique. This technique goes beyond just tracking the error, as it attempts to predict a known value and use the resulting prediction error with the tracking error to adapt control parameters.

Lavretsky (2009) has proposed an improved CMRAC technique, which is much easier to implement compared to the previous CMRAC methods and smoothens the transient response under various operating conditions. Since the improved CMRAC technique does not add too much complexity it is an attractive control solution for small scale UUVs, which have limited computational capabilities. However, the suitability and performance of the improved CMRAC in small scale UUVs are yet to be tested and verified.

The authors have developed a small scale low cost three thruster Remotely Operated Vehicle (ROV) named Australian Maritime College (AMC) ROV (see Fig. 2A.1), with control systems and haptic feedback teleoperation. This paper discusses the suitability of the CMRAC technique in such vehicles and compares its performance against the standard MRAC. The controllers were tested using a nonlinear numerical model of the ROV in a MATLAB/Simulink environment. The results show that CMRAC offers better tracking, faster disturbance rejection, and quick recovery from thruster failure compared to the standard MRAC. In addition, the CMRAC is more robust against parameter uncertainties and thus the control signal shows less oscillation, which in turn reduces the probability of actuator damage.

2A.2 Kinematic and Dynamic Model of the AMC ROV

This section presents the kinematics and the dynamic model of the AMC ROV. Two reference frames namely: Earth-fixed and body fixed, are used for the convenience in modelling the dynamics of the ROV.

2A.2.1 Reference Frames

The Earth-fixed reference $\{E\}$ frame and the body-fixed reference $\{B\}$ frame used in the ROV model are shown in Fig. 2A.1. The $\{E\}$ frame is coupled to the Earth, and acts as the inertial frame as the velocity of the ROV is small enough to neglect the effects of the forces acting on it due to the rotation of the Earth (Perez & Fossen 2005). The $\{B\}$ frame is coupled to the vehicle with the origin chosen to coincide with the Centre of Gravity (CG) denoted by (x_g, y_g, z_g), and acts as the moving frame.

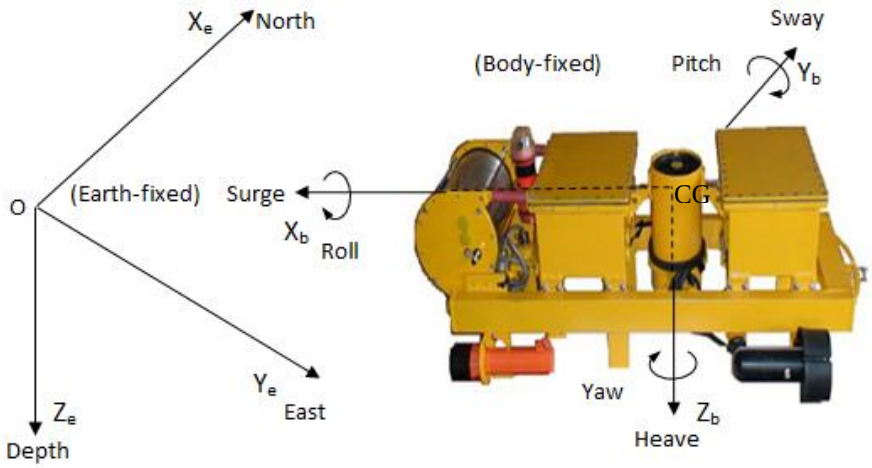

Figure 2A. 1: The three thrusters AMC ROV showing the Earth fixed and body fixed reference frames

2A.2.2 UUV Kinematics

The general motion of a UUV in six Degrees-Of-Freedom (6-DOF) is modelled by using the notation presented in Fossen (2011), which has been adopted from Society of Naval Architects and Marine Engineers (SNAME 1950). The 6-DOF kinematics equations for the UUV is given by Fossen (2011) ,

$$\dot{n} = u\cos\psi\cos\theta + v(\cos\psi\sin\theta\sin\phi - \sin\psi\cos\phi) + w(\sin\psi\sin\phi + \cos\psi\cos\phi\sin\theta) \quad (2A.1)$$

$$\dot{e} = u\sin\psi\cos\theta + v(\cos\psi\cos\phi + \sin\phi\sin\theta\sin\psi) + w(\sin\theta\sin\psi\cos\phi - \cos\psi\sin\phi) \quad (2A.2)$$

$$\dot{d} = -u\sin\theta + v\cos\theta\sin\phi + w\cos\theta\cos\phi \quad (2A.3)$$

$$\dot{\phi} = p + q\sin\phi\tan\theta + r\cos\phi\tan\theta \quad (2A.4)$$

$$\dot{\theta} = q\cos\phi - r\sin\phi \quad (2A.5)$$

$$\dot{\psi} = q\frac{\sin\phi}{\cos\theta} + r\frac{\cos\phi}{\cos\theta}, \quad \theta \neq \pm 90^0 \tag{2A.6}$$

2A.2.3 UUV Dynamics

According to Fossen (2011), Newton's second law can be expressed in an arbitrary body-fixed coordinate frame as,

$$\boldsymbol{M}_{RB}\dot{\boldsymbol{\nu}} + \boldsymbol{C}_{RB}(\boldsymbol{\nu})\boldsymbol{\nu} = \boldsymbol{\tau}_H + \boldsymbol{\tau} \tag{2A.7}$$

where $\boldsymbol{\tau}_H$ is the hydrostatics and hydrodynamic forces vector, $\boldsymbol{\tau}$ is the vector of control inputs, $\boldsymbol{M}_{RB}$ is the mass inertia matrix, and $\boldsymbol{C}_{RB}(\boldsymbol{\nu})$ is the Coriolis and centripetal matrix.

For deeply submerged vehicles equation (2A.7) can be expanded to give,

$$\boldsymbol{M}_{RB}\dot{\boldsymbol{\nu}} + \boldsymbol{C}_{RB}(\boldsymbol{\nu})\boldsymbol{\nu} + \boldsymbol{M}_A\dot{\boldsymbol{\nu}} + \boldsymbol{C}_A(\boldsymbol{\nu})\boldsymbol{\nu} + \boldsymbol{D}(\boldsymbol{\nu})\boldsymbol{\nu} + \boldsymbol{g}(\boldsymbol{\eta}) = \boldsymbol{\tau} \tag{2A.8}$$

where $\boldsymbol{M}_A$ and $\boldsymbol{C}_A(\boldsymbol{\nu})$ represent the added mass matrices that are generated by the forced motion of the vehicle body and $\boldsymbol{g}(\boldsymbol{\eta})$ is the net buoyancy forces and restoring moments matrix. For a UUV it is customary to consider a diagonal $\boldsymbol{M}_A$ because the off-diagonal components are much smaller compared to diagonal terms for low speed underwater vehicles (Eng, Chin & Lau 2014), thus,

$$\boldsymbol{M}_A = -\begin{bmatrix} X_{\dot{u}} & 0 & 0 & 0 & 0 & 0 \\ 0 & Y_{\dot{v}} & 0 & 0 & 0 & 0 \\ 0 & 0 & Z_{\dot{w}} & 0 & 0 & 0 \\ 0 & 0 & 0 & K_{\dot{p}} & 0 & 0 \\ 0 & 0 & 0 & 0 & M_{\dot{q}} & 0 \\ 0 & 0 & 0 & 0 & 0 & N_{\dot{r}} \end{bmatrix} \tag{2A.9}$$

while:

$$\boldsymbol{C}_A(\boldsymbol{\nu}) = \begin{bmatrix} 0 & 0 & 0 & 0 & -Z_{\dot{w}}w & Y_{\dot{v}}v \\ 0 & 0 & 0 & Z_{\dot{w}}w & 0 & -X_{\dot{u}}u \\ 0 & 0 & 0 & -Y_{\dot{v}}v & X_{\dot{u}}u & 0 \\ 0 & -Z_{\dot{w}}w & Y_{\dot{v}}v & 0 & -N_{\dot{r}}r & M_{\dot{q}}q \\ Z_{\dot{w}}w & 0 & -X_{\dot{u}}u & N_{\dot{r}}r & 0 & -K_{\dot{p}}p \\ -Y_{\dot{v}}v & X_{\dot{u}}u & 0 & -M_{\dot{q}}q & K_{\dot{p}}p & 0 \end{bmatrix} \tag{2A.10}$$

where $X_{\dot{u}}, Y_{\dot{v}}, Z_{\dot{w}}, K_{\dot{p}}, M_{\dot{q}}, N_{\dot{r}}$ so forth are the zero-frequency added mass coefficients.

The gravitational force $F_W = mg$ will act through CG, while the buoyancy force $F_B = \rho g \nabla$ will act through the centre of buoyancy (CB). Here g is the gravitational acceleration, ρ is the density of water and ∇ is the displaced water volume. Selecting that the origin of the body-fixed reference frame to coincide with CG (i.e. $x_g = 0, y_g = 0, z_g = 0$), and assuming CG and CB are offset only in the z direction owing to symmetry and is denoted by z_b, $\boldsymbol{g(\eta)}$ is simplified to:

$$\boldsymbol{g}(\boldsymbol{\eta}) = \begin{bmatrix} (F_W - F_B)\sin(\theta) \\ -(F_W - F_B)\cos(\theta)\sin(\phi) \\ -(F_W - F_B)\cos(\theta)\cos(\phi) \\ -(z_b F_B)\cos(\theta)\sin(\phi) \\ -(z_b F_B)\sin(\theta) \\ 0 \end{bmatrix} \tag{2A.11}$$

The damping forces on the UUVs can be written as the sum of the diagonal linear damping terms and nonlinear quadratic damping terms (Chin & Lau 2012). Therefore, the damping matrix $\boldsymbol{D}(\boldsymbol{v})$ is given as:

$$\boldsymbol{D}(\boldsymbol{v}) = -\begin{bmatrix} X_u + X_{u|u|}|u| & 0 & 0 & 0 & 0 & 0 \\ 0 & Y_v + Y_{v|v|}|v| & 0 & 0 & 0 & 0 \\ 0 & 0 & Z_w + Z_{w|w|}|w| & 0 & 0 & 0 \\ 0 & 0 & 0 & K_p + K_{p|p|}|p| & 0 & 0 \\ 0 & 0 & 0 & 0 & M_q + M_{q|q|}|q| & 0 \\ 0 & 0 & 0 & 0 & 0 & N_r + N_{r|r|}|r| \end{bmatrix} \tag{2A.12}$$

AMC ROV is propelled by three thrusters (T_1, T_2 and T_3). T_1 and T_2 are horizontal thrusters. The horizontal distance between the two along the Y_b axis is d_2 and the distance from CG to both thrusters in the direction along the Z_b axis is d_1. T_3 is the vertical thruster and its distance from CG along the direction of the X_b axis is d_4. Thus, the thrust and moment input vector, τ, can be written as,

$$\tau = \begin{bmatrix} T_1 + T_2 \\ 0 \\ T_3 \\ 0 \\ (T_1 + T_2)d_1 - T_3 d_4 \\ (T_1 - T_2)\dfrac{d_2}{2} \end{bmatrix} \tag{2A.13}$$

The hydrodynamic coefficients of the AMC ROV used in the simulations are given in Table 2A.1. Further details of the AMC ROV can be found in Le, Nguyen and Ranmuthugala (2013) .

Table 2A. 1: AMC ROV hydrodynamic coefficients

Parameter	Value	Parameter	Value	Parameter	Value	Parameter	Value
m (Kg)	19.9	$X_{\dot{u}}$ (Kg)	-8.65	X_u (Kgs^{-1})	-0.69	$X_{u\|u\|}$ (Kgm^{-1})	-32.30
I_x (Kgm^2)	0.297	$Y_{\dot{v}}$ (Kg)	-12.23	Y_v (Kgs^{-1})	-0.54	$Y_{v\|v\|}$ (Kgm$^{-1)}$	-96.13
I_y (Kgm$^{2)}$	1.304	$Z_{\dot{w}}$ (Kg)	-15.78	Z_w (Kgs^{-1})	-0.65	$Z_{w\|w\|}$ (Kgm$^{-1)}$	-115.37
I_z (Kgm^2)	1.410	$K_{\dot{p}}$ (Kgm^2)	-0.63	K_p (Kgms$^{-1)}$	-0.19	$K_{p\|p\|}$ (Kgm)	-15.70
d_2 (m)	0.18	$M_{\dot{q}}$ (Kgm^2)	-0.78	M_q (Kgms$^{-1)}$	-0.27	$M_{q\|q\|}$ (Kgm)	-21.25
$F_W - F_B$ (N)	-2	$N_{\dot{r}}$ (Kgm^2)	-0.56	N_r (Kgms$^{-1)}$	-0.23	$N_{r\|r\|}$ (Kgm)	-17.23

2A.4 Model Reference Adaptive Control

As described by Lavretsky (2009) nonlinear uncertain dynamic system can be expressed as,

$$\dot{\boldsymbol{x}}(t) = \boldsymbol{A}\boldsymbol{x}(t) + \boldsymbol{H}\boldsymbol{\Lambda}\left[\boldsymbol{u}(t) + \boldsymbol{\delta}(\boldsymbol{x})\right], \;\; \boldsymbol{x}(0) = \boldsymbol{x}_0, \; t = \bar{\mathbb{R}}_+ \tag{2A.14}$$

where $\boldsymbol{x}(t) \in \mathbb{R}^p$ is the state vector available for feedback, $\boldsymbol{u}(t) \in \mathbb{R}^q$ is the control input vector, $\boldsymbol{\delta}(\boldsymbol{x}) : \mathbb{R}^p \to \mathbb{R}^q$ is the system matched uncertainty, $\boldsymbol{A} \in \mathbb{R}^{p \times p}$ is the constant unknown system matrix, $\boldsymbol{H} \in \mathbb{R}^{p \times q}$ is the constant known control input matrix, and $\boldsymbol{\Lambda} \in \mathbb{R}^{q \times q}$ is a unknown diagonal control effectiveness matrix with positive diagonal elements. It is assumed that the uncertainty vector in (2A.14) is parameterized as $\boldsymbol{\delta}(\boldsymbol{x}) = \boldsymbol{W}^T \boldsymbol{\sigma}(\boldsymbol{x}), \; \boldsymbol{x} \in \mathbb{R}^p$, where $\boldsymbol{W} \in \mathbb{R}^{s \times q}$ is an unknown weight matrix and $\boldsymbol{\sigma} : \mathbb{R}^p \to \mathbb{R}^s$ is a known regression vector of the form $\boldsymbol{\sigma}(\boldsymbol{x}) = \left[\sigma_1(x), \sigma_2(x), \ldots, \sigma_s(x)\right]^T$.

The ideal reference model that specifies a desired closed loop dynamic system is given by:

$$\dot{\boldsymbol{x}}_m(t) = \boldsymbol{A}_m \boldsymbol{x}_m(t) + \boldsymbol{B}_m \boldsymbol{c}(t), \;\; \boldsymbol{x}_m(0) = \boldsymbol{x}_0 \;, \; t = \bar{\mathbb{R}}_+ \tag{2A.15}$$

where $\boldsymbol{x}_m(t) \in \mathbb{R}^p$ is the reference state vector, $\boldsymbol{c}(t) \in \mathbb{R}^q$ is the given uniformly continuous bounded command, $\boldsymbol{A}_m \in \mathbb{R}^{p \times p}$ is a Hurwitz reference system matrix, and $\boldsymbol{B}_m \in \mathbb{R}^{p \times q}$ is the command input matrix.

2A.4.1 Standard Model Reference Adaptive Control (MRAC)

The objective of adaptive control is to design a feedback control law ($\boldsymbol{u}(t)$) such that the state vector ($\boldsymbol{x}(t)$) asymptotically follows the reference state vector ($\boldsymbol{x}_m(t)$), with the above assumptions. If $\boldsymbol{A}$ and $\boldsymbol{\Lambda}$ are known, then $\boldsymbol{u}(t)$ can be an ideal fixed gain control law expressed as,

$$\boldsymbol{u}(t) = \boldsymbol{K}_x^T \boldsymbol{x} + \boldsymbol{K}_c^T \boldsymbol{c} - \boldsymbol{W}^T \boldsymbol{\sigma}(\boldsymbol{x}) \tag{2A.16}$$

where $\boldsymbol{K}_x \in \mathbb{R}^{p \times q}$ is the ideal feedback gain and $\boldsymbol{K}_c \in \mathbb{R}^{q \times q}$ is the ideal feed forward gain that satisfies the matching condition given by:

$$\boldsymbol{A}_m = \boldsymbol{A} + \boldsymbol{H}\boldsymbol{\Lambda}\boldsymbol{K}_x^T, \boldsymbol{B}_m = \boldsymbol{H}\boldsymbol{\Lambda}\boldsymbol{K}_c^T \tag{2A.17}$$

Assuming that (2A.17) holds, it can be easily seen that the closed loop system is exactly the same as the reference model. Therefore, for any bounded command input ($\boldsymbol{c}(t)$), (2A.16) provides a globally asymptotic tracking performance. When $\boldsymbol{A}$ and $\boldsymbol{\Lambda}$ are unknown the previously mentioned ideal gains $\boldsymbol{K}_x$, $\boldsymbol{K}_c$ and $\boldsymbol{W}$ cannot be chosen. Nevertheless, by assuming that such ideal gains exist, the adaptive control law is expressed as:

$$\boldsymbol{u}(t) = \hat{\boldsymbol{K}}_x^T \boldsymbol{x} + \hat{\boldsymbol{K}}_c^T \boldsymbol{c} - \hat{\boldsymbol{W}}^T \boldsymbol{\sigma}(\boldsymbol{x}) \tag{2A.18}$$

where $\hat{\boldsymbol{K}}_x \in \mathbb{R}^{p \times q}$, $\hat{\boldsymbol{K}}_c \in \mathbb{R}^{q \times q}$ and $\hat{\boldsymbol{W}} \in \mathbb{R}^{s \times q}$ are the estimates of the ideal unknown matrices $\boldsymbol{K}_x^T$, $\boldsymbol{K}_c^T$ and $\boldsymbol{W}$ respectively.

From the Lyapunov analysis (Ioannou & Fidan 2006; Narendra & Annaswamy 2005) it can be shown that the system is asymptotically stable, i.e. $\lim_{t\to\infty}\|\boldsymbol{e}_m\|=0$, if the update laws are given as,

$$\begin{aligned}\dot{\hat{\boldsymbol{K}}}_x &= -\boldsymbol{\Gamma}_x \boldsymbol{x}(t)\boldsymbol{e}_m^T\boldsymbol{P}\boldsymbol{H}\\ \dot{\hat{\boldsymbol{K}}}_c &= -\boldsymbol{\Gamma}_c \boldsymbol{c}(t)\boldsymbol{e}_m^T\boldsymbol{P}\boldsymbol{H}\\ \dot{\hat{\boldsymbol{W}}}_\sigma &= \boldsymbol{\Gamma}_\sigma \boldsymbol{\sigma}(\boldsymbol{x})\boldsymbol{e}_m^T\boldsymbol{P}\boldsymbol{H}\end{aligned} \tag{2A.19}$$

where $\boldsymbol{\Gamma}_x=\boldsymbol{\Gamma}_x^T>0$, $\boldsymbol{\Gamma}_c=\boldsymbol{\Gamma}_c^T>0$ and $\boldsymbol{\Gamma}_\sigma=\boldsymbol{\Gamma}_\sigma^T>0$ are learning rates , $\boldsymbol{e}_m=\boldsymbol{x}-\boldsymbol{x}_m$ is the tracking error, and $\boldsymbol{P}=\boldsymbol{P}^T>0$ is the solution of the algebraic Lyapunov equation $\boldsymbol{0}=\boldsymbol{A}_m{}^T\boldsymbol{P}+\boldsymbol{P}\boldsymbol{A}_m+\boldsymbol{Q}$, where $\boldsymbol{Q}=\boldsymbol{Q}^T>0$. A block diagram of the MRAC control architecture is given in Fig 2A.2.

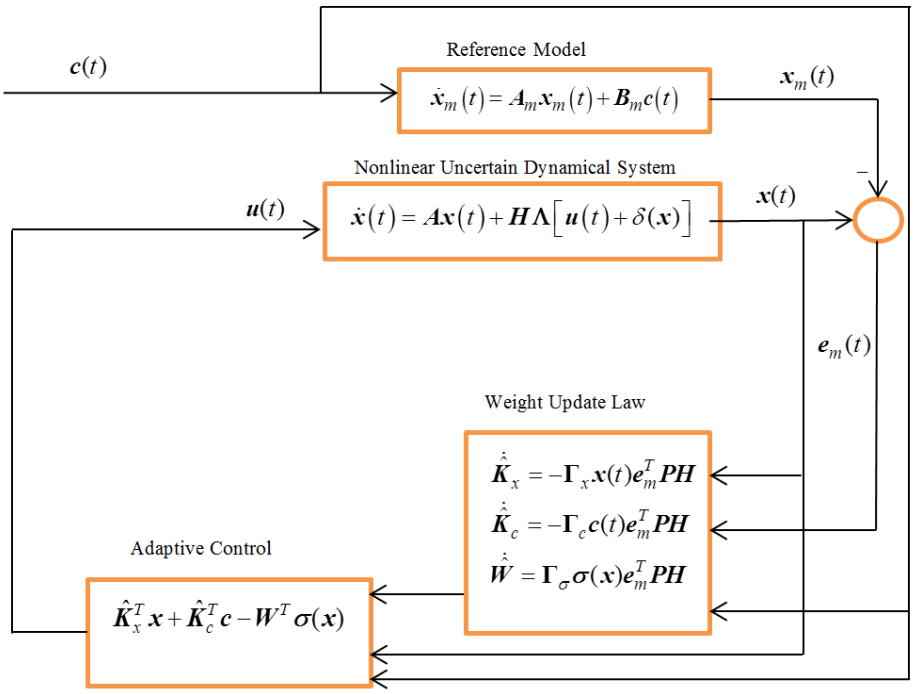

Figure 2A. 2: Standard MRAC control architecture

2A.4.2 Composite Model Reference Adaptive Control (CMRAC)

In the MRAC described earlier, the error between system states and the reference model is used to adjust the parameters. An indirect adaptive component can be added to that by using a prediction error, i.e. the difference between some quantity and its prediction. To

do this it is necessary to generate a suitable prediction error. According to Lavretsky (2009), the quantity used for the prediction ($\boldsymbol{Y}(t)$) is written as:

$$\boldsymbol{Y}(t)=\left(\boldsymbol{H}^T\boldsymbol{H}\right)^{-1}\boldsymbol{H}^T\left(\lambda_f\left(\boldsymbol{x}-\boldsymbol{x}_f\right)-\boldsymbol{A}_m\boldsymbol{x}_f-\boldsymbol{B}_m\boldsymbol{c}_f\right)=\boldsymbol{\Lambda}\left(\boldsymbol{u}_f+\boldsymbol{W}^T\boldsymbol{\sigma}_f\right) \quad (2A.20)$$

where $\boldsymbol{x}_f,\boldsymbol{c}_f,\boldsymbol{\sigma}_f$ and $\boldsymbol{u}_f$ are the filtered versions of $\boldsymbol{x},\boldsymbol{c},\boldsymbol{\sigma}$ and $\boldsymbol{u}$. The filter is a stable first-order filter with the transfer function $G(s)=\frac{\lambda_f}{s+\lambda_f}$, where $\lambda_f>0$ is the filter inverse constant. This expression for $\boldsymbol{Y}(t)$ has the advantage that it can be calculated at any time (t) using the state ($\boldsymbol{x}(t)$), filter state ($\boldsymbol{x}_f(t)$) , and filtered command ($\boldsymbol{c}_f(t)$) without using the state derivative ($\dot{\boldsymbol{x}}(t)$), which would be required if filtering is not used.

It is now possible to estimate $\boldsymbol{Y}(t)$ by using the bilinear predictor model as:

$$\hat{\boldsymbol{Y}}(t)=\hat{\boldsymbol{\Lambda}}\left(\boldsymbol{u}_f+\hat{\boldsymbol{W}}^T\boldsymbol{\sigma}_f\right) \quad (2A.21)$$

which is an estimate of the incalculable signal $\boldsymbol{\Lambda}\left(\boldsymbol{u}_f+\boldsymbol{W}^T\boldsymbol{\sigma}_f\right)$, where $\hat{\boldsymbol{\Lambda}}$ is the estimate of $\boldsymbol{\Lambda}$. The prediction error for CMRAC is defined as $\boldsymbol{e}_Y=\hat{\boldsymbol{Y}}(t)-\boldsymbol{Y}(t)$. It can be shown by the Lyapunov analysis that if the update laws are given as shown in (2A.22), then the tracking error and prediction error are globally asymptotically stable, i.e. $\lim_{t\to\infty}\|\boldsymbol{e}_m\|=0$, $\lim_{t\to\infty}\|\boldsymbol{e}_Y\|=0$.

$$\begin{aligned}
\dot{\hat{\boldsymbol{K}}}_x&=-\boldsymbol{\Gamma}_x\left(\boldsymbol{x}\boldsymbol{e}_m^T\boldsymbol{P}\boldsymbol{H}-\boldsymbol{x}_f\gamma_c\boldsymbol{e}_Y^T\right)\\
\dot{\hat{\boldsymbol{K}}}_r&=-\boldsymbol{\Gamma}_c\left(\boldsymbol{c}\boldsymbol{e}_m^T\boldsymbol{P}\boldsymbol{H}-\boldsymbol{c}_f\gamma_c\boldsymbol{e}_Y^T\right)\\
\dot{\hat{\boldsymbol{W}}}&=\boldsymbol{\Gamma}_\sigma\left(\boldsymbol{\sigma}\boldsymbol{e}_m^T\boldsymbol{P}\boldsymbol{H}-\boldsymbol{\sigma}_f\gamma_c\boldsymbol{e}_Y^T\right)\\
\dot{\hat{\boldsymbol{\Lambda}}}^T&=-\boldsymbol{\Gamma}_\Lambda\left(\boldsymbol{u}_f-\hat{\boldsymbol{K}}_x^T\boldsymbol{x}-\hat{\boldsymbol{K}}_c^T\boldsymbol{c}_f+\hat{\boldsymbol{W}}^T\boldsymbol{\sigma}_f\right)\gamma_c\boldsymbol{e}_Y^T
\end{aligned} \quad (2A.22)$$

where $\Gamma_x = \Gamma_x^T > 0, \Gamma_c = \Gamma_c^T > 0$, $\Gamma_\Lambda = \Gamma_\Lambda^T > 0$ and $\Gamma_\sigma = \Gamma_\sigma^T > 0$ are learning rates and $P = P^T > 0$ is the unique solution of the algebraic Lyapunov equation $0 = A_m{}^T P + P A_m + Q$ where $Q = Q^T > 0$. A block diagram of the CMRAC control architecture is shown in Fig 2A.3.

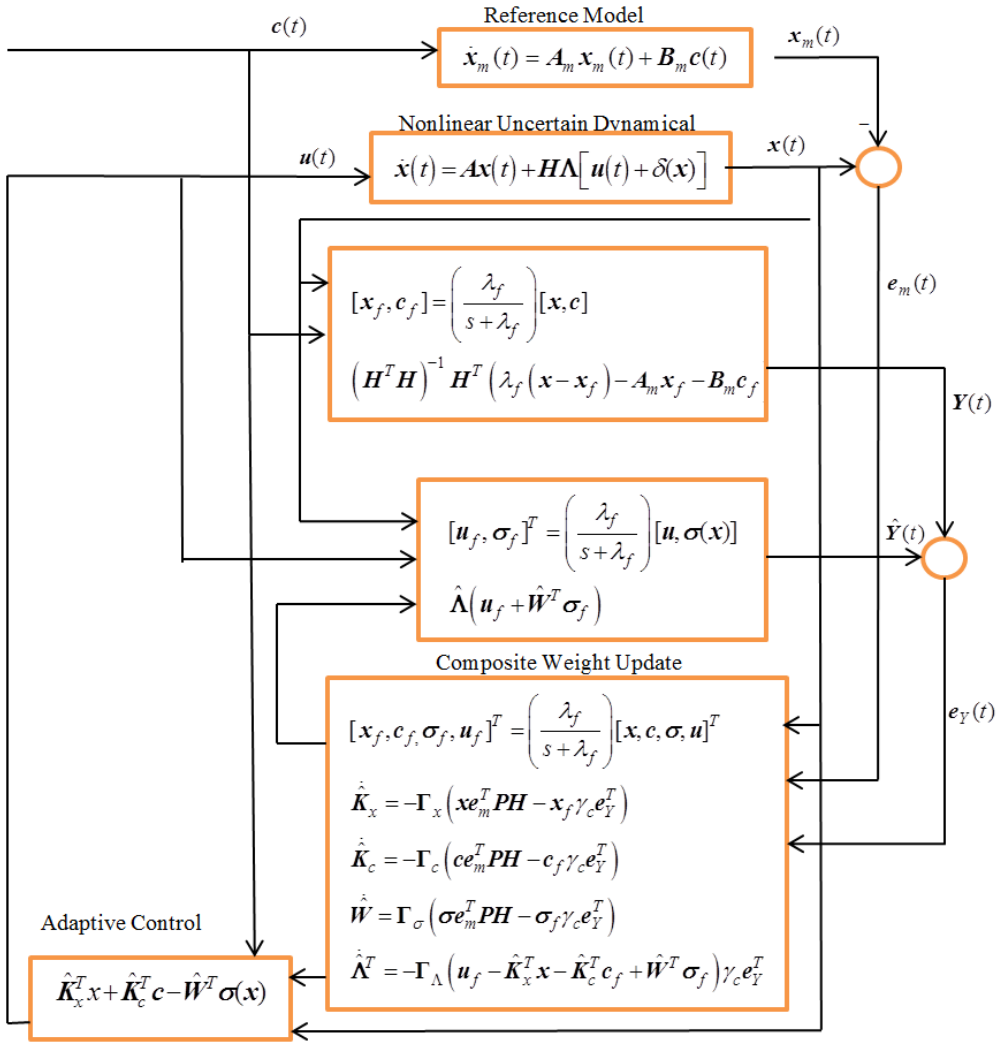

Figure 2A. 3: CMRAC control architecture

2A.4.3 Control Model of the AMC ROV

While the full nonlinear kinematics in (2A.1-2A.6) and dynamics in (2A.8) developed in section 2A.2.2 are used to simulate the motion of the actual ROV, they cannot be used as a base for control design due to limitations in the sensors and actuators on the actual vehicle. The three-thruster configuration allows control of only surge, yaw, and depth, but sway, roll, and pitch remain uncontrolled.

The vehicle is designed to minimise roll and pitch moments, thus supporting the assumption that the pitch and roll DOFs remain stable, which is important for an under-actuated vehicle. This assumption also makes the control design easier, enabling a simpler model, i.e. the control model, to be developed for the purpose of controller design. This model takes the form of (2A.14) in order to apply the previously defined MRAC method. In the control model, the following assumptions are made:

a) uncontrolled DOFs of pitch angle (θ) and roll angle (ϕ) are assumed to be negligible; and
b) the Coriolis forces are assumed to be negligible.

From assumption a) the kinematics in (2A.3) and (2A.6) becomes decoupled. From assumption b) the 6-DOF dynamics in equation (2A.8) also becomes decoupled. This enables each DOF to be considered separately as a second order system. Even though this model is not theoretically justified, it has been successfully implemented with reasonable accuracy in many practical control designs (Smallwood & Whitcomb 2004).

While controllers were built for all three controllable DOFs the surge was not studied due to lack of speed sensor that would make any future experimental verification difficult. With these assumptions, the heading and depth decoupled control models are expressed as,

$$\dot{\psi} = r \tag{2A.23}$$

$$m_r \dot{r} = N_r r + N_{r|r|} r|r| + \tau_r \tag{2A.24}$$

where $m_r = I_z - N_{\dot{r}}$ Dividing by m_r gives,

$$\dot{r} = \left(\frac{N_r}{m_r}\right) r + \left(\frac{N_{r|r|}}{m_r}\right) r|r| + \left(\frac{1}{m_r}\right) \tau_r \tag{2A.25}$$

This can be rearranged to give,

$$\dot{r} = \theta_1 r + \theta_2 \left(\tau_r + \theta_3 r|r|\right) \tag{2A.26}$$

where $\theta_1 = \left(\frac{N_r}{m_r}\right), \theta_2 = \left(\frac{1}{m_r}\right), \theta_3 = N_{r|r|}$.

From equations 2A.23 and 2A.26, the state space form is obtained as:

$$\begin{pmatrix} \dot{\psi} \\ \dot{r} \end{pmatrix} = \begin{pmatrix} 0 & 1 \\ 0 & \theta_1 \end{pmatrix} \begin{pmatrix} \psi \\ r \end{pmatrix} + \begin{pmatrix} 0 \\ 1 \end{pmatrix} \theta_2 \left(\tau_r + \theta_3 r|r| \right) \tag{2A.27}$$

Similarly, the depth of the vehicle is given by:

$$\dot{d} = w \tag{2A.28}$$

$$\dot{w} = \theta_1 w + \theta_2 \left(\tau_w + \theta_3 w|w| + \theta_4 \right) \tag{2A.29}$$

where $\theta_1 = \left(\frac{Z_w}{m_w} \right), \theta_2 = \left(\frac{1}{m_w} \right), \theta_3 = Z_{w|w|}, \theta_4 \approx F_W - F_B, m_w = m - Z_{\dot{w}}$.

Equations 2A.28 and 2A.29 are written in the matrix form as:

$$\begin{pmatrix} \dot{d} \\ \dot{w} \end{pmatrix} = \begin{pmatrix} 0 & 1 \\ 0 & \theta_1 \end{pmatrix} \begin{pmatrix} d \\ w \end{pmatrix} + \begin{pmatrix} 0 \\ 1 \end{pmatrix} \theta_2 \left[\tau_w + \theta_3 w|w| + \theta_4 \right] \tag{2A.30}$$

It is noted that both subsystems represented by equations 2A.27 and 2A.30 have the general state space form of (2A.14), where $\boldsymbol{x} = \begin{pmatrix} x_1 \\ x_2 \end{pmatrix} = \begin{pmatrix} \psi \\ r \end{pmatrix} or \begin{pmatrix} d \\ w \end{pmatrix}, \boldsymbol{A} = \begin{pmatrix} 0 & 1 \\ 0 & \theta_1 \end{pmatrix}, \boldsymbol{H} = \begin{pmatrix} 0 \\ 1 \end{pmatrix}$, $\Lambda = \theta_2, f\left(\boldsymbol{x}\right) = \theta_3 x_2 \left| x_2 \right| + \theta_4,$, and $u = \tau_r \, or \, \tau_w$.

2A.4.4 Reference Model

In order to derive the direct control reference for both the MRAC and CMRAC techniques, an ideal reference model is required. As the control model (see 2A.27 and 2A.30) is of 2nd order, the reference model should also be of the same order for both heading and depth control. Taking $x_1 = \psi or \, d$ and $x_2 = r \, or \, w$ depending on the subsystem, a standard 2nd order transfer function with desired natural frequency (ω_n) and damping ratio (ζ) can be written as:

$$\frac{x_1(s)}{x_{1_{cmd}}(s)} = \frac{\omega_n^2}{s^2 + 2\zeta\omega_n s + \omega_n^2} \tag{2A.31}$$

Converting equation 2A.31 into a state space form gives:

$$\begin{pmatrix} \dot{x}_{1_{ref}} \\ \dot{x}_{2_{ref}} \end{pmatrix} = \begin{pmatrix} 0 & 1 \\ -\omega_n{}^2 & -2\zeta\omega_n \end{pmatrix} \begin{pmatrix} x_1 \\ x_2 \end{pmatrix} + \begin{pmatrix} 0 \\ \omega_n{}^2 \end{pmatrix} x_{1_{cmd}} \tag{2A.32}$$

Applying the matching condition in equation 2A.17 yields:

$$\begin{pmatrix} 0 & 1 \\ -\omega_n{}^2 & -2\zeta\omega_n \end{pmatrix} = \begin{pmatrix} 0 & 1 \\ 0 & \theta_1 \end{pmatrix} + \begin{pmatrix} 0 \\ 1 \end{pmatrix} \theta_2 \begin{pmatrix} k_{x1} & k_{x2} \end{pmatrix} \Rightarrow k_{x1} = \frac{-\omega_n{}^2}{\theta_2}, k_{x2} = \frac{-2\zeta\omega_n - \theta_1}{\theta_2}$$

$$\begin{pmatrix} 0 \\ \omega_n{}^2 \end{pmatrix} = \begin{pmatrix} 0 \\ 1 \end{pmatrix} \theta_2 \begin{pmatrix} k_c \end{pmatrix}, \Rightarrow k_c = \frac{\omega_n{}^2}{\theta_2} \tag{2A.33}$$

Therefore, the ideal feedback gain and feed forward gain can be written as,

$$\boldsymbol{K}_x = \begin{bmatrix} \dfrac{-\omega_n{}^2}{\theta_2} \\ \dfrac{-2\zeta\omega_n - \theta_1}{\theta_2} \end{bmatrix} \text{ and } \boldsymbol{K}_c = \frac{\omega_n{}^2}{\theta_2} \tag{2A.34}$$

2A.5 Simulation Results

The control model of AMC ROV was implemented in the MATLAB/Simulink simulation platform and its behaviour incorporating the MRAC and CMRAC controllers were observed under the following operating scenarios.

2A.5.1 Simulation Scenarios

2A.5.1.1 Initial Operations

In this mode of operation, the standard MRAC and CMRAC control methods are simulated for 400s at the start of a mission. This represents the situation of the initial operation either at the very beginning of a mission or after a task or parameter variation. The objective of this operation is to compare the tracking performance of the two methods for changes in heading and depth at two different forward velocities. The reference model is selected with an approximate rise time of $t_r = 10\,\text{s}$, settling time of $t_s = 20\,\text{s}$, and peak overshoot of $PO = 0\%$. This corresponds to a $\omega_n = 0.3$ rad/s and $\zeta = 1$ for both depth and heading. Furthermore, there is a positive buoyancy of

approximately 2N. This in turn gives the ideal gains for the controllers from Table 2A.1 and equation 2A.34, as shown in Table 2A.2.

Table 2A. 2: Ideal parameters of heading and depth controllers (assuming that all the unknowns are known)

Ideal Parameters	Heading Controller	Depth Controller
K_{x1}	-0.1773	-3.2112
K_{x2}	-0.9518	-20.7580
K_c	0.1773	3.2112
θ_3	-17.23	-115.37
θ_4	N/A	-1.99

2A.5.1.2 External Disturbances

The two control methods were tested under an external disturbance of 10N on the vehicle from top along the Z_b axis against a positive buoyancy of 2N for 1.5m constant depth control. The disturbance was applied after 800s and held for 1s. In order to give sufficient time for the MRAC tracking error to become practically indistinguishable from the CMRAC tracking error, a 800s learning period was applied before introducing the external disturbance. The objective was to see how well the controllers could reject the external disturbance.

2A.5.1.3 Thruster Failure

A vertical thruster failure of 80% was simulated after 800s. This was done with the vehicle holding depth against a positive buoyancy of 2N. The vertical thruster can normally produce close to 20N of thrust, but in the failure case it will reduce close to 4N. This type of failure can occur due to an electrical failure or a snared propeller.

The aim of these tests was to show that the adaptive controllers are able to overcome such disturbance and failures, and to compare the performance of the two control methods in such situations.

2A.5.2 Results of Simulation

The performance of the UUV was measured using six performance indices each for heading and depth given in Table 2A.3; the first four are based on tracking error

$\boldsymbol{e}_m^T = \begin{bmatrix} e_\psi & e_r \end{bmatrix}$ for heading and $\boldsymbol{e}_m{}^T = \begin{bmatrix} e_d & e_w \end{bmatrix}$ for depth while the last two are based on control effort $\tilde{\tau}_r$ for heading and $\tilde{\tau}_w$ for depth. These performance indices were designed based on the work presented in Fossen and Fjellstad (1996).

Table 2A. 3: Performance indices used for quantitative representation of the results.

Description	Equation	Description	Equation
rms heading error	$\psi_{e\_rms} = \sqrt{\frac{1}{N}\sum_{i=1}^{N}\left(e_\psi\right)^2}$	rms depth error	$d_{e\_rms} = \sqrt{\frac{1}{N}\sum_{i=1}^{N}\left(e_d\right)^2}$
rms heading rate error	$r_{e\_rms} = \sqrt{\frac{1}{N}\sum_{i=1}^{N}\left(e_r\right)^2}$	rms depth rate error	$w_{e\_rms} = \sqrt{\frac{1}{N}\sum_{i=1}^{N}\left(e_w\right)^2}$
maximum heading error	$\psi_{e\_\max} = \max(\lvert e_\psi \rvert)$	maximum depth error	$d_{e\_\max} = \max(\lvert e_d \rvert)$
maximum heading rate error	$r_{e\_\max} = \max(\lvert e_r \rvert)$	maximum depth rate error	$w_{e\_\max} = \max(\lvert e_w \rvert)$
rms normalized control effort	$\tilde{\tau}_{r\_rms} = \sqrt{\frac{1}{N}\sum_{i=1}^{N}\left(\tau_r\right)^2}$	rms normalized control effort	$\tilde{\tau}_{w\_rms} = \sqrt{\frac{1}{N}\sum_{i=1}^{N}\left(\tau_w\right)^2}$
maximum normalized control effort	$\tilde{\tau}_{r\_\max} = \max(\lvert \tau_r \rvert)$	maximum normalized control effort	$\tilde{\tau}_{w\_\max} = \max(\lvert \tau_w \rvert)$

2A.5.2.1 Initial Operations

The first task in implementing CMRAC for the ROV was to set the unique parameters. These are the CMRAC gain γ_c and filter constant λ_f. After several trials, it was observed that simply increasing these gains does not always give better performance, thus, it was important to select the values that gave the overall best performance. This was achieved through an iterative process giving suitable values for γ_c and λ_f as 4 and 10 respectively.

Table 2A.4 gives the parameter estimates for the ideal gains in Table 2A.2. It is seen from Tables 2A.2 and 2A.4 that not all parameters converge to the actual value. This is expected as parameter convergence requires persistent excitation while, the simulation used a simple command signal of 400 s. A better way to compare the performance under

initial operation is to look at the tracking error for the MRAC and CMRAC methods given in Table 2A.5.

Table 2A. 4: Comparison of MRAC and CMRAC heading and depth parameter estimates for a learning rate of 100 at u= 0 m/s

Parameter Estimates	Heading Control		Depth Control	
	MRAC	**CMRAC**	**MRAC**	**CMRAC**
$\hat{K}_{x1}$	-0.12908	-0.13986	-3.92363	-2.76506
$\hat{K}_{x2}$	-0.10034	-0.0162	-4.79137	-0.50745
$\hat{K}_c$	0.128897	0.139862	1.807527	0.877888
$\hat{\theta}_3$	0.003453	0.000358	0.185291	0.06049
$\hat{\theta}_4$	N/A	N/A	-1.97112	-1.98634

Table 2A. 5: Comparison of MRAC and CMRAC heading and depth tracking errors at different learning rates at u=0m/s

Tracking Errors	Learning rate of 1		Learning rate of 10		Learning rate of 100	
	MRAC	**CMRAC**	**MRAC**	**CMRAC**	**MRAC**	**CMRAC**
ψ_{e_rms} (deg)	0.836543	0.259213	0.114131	0.00673	0.012856	0.000175
r_{e_rms} (deg/s)	0.220118	0.023329	0.079061	0.002144	0.029858	0.000243
$\psi_{e\_\max}$ (deg)	4.973075	3.348591	1.24143	0.665549	0.212608	0.08163
d_{e_rms} (m)	0.0705	0.003212	0.010007	0.000087	0.001062	0.000002
w_{e_rms} (m/s)	0.022432	0.000277	0.008428	0.00005	0.002943	0.00001
$d_{e\_\max}$ (m)	0.477399	0.415807	0.083731	0.074056	0.009695	0.008283

From Table 2A.5, it is clear that CMRAC is much better at reducing the tracking error in contrast to MRAC. The reduction in heading tracking error for CMRAC versus MRAC at learning rate 1 is 69% (factor of 3) and the reduction in depth tracking error is 95% (factor of 22). When the gain is increased 10 fold, both tracking errors of MRAC reduced by 87% (factor of 7) while both tracking errors for CMRAC reduced by 97% (factor of 38).

Table 2A.6 shows that when the speed is increased, the tracking errors significantly increase; this is due to the simulated Coriolis forces. When speed is increased to 0.4

m/s, the MRAC error is increased by a factor of 28, while CMRAC error is increased by factor of 392 for heading and 476 for depth. However, the heading error of CMRAC is still less than the MRAC by a factor of 5 and the depth error was less by a factor of 31.

To compare the performance further, the speed was increased to 1 m/s which is the theoretically maximum speed for this vehicle. The errors were further increased by factors of 3 and 16 for MRAC and factors 5 and 23 for CMRAC. However, CMRAC still had errors less than MRAC by factors of 3 and 2 for heading and depth respectively. While the degradation in heading error is skewed due to a large error initially, the underactuation prevents recovery of pitch change. This is because of the Munk moment that violates the negligibility of the pitch angle, leading to a larger error in depth. It is clear for a high speed UUV, the Coriolis effects cannot be neglected in the control model. It would also be interesting to see in experimental trials if the unmodelled coupled damping terms will have a stabilizing effect that counteracts the destabilizing moment.

Table 2A. 6: Comparison of MRAC and CMRAC heading and depth tracking error at learning rate 100 and u= 0.4 m/s and 1.0 m/s

Tracking error	**U=0.4 m/s**		**U=1.0 m/s**	
	MRAC	**CMRAC**	**MRAC**	**CMRAC**
ψ_{e_rms} (deg)	0.364533	0.068744	1.119117	0.348575
r_{e_rms} (deg/s)	0.120072	0.010769	0.432113	0.047405
$\psi_{e\_\max}$ (deg)	2.810244	2.210998	6.362412	5.233558
d_{e_rms} (m)	0.029654	0.000953	0.453423	0.221136
w_{e_rms} (m/s)	0.008001	0.000032	0.062124	0.006830
$d_{e\_\max}$ (m)	0.139869	0.140079	1.174144	1.176519

Table 2A.7 looks at the control input for depth and heading, where another possible advantage of the CMRAC method is evident. This method always has a reduced maximum signal compared to MRAC, which could be important in conditions where the vehicle is operating near actuator saturation limits. That advantage increase with the learning rate, thus at learning rate of 1 the reduction is only 3.5% but at a learning rate of 100 the reduction is 14%. Another advantage is that the high frequency content in the

control signal of CMRAC is less compared to that of MRAC. However, Table 2A.6 also provides a possible disadvantage of the CMRAC method, especially if the UUV is autonomous. It shows that the root mean square (RMS) value of the CMRAC control signal is greater than MRAC at higher learning rates. This results in an overall increase in power consumption. For a learning rate of 100 this increase is 21%.

Table 2A. 7: Comparison of control input at different learning rates

Control Input	Learning rate 1		Learning rate 10		Learning rate 100	
	MRAC	**CMRAC**	**MRAC**	**CMRAC**	**MRAC**	**CMRAC**
τ_{r_rms} (Nm)	0.008432	0.008822	0.008350	0.013139	0.007844	0.017548
$\tau_{r\_\max}$ (Nm)	0.039357	0.040294	0.047701	0.051586	0.065525	0.061448
τ_{w_rms} (N)	2.162904	2.111423	2.168059	2.340919	2.149274	2.609471
$\tau_{w\_\max}$ (N)	6.680641	6.452177	9.239823	8.630128	11.679424	10.035248

An interesting point regarding the control signal is that all these comparisons are done at the same learning rate. However, as seen before, if the same tracking error is to be maintained by both controllers, the learning rate of MRAC has to be increased. Thus, assuming the tracking error of CMRAC at a learning rate of 10 is acceptable; an equivalent tracking error with MRAC corresponds to learning rates of 200 and 1000 for heading and depth.

2A.5.2.2 External Disturbances

Table 2A.8 shows that at a gain of 10 the maximum displacement of the vehicle is marginally better for the CMARC method but recovers faster from the disturbance compared to MRAC (see Fig. 2A.4). In addition, Fig. 2A.5 shows that the CMRAC method has less oscillatory control signal. This effect on the control signal becomes clearer when the gain is increased to 100, while the change in depth is negligible for both cases. The difference in control signals is more pronounced as shown in Fig. 2A.6. The recovery time for MRAC increases four-fold when learning rate is increased in contrast to CMRAC, where the recovery time decreases by a factor of 5.5.

Table 2A. 8: Comparison of depth controller response to an impact of 10 N

	Learning Rate=10		**Learning Rate=100**	
	MRAC	**CMRAC**	**MRAC**	**CMRAC**
Maximum depth change	0.075 m	0.073 m	0.01 m	0.01 m
Time to depth error to get below 0.01m	20 s	7 s	N/A	N/A
Maximum control signal value	16 N	15.6 N	17.7 N	17.2 N
Time for control signal to settle to final value	190 s	11 s	75 s	2 s

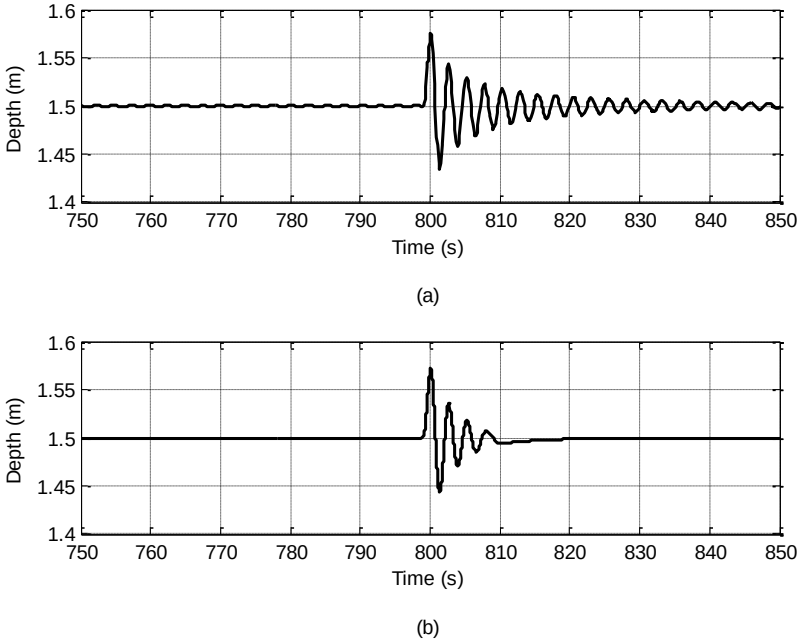

Figure 2A. 4: Depth change for 10N impact with learning rate=10 for (a) MRAC (b) CMRAC

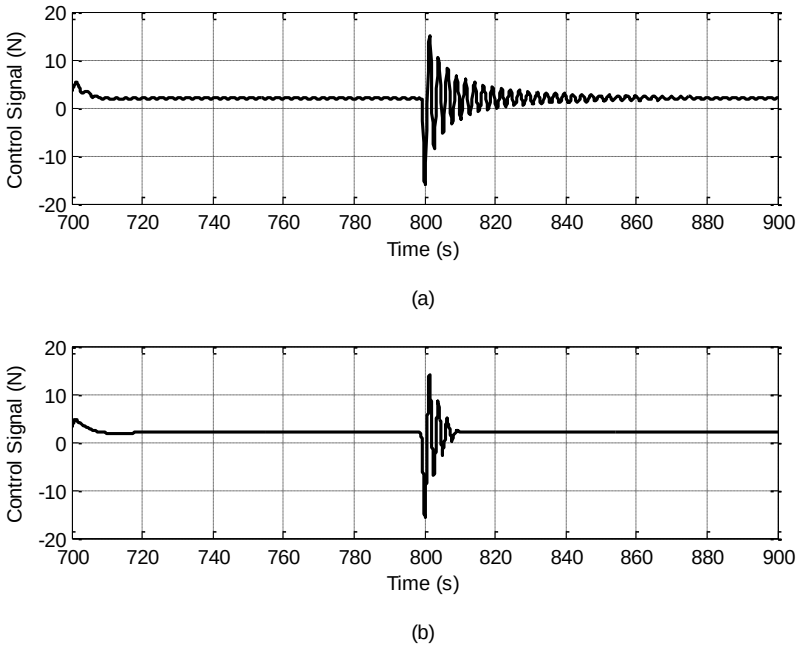

Figure 2A. 5: Control signal for 10N impact with learning rate=10 for (a) MRAC and (b) CMRAC

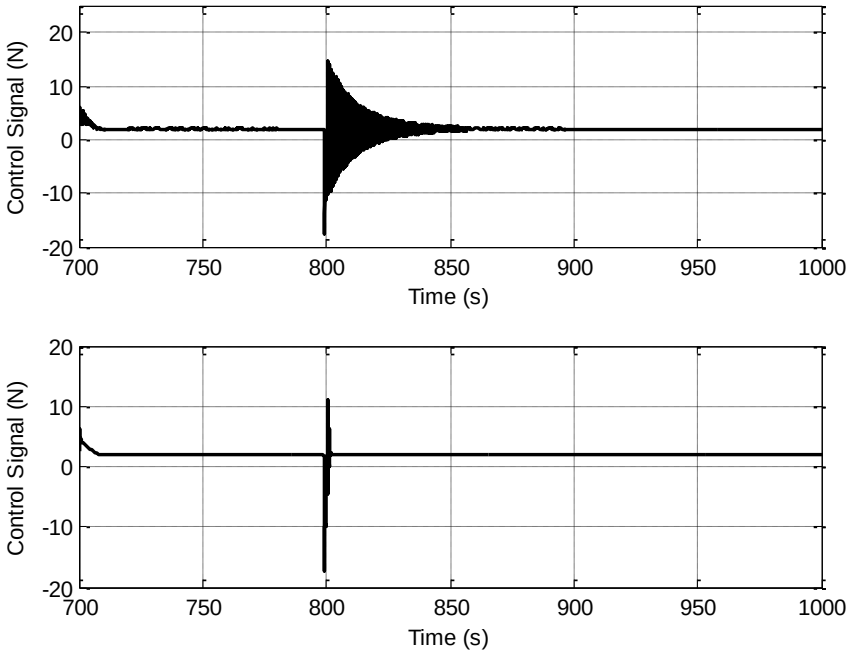

Figure 2A. 6: Control signal for 10N impact with learning rate=100 for (a) MRAC and (b) CMRAC

2A.5.2.3 Thruster Failure

The plots in Fig. 2A.7 show that the depth is quickly recovered by CMRAC, while MRAC tends to oscillate around the required depth after the thruster failure when learning rate is set to 10. The control signal also has a similar difference with long-term oscillations manifesting in MRAC, as seen in Fig. 2A.8. When learning rate is 100, the depth hardly varies for both methods with smaller oscillations for CMRAC when the thruster fails, as seen in Table 2A.9. These results prove suitability of both MRAC and CMRAC as the controller in UUVs and their ability to adapt to the changes in the system. The difference in the two methods is more evident in the control signal. Fig. 2A.9 shows that MRAC has much larger oscillations that last for a longer duration, while the CMRAC has small oscillations for a shorter duration. Therefore, overall the CMRAC method exhibits better performance than MRAC.

Table 2A. 9: Comparison of MRAC and CMRAC for 80% loss of thrust

	Gain=10		**Gain=100**	
	MRAC	**CMRAC**	**MRAC**	**CMRAC**
Maximum depth change	0.06 m	0.06 m	<0.01 m	<0.01 m
Time to depth error to get below 0.01m	large	22 s	N/A	N/A
Maximum control signal value	17.8 N	17.3 N	23.6 N	17.5 N
Time for control signal to settle to final value	large	28 s	large	5 s

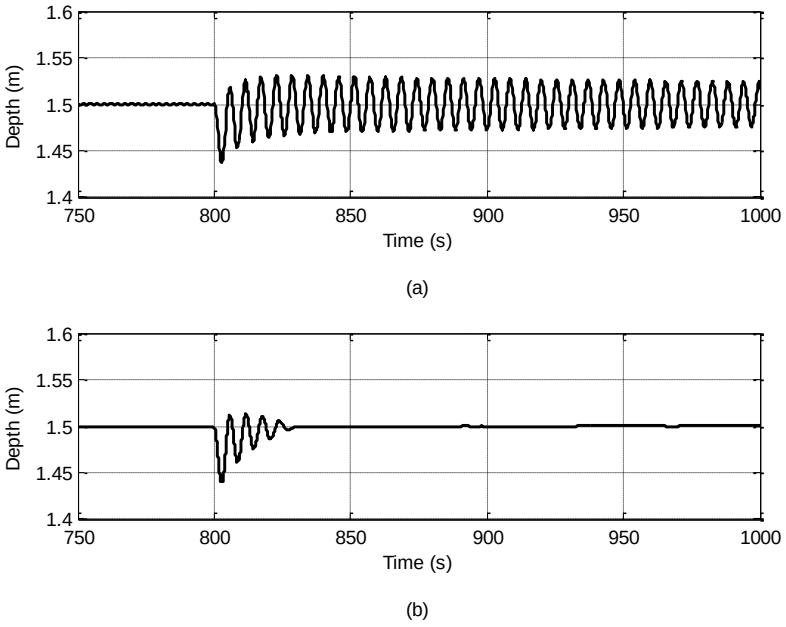

Figure 2A. 7: Depth change for 80% thrust loss with learning rate=10 for (a) MRAC and (b) CMRAC

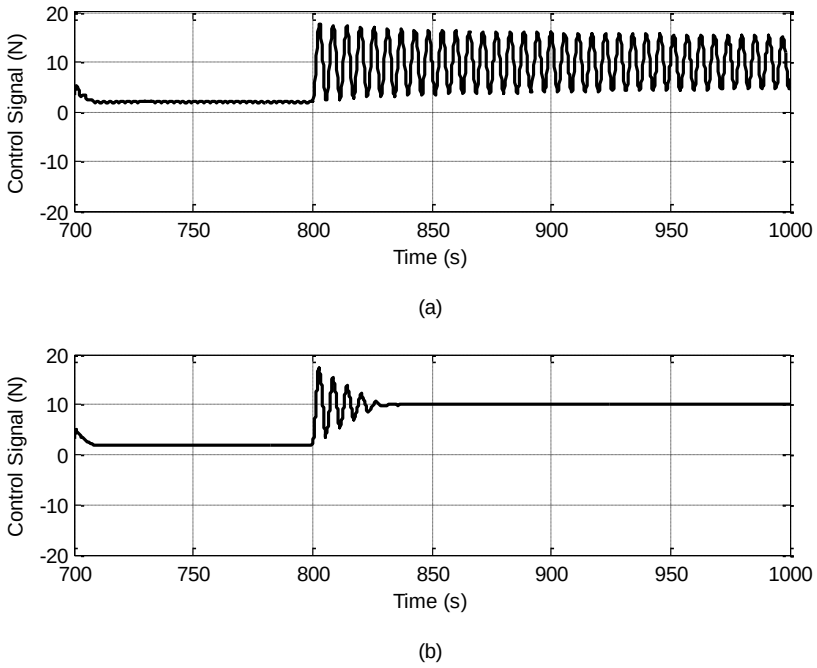

Figure 2A. 8: Control signal for 80% thrust lost with learning rate=10 for (a) MRAC and (b) CMRAC

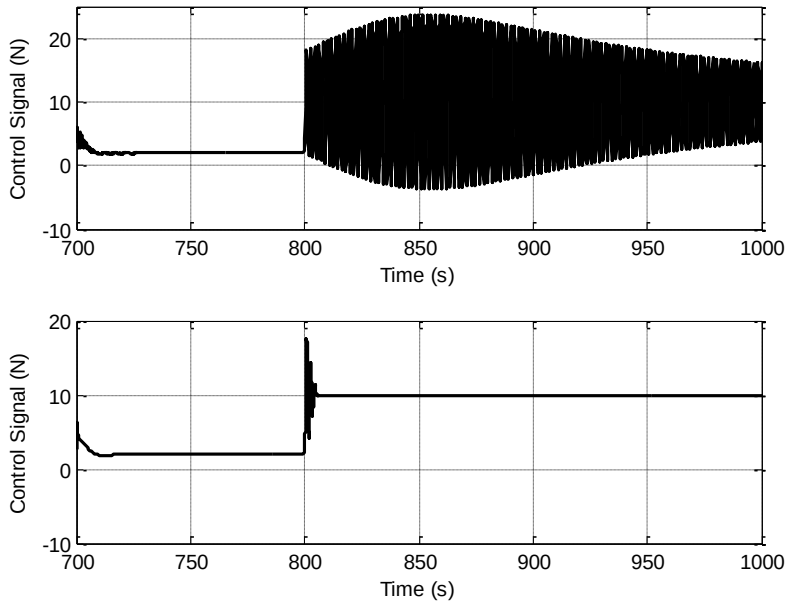

Figure 2A. 9: Control signal for 80% thrust lost with learning rate =100 for (a) MRAC and (b) CMRAC

2A.6 Conclusion

In this work, the suitability of CMRAC as a controller for an UUV and its performance against the standard MRAC were studied using numerical simulations. For the same

learning rate, the CMRAC method has shown better tracking performance compared to MRAC for heading and depth changes during a mission or after a task or parameter variation. In addition, as the learning rate is increased, the improvement in tracking error is higher with CMRAC, and the external disturbance rejection and recovery are better.

Furthermore, the control signal produced by CMRAC contains fewer oscillations compared to that of the standard MRAC. Even though both controllers are capable of overcoming thruster failures, CMRAC is more robust to such effects with fewer oscillations in both the output and control signals. Overall, it can be concluded that CMRAC with its additional predictive error is preferred over standard MRAC for the control of UUVs. Future work will concentrate on adding integral feedback and testing CMRAC experimentally.

Chapter 2:

Part B –

Predictor-Based Model Reference Adaptive Control for an Unmanned Underwater Vehicle

This subchapter has been published in the "*Proceedings of the 14th International Conference on Control, Automation, Robotics and Vision*". The citation for the research article is:

Makavita, CD and Nguyen, HD and Jayasinghe, SG and Ranmuthugala, D, Predictor-based model reference adaptive control of an unmanned underwater vehicle, *Proceedings of the 14th International Conference on Control, Automation, Robotics & Vision*, 13-15 November 2016, Phuket, Thailand, pp. 1-7. ISBN 978-1-5090-3549-6 (2016) [Refereed Conference Paper]

Chapter 2B has been removed for copyright or proprietary reasons.

Chapter 3:

Simulation & Verification of Command Governor-based Adaptive Control for an Unmanned Underwater Vehicle

This chapter consists of two subchapters:

Part A: Command Governor Adaptive Control for an Unmanned Underwater Vehicle.

Part B: Command Governor Adaptive Control for an Unmanned Underwater Vehicle with Measurement Noise and Actuator Dead-Zone.

This chapter continuous the simulation study by analysing a command governor based modification instead of the composite adaptation modifications used in chapter 2. In part A, CGAC performance is analysed by numerical simulation using a dynamic model of the UUV while part B extends on part A by focusing on measurement noise and actuator dead-zone effect on CGAC. The results provided the verification of the suitability of command governor method for UUV applications and formed the foundation for experimental validation in Chapter 5.

Chapter 3:

Part A –

Command Governor Adaptive Control for an Unmanned Underwater Vehicle

This subchapter has been published in the "*Proceedings of the 2015 IEEE Conference on Control Applications"*. The citation for the research article is:

Makavita, CD and Nguyen, HD and Ranmuthugala, D and Jayasinghe, SG, Command governor adaptive control for an unmanned underwater vehicle, *Proceedings of 2015 IEEE Conference on Control and Applications (CCA 2015)*, 21-23 September, Novotel Sydney Manly Pacific, pp. 1096-1102. ISBN 978-1-4799-7787-1 (2015) [Refereed Conference Paper]

Chapter 3A has been removed for copyright or proprietary reasons.

Chapter 3:

Part B –

Command Governor Adaptive Control for an Unmanned Underwater Vehicle with Measurement Noise and Actuator Dead-Zone

This subchapter has been published in the "*Proceedings of the 2016 Moratuwa Engineering Research Conference*". The citation for the research article is:

Makavita, CD and Nguyen, HD and Jayasinghe, SG and Ranmuthugala, D, Command Governor Adaptive Control for Unmanned Underwater Vehicles with Measurement Noise and Actuator Dead-Zone, *Proceedings of 2016 Moratuwa Engineering Research Conference (MERCon*), 5-6 April 2016, Moratuwa, Sri Lanka, pp. 384-379. ISBN 978-1-5090-0645-8 (2016) [Refereed Conference Paper]

Chapter 3B has been removed for copyright or proprietary reasons.

Chapter 4:

Experiments & Validation of Composite Model Reference Adaptive Controllers

This chapter has been submitted to the journal "*IEEE Journal of Oceanic Engineering"* and at the time of writing is under review. The citation for the research article is:

Makavita, C.D., Nguyen, H.D., Jayasinghe, S.G, & Ranmuthugala, D. 2017. 'Experimental Comparison of Two Composite MRAC methods for UUV Operations under Low Adaptation Gains', *IEEE Journal of Oceanic Engineering*. [Under review, 2017]

In this chapter, the CMRAC and PMRAC methods that were tested using simulations in Chapter 3 are experimentally tested to validate the simulations results. The results are used to determine which method is more suitable for UUV applications. Moreover, this chapter provides an insight into implementation differences of the two methods.

Chapter 4 has been removed for copyright or proprietary reasons.

Chapter 5:

Experiments & Validation of Command Governor-based Adaptive Control

This chapter consists of two subchapters:

Part A: Experimental Study of Command Governor Adaptive Heading Control for Unmanned Underwater Vehicles.

Part B: Experimental Study of a Command Governor Adaptive Depth Controller for an Unmanned Underwater Vehicle.

In this chapter CGAC method that was tested using simulations in Chapter 4 is experimentally tested to validate the simulation results. Part A looks at heading control with an emphasis on normal operations, disturbances and actuator dead-zone while Part B looks at depth control with an emphasis on measurement noise and robustification filter.

Chapter 5:

Part A –

Experimental Study of Command Governor Adaptive Heading Control for Unmanned Underwater Vehicles

A revised version of this subchapter has been published in the journal "*IEEE Transaction on Control Systems Technology"* and is currently available as an "Early Access Article". The citation for the research article is:

Makavita, C.D., Nguyen, H.D., Jayasinghe, S.G, & Ranmuthugala, D, 'Experimental Study of Command Governor Adaptive Control for Unmanned Underwater Vehicles', *IEEE Transactions on Control Systems Technology*, pp. 1-14. ISSN 1063-6536 (2017) [Refereed Article]

Chapter 5A has been removed for copyright or proprietary reasons.

Chapter 5:

Part B –

Experimental Study of a Command Governor Adaptive Depth Controller for an Unmanned Underwater Vehicle

This subchapter was submitted to the journal "*Control Engineering Practice"* and is currently being revised based on the response of the reviews before resubmitting.

Abstract

Unmanned Underwater Vehicles (UUVs) are increasingly being used in advanced applications that require them to operate in tandem with human divers and around underwater infrastructure and other vehicles. These applications require precise control of the UUVs which is challenging due to the non-linear and time varying nature of the hydrodynamic forces, presence of external disturbances, uncertainties and unexpected changes that can occur within the UUV's operating environment. Adaptive control has been identified as a promising solution to achieve desired control within such dynamic environments. Nevertheless, adaptive control in its basic form, such as standard Model Reference Adaptive Control (MRAC) has a trade-off between the learning rate and transient performance. Even though, higher learning rates produce better performance they can lead to instabilities and actuator fatigue due to high frequency oscillations in the control signal. Command Governor Adaptive Control (CGAC) is a possible solution to achieve better transient performance at low learning rates. In this study, the suitability of the CGAC for depth control of a UUV has been experimentally validated and its performance compared against MRAC for several operating conditions, including normal operation, external impact disturbance and partial thruster failure. This is uniquely challenging due to the unavailability of full state measurement, additional noise due to state estimation, and time-delays from input noise filters. Experimental results show that the CGAC offers better tracking, disturbance rejection and tolerance to partial thruster failure compared to the MRAC. In addition, the CGAC is shown to be more robust against noise and time-delays.

Keywords: adaptive control, command governor adaptive control, external disturbances, measurement noise, thruster failure, time-delay, unmanned underwater vehicles

5B.1 Introduction

Unmanned Underwater Vehicles (UUVs) can be divided broadly into ROVs and AUVs. Both types are increasingly being used in a wide range of applications such as marine archaeology (L'Hour & Creuze 2016), ship hull inspection (Lynn & Bohlander 1999) underwater drilling and maintenance (Solvang, Deng & Lien 2001), oceanography (Wynn et al. 2014), and underwater surveillance (Kemna et al. 2011). Over the years the distinction between ROVs and AUVs has somewhat blurred, mainly due to the continuous efforts to add autonomous features to ROVs. This resulted in semi-autonomous ROVs (Kim & Yuh 2004), i.e. ROVs with low level automation and Hybrid ROV/AUVs (Bowen et al. 2009), i.e. vehicles that function both as a ROV or AUV as required. Numerous control techniques from PID (Zanoli & Conte 2003) to adaptive control (Yuh, Nie & Lee 1999) has been successfully implemented in UUVs and experimentally verified, although PID and sliding mode control techniques (Healey & Lienard 1993) are still the most popular due to their relatively straightforward control structure and ease of implementation. Furthermore, they provide adequate performance in traditional UUV applications.

Recently there has been an uptake in research into advanced applications that require a rethink of UUV control techniques, as popular control methods may no longer be able to provide adequate performance (McFarland & Whitcomb 2014). These advanced applications include the use of mini AUVs to help divers, i.e. remote diver assistant (DeMarco, West & Howard 2014), launching and recovering AUVs from larger vehicles (Leong et al. 2015) and docking stations for AUVs (Jin-Yeong et al. 2011). These require very precise manoeuvring in constrained environments to ensure safe operation, mainly due to involvement of humans and other underwater assets. This includes smooth and fast transient response as well as zero steady-state error. In addition, quick recovery from external disturbances and sufficient operational control under partial-fault conditions are also essential. Therefore, many researches have recommended adaptive control as the most suitable and promising control technique for these applications (Maalouf 2013; Valladarez 2015).

Adaptive control attempts to change the internal parameters of the control system based on the operating conditions. Therefore, it has the ability to adapt to changes in the

operating environment and vehicle configuration, and thereby ensure desired performance even under changing conditions. In order to achieve this adaptive controllers use a learning mechanism, which could be accomplished by either directly learning the control parameters (direct adaptive control) or by learning the plant parameters and using them to set the control parameters (indirect adaptive control) (Åström & Wittenmark 1995). Model Reference Adaptive Control (MRAC) is one of the direct adaptive control methods, where the system attempts to follow a reference signal generated by an ideal model (Åström & Wittenmark 1995). The control parameters are learned based on the error between the reference and actual states.

Although quite promising adaptive control techniques, including MRAC, face certain challenges. These include, difficulty in achieving good performance (i.e. reference tracking) throughout the operating region while ensuring stable operation with smooth control signals, and achieving robust control in the presence of measurement noise and time-delays. It is well know that once all the parameter values have been completely learned MRAC provides good reference tracking in steady state, but does not have guaranteed tracking performance during the transient time where the parameters are being learned (Cao & Hovakimyan 2006a). The length of this transient stage depends on the speed of learning, which in turn depends on the learning rates or adaptive gains. At higher gains, learning is faster and thus the transient stage is shorter. Nevertheless, high gains leads to oscillatory and erratic parameter estimates that results in oscillatory control signals and instability. In addition, robustness to noise and time-delay is drastically reduced at high gains, which can also result in instability. A similar effect is observed under disturbances, where low gains result in slow but stable recovery while high gains can have fast recovery with saturated control signals and potential instability. There are two main solutions to this conundrum, namely: the use of high gains with some additional modification to add more robustness and remove the high frequency system oscillations, or the use of low gains and add some additional modifications to ensure better tracking in the transient region. Adaptive control strategies that fall into the former category are L1 Adaptive Control (Cao & Hovakimyan 2008) and Frequency Limited Adaptive Control (Yucelen, Torre & Johnson 2013), while strategies for the latter category are Composite Adaptive Control (Slotine & Li 1989) and Command Governor Adaptive Control (CGAC) (Yucelen & Johnson 2012a).

CGAC is a method in which standard MRAC is modified by adding a linear dynamical system referred to as the command governor that modifies the command based on the tracking error. This in turn leads to a modification in the reference model that allows better performance in the transient region even with low gain. In addition, CGAC has an inherent ability to reject disturbances. The authors previously have verified the suitability of CGAC for UUV applications using simulations (2016a; Makavita et al. 2015a). In Makavita et al. (2015a) the considerable improvement in reference tracking in transient region was verified for both heading and depth control of a mini ROV/AUV with full state feedback under assumptions of no actuator nonlinearities, negligible sensor noise and time-delays. These simulations of heading control where extended to include actuator dead-zone and sensor noise in Makavita et al. (2016a). It was shown that CGAC overcame a substantial dead-zone without any additional dead-zone inverse, while the requirement of the robustification filter introduced by Yucelen and Johnson (2013) to reduce noise in the control signal was confirmed. In addition, it also demonstrated that time-delay induced instability can be mitigated by the above robustification filter. More recently experimental validation of heading control carried out by the authors were presented in Makavita et al. (2017c). The validation that compared MRAC and CGAC showed that the latter did indeed improve tracking at low gain, had less control signal oscillations, overcame actuator dead-zone and had better disturbance rejection. On the other hand, the noise was sufficiently small that it did not require input filtering; thus the time-delay was negligibly small. Therefore, while the robustification filter was implemented, it had only a minor role in the operation.

The natural extension of the abovementioned study is to experimentally validate the results of the depth control. This has a special significance due to some crucial differences between heading and depth motions for the AMC ROV used for validation programme (Fig. 2). Firstly, the full state feedback was not available as there was no measurement of the depth rate. This led to estimation of the depth rate, which in turn adds significant amount of noise that requires input filtering causing time-delay. Therefore, the noise and time-delay are no longer negligible and thus careful considerations must be taken in the design of the robustification filter and its effect on reference tracking. Secondly, in contrast to the heading, the vertical movement is achieved with a single thruster compared to the two thruster operation for horizontal

movements. In addition, the drag in the vertical direction is significantly larger and the vehicle is positively buoyant. Therefore, a much larger control effort and continuous operation of the thruster was required even to maintain a constant depth. This larger effort brings thruster saturation as well as overall energy expenditure into consideration.

The depth control tests were carried out for both CGAC and MRAC to compare their performance under normal operation in the transient region, under external impact disturbance and in the event of a partial thruster failure. In addition, this paper also serves to illustrate the effect of noise and time-delay as well as the prominent role played by the robustification filter in CGAC design. The definitions of the variables and symbols are given in the Nomenclature section.

5B.2 Command Governor Adaptive Control Architecture

This section provides a brief introduction to the standard MRAC and extension of MRAC to CGAC using a linear dynamical system.

5B.2.1 Model Reference Adaptive Control (MRAC)

This MRAC architecture has been described in Chapter 3 section 3A.3 and 3A.3.1, and for the sake of brevity will not be repeated here

5B.2.2 Command Governor Adaptive Control (CGAC)

This CGAC architecture has been described in section 5A.2.2 and for the sake of brevity will not be repeated here.

5B.3 Kinematic and Dynamic Model of the AMC ROV

It is common practice in marine control systems to have two models, namely the highly detailed PPM and a more simplified CPM, at two different complexity levels (Sørensen, AJ 2005). The PPM is used for test and calibration of controllers, training simulators, and hardware-in-the-loop testing and thus it should capture all the components of the real vehicle as accurately as possible. The CPM is used in analytical stability analysis and as the basis for controller design and thus it should capture only the essential

features of the system. The importance of having two separate models and their efficacy is explained in Refsnes (2007).

5B.3.1 Process Plant Model

The PPM has been described in Chapter 4 section 4.3.1 and for the sake of brevity will not be repeated here.

5B.3.2 Control Plant Model

The CPM has been described in Chapter 4 section 4.3.2 and for the sake of brevity will not be repeated here. The depth CPM is given below as its structure is slightly different from the structure of depth CPM in chapter 4.

5B.3.2.1 Depth CPM

Thus, the depth control model was developed as follows. Simplifying (4.6) using **Assumptions 4.9** and **4.10** gives,

$$\dot{d} = w \tag{5B.1}$$

From (4.7), considering only the depth DOF ignoring the buoyancy term due to **Assumptions 4.9** and **4.10** the following equation is obtained,

$$m_w \dot{w} = Z_w w + Z_{w|w|} w|w| + (F_W - F_B) + \tau_w \tag{5B.2}$$

Rearranging (5B.2) for $\dot{w}$ yields,

$$\dot{w} = \left(\frac{Z_w}{m_w}\right) r + \left(\frac{Z_{w|w|}}{m_w}\right) w|w| + \frac{F_W - F_B}{m_w} + \left(\frac{1}{m_w}\right) \tau_w \tag{5B.3}$$

Replacing τ_w with the normalized moment using (4.13) yields,

$$\dot{w} = \left(\frac{Z_w}{m_w}\right) r + \left(\frac{Z_{w|w|}}{m_w}\right) w|w| + \frac{F_W - F_B}{m_w} + \left(\frac{K_{vf} K_{iv}}{m_w}\right) \tilde{\tau}_w \tag{5B.4}$$

or

$$\dot{w} = \theta_1 w + \theta_2 w|w| + \theta_4 + \theta_3 \tau_w \tag{5B.5}$$

where $\theta_1 = \left(\frac{Z_w}{m_w}\right)$, $\theta_2 = \left(\frac{Z_{w|w|}}{m_w}\right)$, $\theta_3 = \left(\frac{K_{vf} K_{iv}}{m_w}\right)$, $\theta_4 = \frac{F_W - F_B}{m_w}$, $m_w = m - Z_{\dot{w}}$.

From (5B.1) and (5B.5), the state space form of the depth control model is given as,

$$\begin{pmatrix} \dot{d} \\ \dot{w} \end{pmatrix} = \begin{pmatrix} 0 & 1 \\ 0 & 0 \end{pmatrix} \begin{pmatrix} \dot{d} \\ w \end{pmatrix} + \begin{pmatrix} 0 \\ 1 \end{pmatrix} \left[\theta_4 + \theta_1 w + \theta_2 w|w| \right] + \begin{pmatrix} 0 \\ 1 \end{pmatrix} \theta_3 \tilde{\tau}_w \tag{5B.6}$$

Equation (5B.6) has the general state space form of (3A.9) where, $\boldsymbol{x} = \begin{pmatrix} x_1 \\ x_2 \end{pmatrix} = \begin{pmatrix} d \\ w \end{pmatrix}$, $\boldsymbol{A} = \begin{pmatrix} 0 & 1 \\ 0 & 0 \end{pmatrix}$, $\boldsymbol{H} = \begin{pmatrix} 0 \\ 1 \end{pmatrix}$, $\boldsymbol{B} = \boldsymbol{H}\Lambda = \begin{pmatrix} 0 \\ \theta_3 \end{pmatrix}$, $\Lambda = \theta_3$, $\delta(\boldsymbol{x}) = \theta_1 x_2 + \theta_2 x_2 |x_2| + \theta_4$, and $u = \tilde{\tau}_w$. Thus, $p = 2$ and $q = 1$.

5B.3.3 Reference Model

This reference model has been described in Chapter 3 section 3A.3.2 and for the sake of brevity will not be repeated here.

5B.4 Experimental Setup

The experimental setup has been described in Chapter 4 section 4.4 and for the sake of brevity will not be repeated here.

5B.4.1 Parameter Values

The adaptive control parameters were set as follows. For simplicity, all adaptive gains were taken as dependent on a single positive constant γ such that $\boldsymbol{\Gamma}_\sigma = \gamma \boldsymbol{I}_{3\times 3}$ and $\Gamma_{un} = \gamma$. CGAC always uses $\gamma = 1$, with a command governor gain of $\lambda = 100$. The values of $\gamma = 100$ for MRAC and filter gain of $\kappa = 3$ were selected based on preliminary experiments as described in Section 5B.5.1. All the initial values of the model parameters were set to zero ($\hat{W}_{un} = 0$ and $\hat{\boldsymbol{W}}_\sigma = [0 \quad 0 \quad 0]$), thus assuming no *a priori* knowledge. While this is an extreme assumption considering that some values are known, albeit approximately (e.g. mass), it provides a good basis to test the ability of the controller under severe uncertainty. The reference model parameters were set to $\omega_n = 0.3$ rad/s and $\zeta = 1$, which yields $\boldsymbol{K}_1 = [-0.09 \quad -0.6]$ and $K_2 = 0.09$.

5B.4.2 Experimental Scenarios

The experiments were conducted for both CGAC and MRAC under four different scenarios. The first scenario was a preliminary run to determine which parameter values to use for learning rates and filter gain. The three remaining scenarios are normal operation, disturbance rejection, and partial thruster failure, which are conditions usually encountered in practice. More details on the experimental scenarios are given below:

5B.4.2.1 Preliminary operation

The preliminary tests were carried out to determine the learning rates to be used in MRAC and also to determine the robustification filter gain. In addition, these tests were used to show the effect of noise, time-delay and robustification filter on the performance of MRAC and CGAC.

5B.4.2.2 Normal operation

The vehicle was tested for depth change without disturbances for a short duration with initial parameter values set to zero to recreate a transient region. The tests were conducted with forward speed of 0m/s. The objective of these tests was to assess the tracking performance and control effort of CGAC compared to MRAC for depth control in the transient period.

5B.4.2.3 External disturbance

The ability of MRAC and CGAC to overcome an external disturbance in the form of an external vertical impact was tested. The ROV was initially given some time to settle to a fixed depth and then a sudden vertical force was applied to mimic an external disturbance.

5B.4.2.4 Thruster failure

This represents a 50% loss of thrust in the vertical thruster during operation. This type of partial failure can occur due to an electrical or mechanical malfunction. This situation was recreated by halving the voltage to the motor controllers. The partial failure was activated at 150s from the start at a depth of 1m. The objective was to ascertain the ability of MRAC and CGAC to overcome such a failure and maintain the depth.

5B.5 Experimental Results

Performance of CGAC and MRAC in depth control was measured using six performance indices. The first four indices were based on the errors in depth (e_d) and depth rate (e_w), where $\boldsymbol{e}_m{}^T = \begin{bmatrix} e_d & e_w \end{bmatrix}$, and the last two are based on the control effort. These performance indices were designed based on the work of Fossen and Fjellstad (1996).

$$d_{e\_rms} = \sqrt{\frac{1}{N}\sum_{i=1}^{N}\left(e_d\right)^2} \quad \text{(rms depth error)} \tag{5B.7}$$

$$w_{e\_rms} = \sqrt{\frac{1}{N}\sum_{i=1}^{N}\left(e_w\right)^2} \quad \text{(rms depth rate error)} \tag{5B.8}$$

$$d_{e\_\max} = \max(\left|e_d\right|) \text{ (maximum depth error)} \tag{5B.9}$$

$$w_{e\_\max} = \max(\left|e_w\right|) \text{ (maximum depth rate error)} \tag{5B.10}$$

$$\tilde{\tau}_{w\_rms} = \sqrt{\frac{1}{N}\sum_{i=1}^{N}\left(\tau_w\right)^2} \quad \text{(rms normalized control effort)} \tag{5B.11}$$

$$\tilde{\tau}_{w\_\max} = \max(\left|\tau_w\right|) \text{ (maximum normalized control effort)} \tag{5B.12}$$

In addition, other performance indices such as settling time were used as required. The vertical thruster force, when given numerically or graphically, is the value before adding the dead-zone inverse value.

5B.5.1 Preliminary operations

As a preliminary requirement before testing the realistic scenarios it was important to determine the command governor filter gain (κ) and learning rate γ. To this end a set of experiments were carried out as described below.

5B.5.1.1 Determination of the command governor filter gain

The $\kappa = 20$ used in the experiments (Makavita et al. 2017c) for heading control was initially used for depth control experiments as well, although depth control differs from

heading control for the UUV as it does not have full state measurement. Therefore, the depth rate was estimated as the derivative of depth under the assumption of negligible roll and pitch. As expected, this adds considerable noise into the rate estimate as seen in Fig. 5B.1 (b). Thus, for $\kappa = 20$ it is observed that while the depth tracking performance is very good as seen in Fig. 5B.1 (a), the control signal quickly becomes unacceptably noisy as seen in Fig. 5B.1(c).

As a possible solution, the depth and depth rate estimates were low pass filtered to reduce noise. The selected filter was a 2nd order Butterworth filter with a cut-off frequency of 12 rad/s. The experiment was re-run with the filter and the corresponding results are shown in Fig. 5B.2. As observed in Fig. 5B.2 (a), the depth tracking is still very good but the depth rate in Fig. 5B.2 (b) undergoes severe oscillation as it tries to track the depth command. In addition, as seen in Fig. 5B.2 (c), the control signal also shows large oscillations which exceed the saturation limits. The cause of this poor performance is the time-delay created by the input filter.

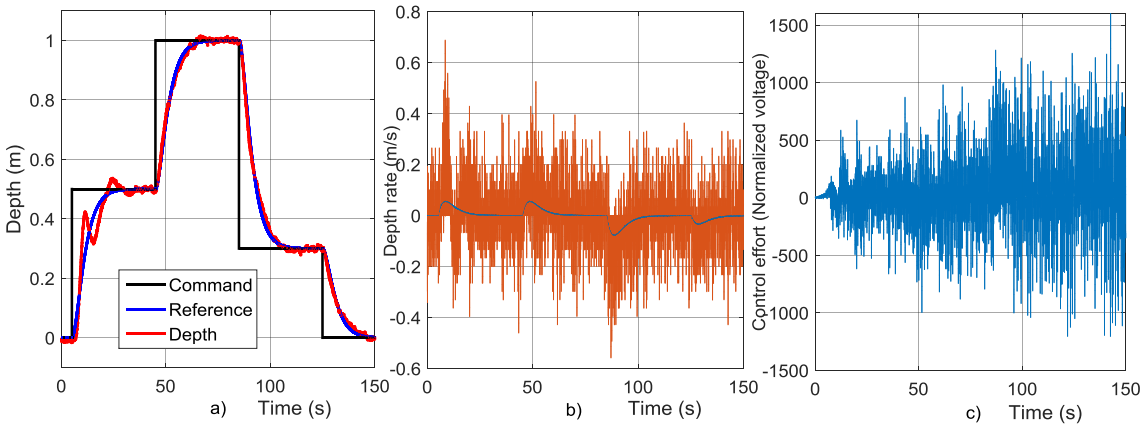

Figure 5B. 1: a) Depth b) depth rate and c) control signal for CGAC with $\kappa = 20$, without an input filter.

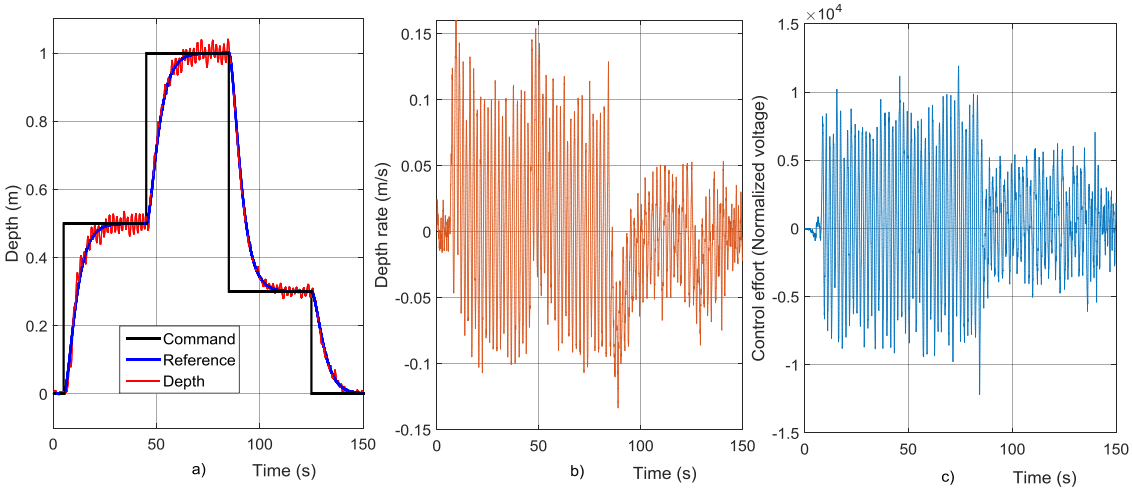

Figure 5B. 2: a) Depth, b) depth rate and c) control signal for CGAC with $\kappa = 20$, with the input filter

It was already shown by the authors in previous simulation studies (Makavita et al. 2016a) that lowering κ can overcome noise as well as increase robustness to time-delay. Thus, κ must be selected such that the input filter and robustification filter reduce noise to an acceptable level while the robustification filter counteracts the time-delay effects. In addition, considerable attention must be placed on the judicious selection of κ, as it has a significant effect on the initial tracking performance of CGAC as described in Section 5B.5.2. After several experiments using different values and considering the balance between performance and robustness the final κ value was selected as 3.

5B.5.1.2 Determine MRAC learning rates

In both simulations (Makavita et al. 2016a) and experiments (Makavita et al. 2017c) of the heading controller, CGAC was compared with both MRAC with low gain (MRAC-LG) and MRAC with high gain (MRAC-HG). In that work MRAC-LG had the same learning rate as CGAC of $\gamma = 1$ while MRAC-HG had the learning rate of $\gamma = 10^4$. The same settings when used for depth control yielded the results tabulated in Table 5B.1, with the depth tracking performance shown graphically in Fig. 5B.3. A relatively poor tracking performance was expected from MRAC-LG due to the low learning rate, confirmed by the poor performance with d_{e_rms} of 0.58m and $d_{e\_\max}$ of 1.36m with a commanded maximum depth of only 1m. On the other hand, a good tracking performance was expected from MRAC-HG, albeit with high frequencies in the control signal. Unexpectedly, the tracking performance of MRAC-HG was also relatively poor,

with d_{e_rms} and $d_{e\_\max}$ only marginally better than those for MRAC-LG, and w_{e_rms} and $w_{e\_\max}$ faring worse than for MRAC-LG by 53% (a factor of 2.1) and 42% (a factor of 1.7) respectively (note, in the interest of brevity, in future the change factor for the performance indices will simply be given as a number within brackets following the respective percentage change). Furthermore, as $\tilde{\tau}_{w\_rms}$ and $\tilde{\tau}_{w\_\max}$ clearly indicate, the control signal has gone out of bounds and the system is unstable. The cause of this was the lack of robustness of MRAC-HG to the time-delay caused by the input filter.

Table 5B. 1: Performance indices of tracking error and control effort for MRAC with, $\gamma = 1, 10^4$ and 10^2

Performance Indices	MRAC (1)	MRAC (10000)	MRAC (100)
d_{e_rms} (m)	0.579	0.497	0.047
$d_{e\_\max}$ (m)	1.359	1.148	0.141
w_{e_rms} (m/s)	0.076	0.116	0.054
$w_{e\_\max}$ (m/s)	0.248	0.353	0.200
$\tilde{\tau}_{w\_rms}$	45.478	330461	50.756
$\tilde{\tau}_{w\_\max}$	92.056	634534	154.427

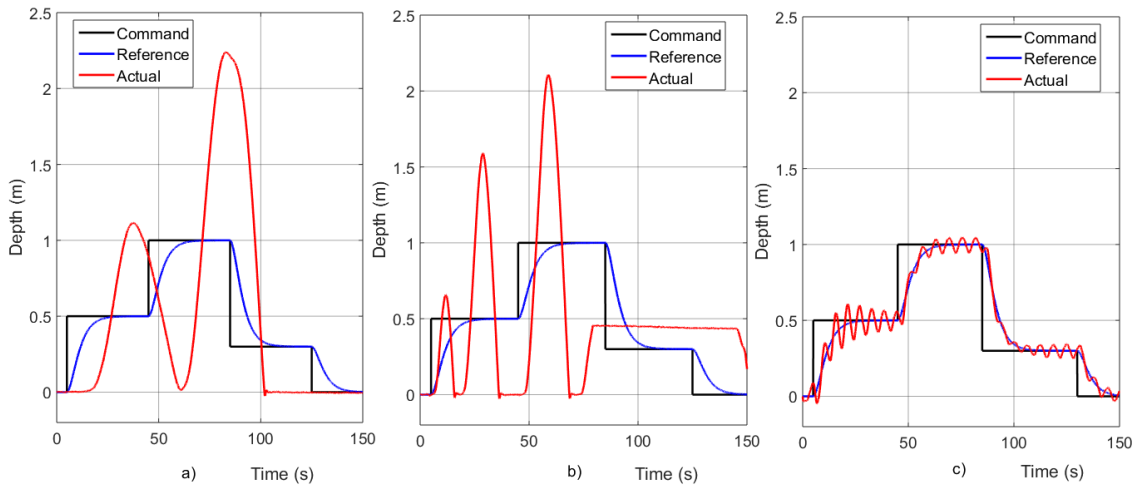

Figure 5B. 3: MRAC depth response with a) $\gamma = 1$, b) $\gamma = 10000$, and c) $\gamma = 100$

Thus, both these learning rates cannot be used for MRAC as a meaningful comparison against CGAC. In an effort to identify a reasonably low and high gain, several different values were tested, which lead to the conclusion that MRAC was not well suited for depth control irrespective of the gain. As a compromise between the two extremes a

single value of $\gamma = 100$ was selected as it had the best performance with d_{e_rms} reduced by 92% (12.3), $d_{e\_\max}$ reduced by 90% (10), w_{e_rms} reduced by 29% (1.4), and $w_{e\_\max}$ reduced by 19% (1.2) over MRAC-LG. Thus, for all further test scenarios, the optimal MRAC with $\gamma = 100$ was compared against the CGAC with $\gamma = 1$.

5B.5.2 Normal Operations

Normal operations were tested using the depth command shown in Fig. 5B.4, with a duration of 150 s at a forward speed u=0m/s.

In Table 5B.2, the MRAC and CGAC performance indices are given in three parts: full run, first 50s, and last 100s. As observed from Fig. 5B.4 (b), there is a clear distinction between first 50s and next 100s of the CGAC depth response which cannot be captured by the single full run indices. Thus, this analysis will look at the first 50s and next 100s separately and compare the performances. It is clear that in the first 50s, due to the significant negative effect of the robustification filter on CGAC, the MRAC performed better than CGAC with respect to both depth response and control signal. Considering tracking, for MARC d_{e_rms} is lower by 73% (3.8), $d_{e\_\max}$ is lower by 76% (4.2), and $w_{e\_\max}$ is lower by 25% (1.3) compared to CGAC. The only exception is in w_{e_rms} which is increased by 8% (1.08). Considering the control effort, $\tilde{\tau}_{w\_rms}$. is lower by 35% (a factor of 1.5) and $\tilde{\tau}_{w\_\max}$ is lower by 54% (a factor of 2.2) for MARC in comparison to CGAC.

Table 5B. 2: Performance indices of tracking error and control effort for MRAC and CGAC for normal operation

Performance Indices	MRAC			CGAC		
	Full run	**First 50s**	**Next 100s**	**Full run**	**First 50s**	**Next 100s**
d_{e_rms} (m)	0.047	0.070	0.032	0.153	0.265	0.018
$d_{e\_\max}$ (m)	0.142	0.142	0.091	0.600	0.600	0.064
w_{e_rms} (deg/s)	0.054	0.081	0.035	0.045	0.075	0.017
$w_{e\_\max}$ (deg/s)	0.200	0.200	0.097	0.267	0.267	0.067
$\tilde{\tau}_{w\_rms}$	50.756	74.660	35.027	70.588	116.619	25.942
$\tilde{\tau}_{w\_\max}$	154	154	109	334	334	104

A more realistic comparison of the actual performance of the two methods can be obtained by looking at the next 100s of the run, i.e. after the filter effect has died down. In this case the tracking performance indices that d_{e_rms}, w_{e_rms}, $d_{e\_\max}$, and $w_{e\_\max}$ is lower for CGAC than MRAC by 44% (1.8), 51% (2.1), 42% (1.7), and 45% (1.8) respectively. Furthermore, the control effort indices of $\tilde{\tau}_{w\_rms}$ is lower for CGAC by 26% (1.4) while $\tilde{\tau}_{w\_\max}$ is approximately the same for CGAC and MRAC. While the initial poor performance of CGAC is a cause for concern, this only manifest at the very beginning of a run, and once the filter effect has died down, CGAC does perform better than MRAC in reference tracking and energy usage.

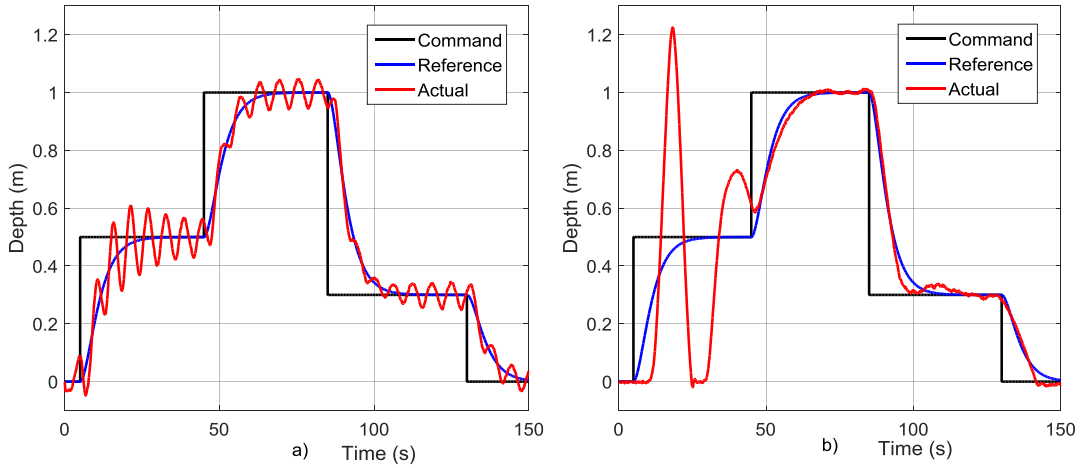

Figure 5B. 4: Depth response of a) MRAC and b) CGAC under normal operations

In addition to the performance indices, Fig. 5B.4 indicates another advantage of CGAC over MRAC. As observed from Fig. 5B.4(a), the MRAC response is continuously oscillatory in contrast to that for CGAC shown in Fig. 5B.4(b). Therefore, even if the average error of MRAC is acceptable for a given task, the oscillatory nature of it makes MRAC much less suitable for most operations such as image capturing or manipulation tasks. Further analysis conducted in the frequency domain is shown in Fig. 5B.5, where the y-axis represents normalized magnitudes of the frequencies present in the control signal. As seen it is clear that both spectrums have only low frequencies as they do not use very high learning rates. The major difference is that there is a peak for MRAC at 0.16Hz that represents the slow control signal oscillations that correspond to the oscillations in the depth response.

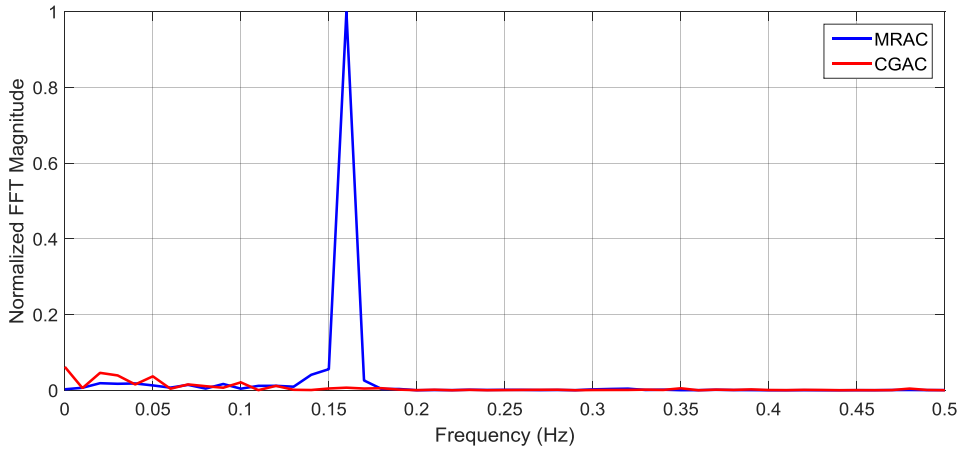

Figure 5B. 5: Normalized frequency spectrum of the control signals produced by MRAC and CGAC under normal operation.

5B.5.3 External Disturbances

In this set of tests the UUV is subjected to a sudden impact once it has settled at a depth of 1m, with the results presented in Figs. 5B.6 and 5B.7 and Table 5B.3. Time is measured by taking the moment of impact as zero. As can be seen in Fig. 5B.6(a) the MRAC depth response has an initial peak deviation of 26cm at around 2s, and then continues to increase to a maximum deviation of 48.5cm at around 11s, and then reduces until it settles to the final value within 5% of the original depth in a settling time of 34s. On the other hand CGAC depth response in Fig. 5B.6(b) has an initial peak deviation of 24cm and then continuously decrease until it settles to within 5% of the original depth in a settling time of 12.5s. Furthermore, the CGAC maximum deviation and settling time are lower than MRAC by 46% (1.9) and 63% (2.7) respectively. Therefore, CGAC is less affected by the disturbance and recovers faster to the original depth.

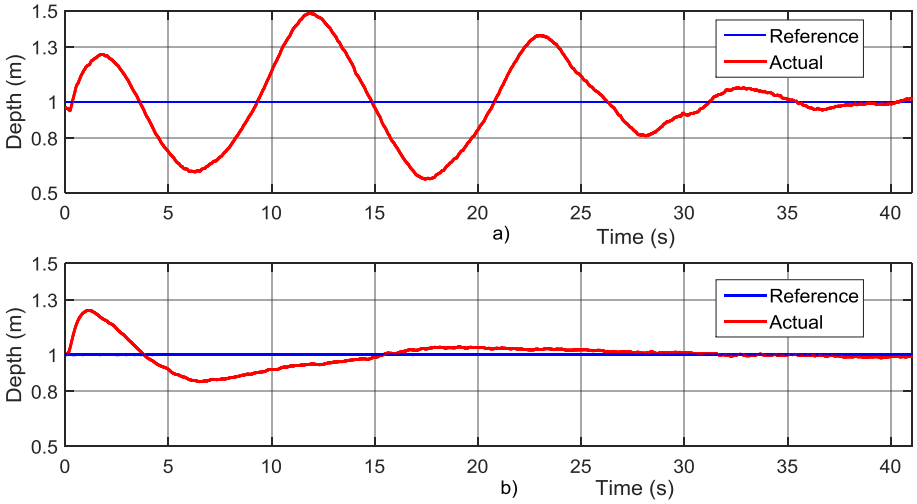

Figure 5B. 6: Depth response of a) MRAC and b) CGAC under an impact disturbance

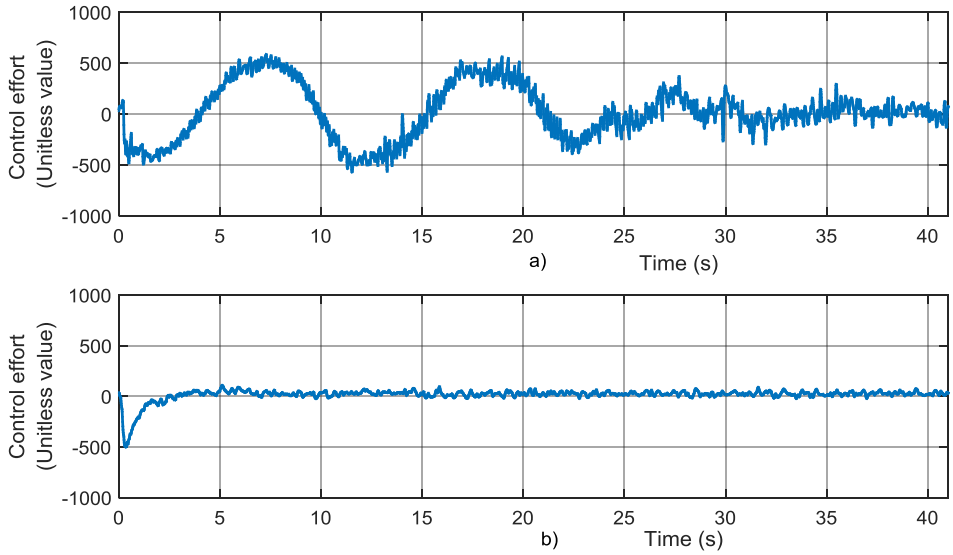

Figure 5B. 7: Control signal of a) MRAC and b) CGAC under an impact disturbance

Table 5B. 3: Performance metrics of MRAC and CGAC for an impact disturbance

	MRAC	**CGAC**
Maximum depth change	0.485 m	0.242 m
Time to depth error to get below 0.05m (5% settling time)	34s	12.5s
Maximum control signal value	586	490
Duration of thruster saturation	20s	1s

From the MRAC control effort shown in Fig. 5B.7(a), it is seen that the controller output exceeds the upper saturation limit of 128 with a maximum of 589 (see Table

5B.3). The MRAC control effort remains above saturation for a total duration of approximately 20s. In contrast, as seen in Fig.5B.7(b), the maximum CGAC control effort is somewhat lower than 490, still well above saturation. Nevertheless, the CGAC control effort remains above saturation only for a total duration of 1s, giving CGAC a much more acceptable control signal compared to MRAC.

5B.5.4 Thruster Failure

As before the UUV is maintained at a constant depth of 1m before thruster failure is initiated. The plots in Fig. 5B.8 show the depth response of the UUV to a 50% thruster failure at 150s after commencing operation. As seen in Fig. 5B.8(a), after thruster failure the MRAC depth response has a large deviation that settles slowly towards the initial value at around t=350s. However around t=380s the error begins to increase again. In contrast as seen in Fig. 5B.8(b), the CGAC has a much smaller increase in depth error after the failure, which remains almost constant throughout the run.

These observations are further elucidated below using the performance indices presented for both before thrust loss (i.e. from 100s to 150s) and after thrust loss (from 150s to 200s) in Table 5B.4. The MRAC response oscillates around the 1m depth with an average depth error (d_{e_rms}) of 3.2cm and maximum depth error ($d_{e\_\max}$) of 5.5cm before thruster failure. After failure, d_{e_rms} increases by 131% (2.3) to 7.4cm and $d_{e\_\max}$ increases by 142% (2.4) to 13.3cm. Afterwards, the oscillation amplitude reduced from the peak of 13.3cm at 175s to around 5cm at 300s but then again increased to above 6cm at 380s. On the other hand the CGAC had d_{e_rms} of 0.6cm and $d_{e\_\max}$ of 1.6cm before thrust loss, which increased by 133% (2.3) and 119% (2.2) to 1.4cm and 3.5cm respectively after thrust loss. Furthermore, the increased error amplitude reduced to around 2cm within 22s and then remained at that value throughout the rest of the run. Therefore, CGAC maintains its relative reference tracking advantage over MRAC under partial thruster failure. In addition, the CGAC not only settles much faster to its final error value but also maintains the error without variation compared to the MRAC.

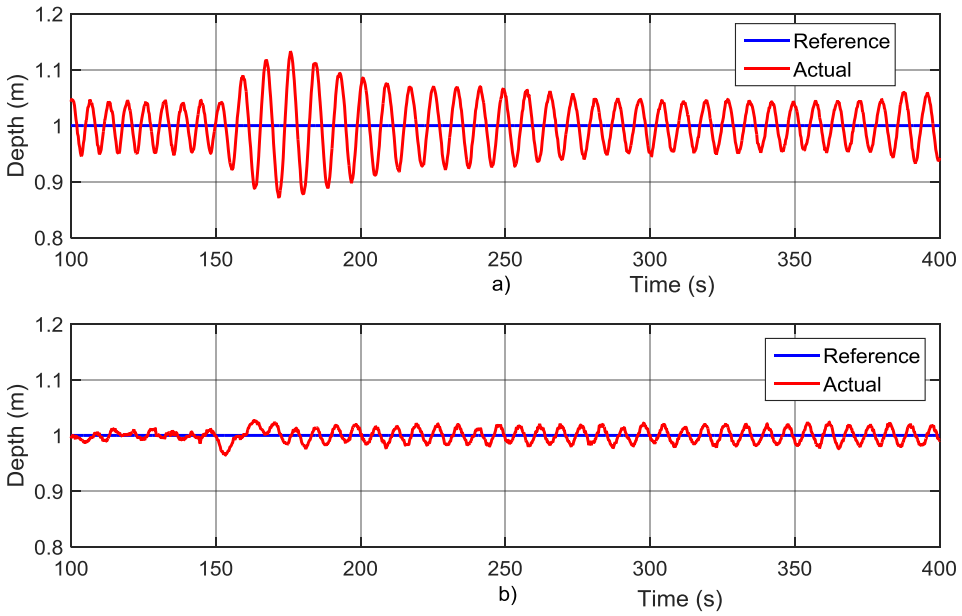

Figure 5B. 8: Depth response of a) MRAC and b) CGAC for partial thruster failure at t=150s

Table 5B. 4: Performance metrics of MRAC and CGAC for partial thruster failure

	MRAC	**CGAC**
d_{e_rms} before thrust loss	0.032 m	0.006 m
d_{e_rms} after thrust loss	0.074 m	0.014 m
$d_{e\_\max}$ after thrust loss	0.133 m	0.035 m
Time to depth response to settle to final value	large	22 s
$\tilde{\tau}_{w\_rms}$ before thrust loss	34.54	21.04
$\tilde{\tau}_{w\_rms}$ after thrust loss	81.71	34.49
$\tilde{\tau}_{w\_\max}$ before thrust loss	78	77
$\tilde{\tau}_{w\_\max}$ after thrust loss	184	82
Time for control signal to settle to final value	large	28 s

Looking at the control effort in Table 5B.4, it is seen that for MRAC the average control effort ($\tilde{\tau}_{w\_rms}$) has increased from 34.54 by 136% (2.4) to 81.71 after thrust loss while maximum control effort ($\tilde{\tau}_{w\_\max}$) has increased by the same factor from 78 to 184. For CGAC, $\tilde{\tau}_{w\_rms}$ has increased from 21.04 by 64% (1.6) to 34.49 after thrust loss while $\tilde{\tau}_{w\_\max}$ marginally changes from 77 to 82.

These results clearly show the advantage of CGAC in terms of control effort. Firstly, the average control effort of the CGAC, even after thrust loss, is still smaller than that of the MRAC before thrust loss. Secondly, the factor of increase of $\tilde{\tau}_{w\_rms}$ is lower for the CGAC than the MRAC. Therefore, CGAC not only has the lower overall energy consumption, but also its relative energy efficiency compared to MRAC improves from a 64% reduction before thrust loss to 137% reduction after thrust loss. Finally, the maximum control effort of CGAC shows only a small change after the loss of thrust which is well below saturation limit while for MRAC it increases by a large factor to a value well above the saturation limit.

5B.6 Conclusion

This paper presents the results of an experimental study conducted to compare the performance of CGAC and MRAC in the depth control of an UUV. In this study, it was found that the measurement noise and time-delay introduced by input filters cause significant performance degradations and thus filter parameters should be carefully chosen in the design stage of the controller in order to minimise the loss of performance. The command governor filter gain is judiciously selected to ensure sufficient robustification for noise and time-delay.

Through comparative experimental results it was shown that in normal operations the robustification filter adversely affects the CGAC for an initial time period, however once settled it outperforms the MRAC on all performance metrics. Moreover, the selection of appropriate learning rates for MRAC is important to achieve acceptable performance, as low learning rates results in poor tracking while high learning rates lead to instability. Under an external impact disturbance, the CGAC has a significantly lower deviation from the commanded depth as well as a shorter recovery time than the MRAC. Subjected to partial vertical thruster failure, the CGAC response showed minimum deviation, recovering quickly, and continued to maintain the depth with a relatively small error. In comparison, the MRAC experienced much larger deviation, recovering relatively slowly and was unable to maintained or significantly reduce the error throughout the run.

Overall CGAC showed consistently improved performance over MRAC except for the negative effect of the robustification filter on tracking in the initial phase. Future research through numerical simulations and experimental validation will concentrate on improving the tracking performance of the CGAC in the initial phase without compromising the robustness improvements of the robustification filter.

Chapter 6:

Extended Command Governor Adaptive Control for Unmanned Underwater Vehicles

This chapter was submitted to the journal "*International Journal of Adaptive Control and Signal Processing"* and is currently being revised based on the response of the reviews before resubmitting.

In this chapter, further modifications are suggested to improve adaptive control of a UUV based on the results from Chapters 4 & 5. The CGAC method which showed the best results is extended by adding a closed loop state predictor from PMRAC to improve the learning in transient stage and by introducing a weight filter to replace the robustification filter for noise removal. This method improves tracking, especially in transient stage without increasing high frequency signals or being too susceptible to noise.

Abstract

Command Governor-based Adaptive Control (CGAC) is an extension of the standard adaptive control which is capable of achieving improved transient tracking performance without compromising the system stability and smoothness of the final control signal. Nevertheless, in both simulation and experimental studies, the authors have observed poor initial tracking performance in CGAC, which is caused by the filter added to improve the robustness against noise and time delay of the feedback signal. As a solution, this paper proposes a novel extension to CGAC, named as Extended CGAC (ECGAC), which replaces the robustification filter by a weight filter and modifies the update law with the prediction error from a closed loop state predictor. The new scheme is validated through experiments in an Unmanned Underwater Vehicle (UUV). The results indicate that ECGAC substantially improves the tracking performance with less control effort and increased robustness to noise and time-delay.

Keywords: Adaptive control, measurement noise, time-delay, transient tracking, unmanned underwater vehicle, robustness.

6.1 Introduction

Adaptive control is an important control methodology for Unmanned Underwater Vehicles (UUVs) due to its inherent ability to adapt to changes that affect the vehicle behaviour. During operations UUVs are consistently subjected to various parameter changes that affect the vehicle motion such as changes in the weight due to different payloads (Cavalletti, Ippoliti & Longhi 2011), changes in buoyancy due variations in the pressure, temperature and salinity (Wu, Liu & Xu 2014), change in the control effectiveness due to partial loss of thrust (Pivano 2008) and changes in the hydrodynamic load near the free surface (Sayer 1996). The mitigation of the effects of such changes on the motion of the vehicle is a crucial factor in complex UUV applications that require precise manoeuvres. These include semi-autonomous ROVs used in applications such as tidal energy infrastructure servicing under high-flow conditions (Proctor et al. 2015), AUVs used for assisting divers to carry out underwater task (Stilinović, Nađ & Mišković 2015), launching and recovering of torpedo shaped AUVs from submarines for military purposes (Rodgers et al. 2008). To enable these applications it is essential that UUVs have good tracking performance throughout their entire mission. Therefore, the controllers used in UUVs should adapt to the changes and ensure good tracking in both steady state and, more importantly, transient time.

Even though adaptive control has been proposed as a promising solution (Antonelli et al. 2001; Fossen & Fjellstad 1996; McFarland & Whitcomb 2014; Valladarez & Toit 2015; Yuh, Nie & Lee 1999), there are certain drawbacks that prevent their widespread use in advanced UUV applications. One of the major drawbacks is the trade-off between transient tracking performance and adaptation gains. High adaptation gains are known to achieve accurate transient tracking, which in turn leads to oscillations in the control signal (Stepanyan & Krishnakumar 2012a), reduced robustness to noise and time-delay, and instability (Crespo, Matsutani & Annaswamy 2010). On the other hand low adaptation gain mitigates the above issues, but it leads to poor reference tracking in the transient region (Zang & Bitmead 1994) that can be dangerous in cluttered environments. Several solutions (Cao & Hovakimyan 2006a; Stepanyan & Krishnakumar 2010; Yucelen & Haddad 2012; Yucelen & Johnson 2012a) to this conundrum have been proposed in the past decade including L1 adaptive control (Cao & Hovakimyan 2006a) which has been applied to UUVs by Maalouf (2013) and

Valladarez (2015) with encouraging results. This method uses a modified Model reference Adaptive Control (MRAC) architecture that places a low pass filter in a unique position that subverts the high frequency signals and decouples adaptation from robustness (Cao & Hovakimyan 2006a). This decoupling theoretically enables the use of high adaptation gains to increase transient tracking but concern has been expressed by several researches that high adaptation gains could lead to numerical instability (Campbell et al. 2010b; Ioannou et al. 2014) and parameter freezing (Ortega & Panteley 2014). Some of the other solutions (Stepanyan & Krishnakumar 2010; Yucelen & Haddad 2012), although not widely applied, also use some form of filtering with high adaptation gains and could face the same questions as L1 adaptive control.

Therefore, the authors have focused on modifications to MRAC that uses low adaptive gains, which provide an emphasis on stability and smooth control signals while improving transient performance. One such method is composite adaptation, which was verified through simulations by the authors in Makavita et al. (2015b) and Makavita et al. (2016b) for two different variants proposed by Lavretsky et al. namely Composite MRAC (CMRAC) (Lavretsky 2009) and Predictor-based MRAC (PMRAC) (Lavretsky, Gadient & Gregory 2010). Experimental work carried out by the authors comparing CMRAC and PMRAC with MRAC validated the simulation results while indicating PMRAC performed significantly better than both MRAC and CMRAC (Makavita et al. 2017a).

Another method is Command Governor Adaptive Control (CGAC) (Yucelen & Johnson 2012b) which uses an additional linear dynamical system, driven by the system error, named command governor to modify the command signal. This in turn leads to improved transient performance at low adaptation gains and an inherent disturbance rejection capability (Yucelen & Johnson 2012b). The authors initially applied CGAC to a UUV in simulation to verify the tracking and disturbance rejection improvements in Makavita et al. (2015a). A possible drawback of CGAC is that the command governor has the tendency to amplify measurement noise (Yucelen & Johnson 2012b). A solution to this was provided in Yucelen and Johnson (2012b) that uses a low pass filter termed robustification filter to filter out noise from the command governor signal. The authors confirmed through simulations the efficacy of this solution named Robust CGAC (RCGAC) for UUV operations in Makavita et al. (2016a) and showed that at high noise

levels the robustification filter by itself was insufficient and some input filtering was also required. In addition, it was shown that time-delay due to input filtering can cause instability and the robustification filter can also increase robustness to such time-delays. Furthermore, in the same study it was confirmed that RCGACs disturbance rejection ability allowed it to overcome a significant actuator dead-zone without using an additional dead-zone inverse. The authors validated through experiments the tracking improvement, disturbance rejection, and dead-zone overcoming effect in Makavita et al. (2017c) for heading control of the AMC ROV (Fig. 2). A further experimental study (Makavita et al. 2017b) of RCGAC applied to depth control provided an opportunity to validate the effect of robustification filter due to high input noise from depth rate estimation. It was seen that while the robustification filter is required to increase robustness to measurement noise and time-delay, a filter designed to handle high noise levels cause a short initial period of very poor reference tracking. Apart from this initial period RCGAC outperformed MRAC in tracking, disturbance rejection, operation under thrust loss, control effort and smooth control signal.

Although these experimental results were promising it was determined that a solution was required for this initial period of poor performance as well as further reducing noise levels without sacrificing tracking performance. This paper presents a possible solution by removing the robustification filter and replacing it with a weight filter based on the approach by Yucelen and Haddad (2013) to provide an improved robustness to noise and time-delay without incurring an initial period of poor tracking. In addition, it is combined with the state predictor modification introduced in Lavretsky, Gadient and Gregory (2010) for PMRAC to improve the overall tracking performance. The final control system with these modifications is termed ECGAC, which is tested using experiments for depth control and compared with previous results derived in Makavita et al. (2017b) for depth control using RCGAC.

6.2 Adaptive Control Architecture

This section gives a brief introduction to standard MRAC, the command governor modification, the weight filter modification and the state predictor modification.

6.2.1 Model Reference Adaptive Control (MRAC)

As described in Yucelen and Johnson (2013), consider the nonlinear uncertain

dynamical system given by,

$$\dot{\boldsymbol{x}}(t)=\boldsymbol{A}\boldsymbol{x}(t)+\boldsymbol{H}\boldsymbol{\delta}\left(\boldsymbol{x}(t)\right)+\boldsymbol{B}u(t),\ \ \boldsymbol{x}(0)=\boldsymbol{x}_0,\ t=\bar{\mathbb{R}}_+ \tag{6.1}$$

where $\boldsymbol{x}(t)\in\mathbb{R}^p$ is the state vector, $\boldsymbol{u}(t)\in\mathbb{R}^q$ is the control input, $\boldsymbol{\delta}:\mathbb{R}^p\to\mathbb{R}^q$ is an uncertainty, $\boldsymbol{A}\in\mathbb{R}^{p\times p}$ is a known system matrix, $\boldsymbol{B}\in\mathbb{R}^{p\times q}$ is an unknown control input matrix, $\boldsymbol{H}\in\mathbb{R}^{p\times q}$ is a known uncertainty input matrix, and the pair $(\boldsymbol{A},\boldsymbol{B})$ is controllable. It is also assumed that $\delta(\boldsymbol{x})$ is parameterized as $\delta(\boldsymbol{x})=\boldsymbol{W}^T\boldsymbol{\sigma}(\boldsymbol{x})$, where $\boldsymbol{W}\in\mathbb{R}^{s\times q}$ is an unknown weight matrix, and $\boldsymbol{\sigma}:\mathbb{R}^q\to\mathbb{R}^s$ is a known basis function of the form $\boldsymbol{\sigma}(\boldsymbol{x})=\left[\sigma_1(\boldsymbol{x}),\sigma_2(\boldsymbol{x}),\ldots..,\sigma_s(\boldsymbol{x})\right]^T$. It is further assumed that $\boldsymbol{B}$ is parameterized as $\boldsymbol{B}=\boldsymbol{H}\Lambda$, where $\det\left(\boldsymbol{H}^T\boldsymbol{H}\right)\neq 0$, and $\boldsymbol{\Lambda}\in\mathbb{R}^{q\times q}$ is an unknown control effectiveness matrix with positive diagonal elements.

The ideal reference model that specifies a desired closed loop dynamical system performance is given by,

$$\dot{\boldsymbol{x}}_m(t)=\boldsymbol{A}_m\boldsymbol{x}_m(t)+\boldsymbol{B}_m\boldsymbol{c}(t),\ \ \boldsymbol{x}_m(0)=\boldsymbol{x}_0,\ t=\bar{\mathbb{R}}_+ \tag{6.2}$$

where $\boldsymbol{x}_m(t)\in\mathbb{R}^p$ is the reference state vector, $\boldsymbol{c}(t)\in\mathbb{R}^q$ is the given uniformly continuous bounded command, $\boldsymbol{A}_m\in\mathbb{R}^{p\times p}$ is the Hurwitz reference system matrix, and $\boldsymbol{B}_m\in\mathbb{R}^{p\times q}$ is the command input matrix.

The objective of MRAC is to design a feedback control law $\boldsymbol{u}(t)$ such that $\boldsymbol{x}(t)$ asymptotically follows $\boldsymbol{x}_m(t)$, i.e. $\lim_{t\to\infty}\|\boldsymbol{e}_m\|=0$, where $\boldsymbol{e}_m\triangleq\boldsymbol{x}-\boldsymbol{x}_m$ is the system error. Let $\boldsymbol{u}(t)$ be given by,

$$\boldsymbol{u}(t)=\boldsymbol{u}_n(t)+\boldsymbol{u}_a(t) \tag{6.3}$$

where $\boldsymbol{u}_n(t)\in\mathbb{R}^q$ is the nominal feedback control law and $\boldsymbol{u}_a(t)\in\mathbb{R}^q$ is the adaptive feedback control law. The nominal control law is given by

$$\boldsymbol{u}_n(t)=\boldsymbol{K}_1\boldsymbol{x}(t)+\boldsymbol{K}_2\boldsymbol{c}(t) \tag{6.4}$$

where $\boldsymbol{K}_1 \in \mathbb{R}^{q\times p}$ is the nominal feedback gain and $\boldsymbol{K}_2 \in \mathbb{R}^{q\times q}$ is the nominal feedforward gain, such that the following matching condition holds.

$$\boldsymbol{A}_m = \boldsymbol{A} + \boldsymbol{H}\boldsymbol{K}_1,\ \boldsymbol{B}_m = \boldsymbol{H}\boldsymbol{K}_2 \text{ and } det(\boldsymbol{K}_2) \neq 0. \tag{6.5}$$

Applying the control law defined in (6.3) into (6.1) and simplifying yields,

$$\dot{\boldsymbol{x}}(t) = \boldsymbol{A}_m \boldsymbol{x}(t) + \boldsymbol{B}_m \boldsymbol{c}(t) + \boldsymbol{H}\boldsymbol{\Lambda}\left[\boldsymbol{W}_{un}^T \boldsymbol{u}_n(t) + \boldsymbol{u}_a(t) + \boldsymbol{W}_{\sigma}^T \boldsymbol{\sigma}(\boldsymbol{x})\right] \tag{6.6}$$

where $\boldsymbol{W}_{un} \triangleq 1 - \boldsymbol{\Lambda}^{-1} \in \mathbb{R}^{q\times q}$ and $\boldsymbol{W}_{\sigma} \triangleq \boldsymbol{W}\boldsymbol{\Lambda}^{-1} \in \mathbb{R}^{s\times q}$. Furthermore, the adaptive feedback law is selected as,

$$\boldsymbol{u}_a(t) = -\hat{\boldsymbol{W}}_{un}{}^T(t)\boldsymbol{u}_n(t) - \hat{\boldsymbol{W}}_{\sigma}{}^T(t)\boldsymbol{\sigma}(\boldsymbol{x}) \tag{6.7}$$

where $\hat{\boldsymbol{W}}_{un}(t) \in \mathbb{R}^{q\times q}$ and $\hat{\boldsymbol{W}}_{\sigma}(t) \in \mathbb{R}^{s\times q}$ are estimates of $\boldsymbol{W}_{un}$ and $\boldsymbol{W}_{\sigma}$, satisfying the update laws given by,

$$\dot{\hat{\boldsymbol{W}}}_{un}(t) = \boldsymbol{\Gamma}_{un}\boldsymbol{u}_n(t)\boldsymbol{e}_m{}^T\boldsymbol{P}\boldsymbol{H} \tag{6.8}$$

$$\dot{\hat{\boldsymbol{W}}}_{\sigma}(t) = \boldsymbol{\Gamma}_{\sigma}\boldsymbol{\sigma}\left(\boldsymbol{x}(t)\right)\boldsymbol{e}_m{}^T\boldsymbol{P}\boldsymbol{H} \tag{6.9}$$

where $\boldsymbol{\Gamma}_{un} \in \mathbb{R}^{q\times q}$ and $\boldsymbol{\Gamma}_{\sigma} \in \mathbb{R}^{s\times s}$ are learning rates and $\boldsymbol{P} = \boldsymbol{P}^T > 0$ is the solution of the Lyapunov equation $\boldsymbol{0} = \boldsymbol{A}_m^T\boldsymbol{P} + \boldsymbol{P}\boldsymbol{A}_m + \boldsymbol{Q}$ for some $\boldsymbol{Q} = \boldsymbol{Q}^T > 0$.

Now using (6.7) in (6.6) yields

$$\dot{\boldsymbol{x}}(t) = \boldsymbol{A}_m \boldsymbol{x}(t) + \boldsymbol{B}_m \boldsymbol{c}(t) - \boldsymbol{H}\boldsymbol{\Lambda}\left[\tilde{\boldsymbol{W}}_{un}^T(t)\boldsymbol{u}_n(t) + \tilde{\boldsymbol{W}}_{\sigma}^T(t)\boldsymbol{\sigma}(\boldsymbol{x})\right] \tag{6.10}$$

where $\tilde{\boldsymbol{W}}_{un}(t) \triangleq \hat{\boldsymbol{W}}_{un}(t) - \boldsymbol{W}_{un} \in \mathbb{R}^{q\times q}$ and $\tilde{\boldsymbol{W}}_{\sigma}(t) \triangleq \hat{\boldsymbol{W}}_{\sigma}(t) - \boldsymbol{W}_{\sigma} \in \mathbb{R}^{s\times q}$. The system error dynamics is derived by subtracting (6.2) from (6.10) to give,

$$\dot{\boldsymbol{e}}_m(t) = \boldsymbol{A}_m \boldsymbol{e}_m(t) - \boldsymbol{H}\boldsymbol{\Lambda}\left[\tilde{\boldsymbol{W}}_{un}{}^T(t)\boldsymbol{u}_n(t) + \tilde{\boldsymbol{W}}_{\sigma}{}^T(t)\boldsymbol{\sigma}(\boldsymbol{x})\right] \tag{6.11}$$

It is shown by the Lyapunov analysis in Yucelen and Johnson (2013) that for the update laws (6.8) and (6.9) $\lim_{t\to\infty} \|\boldsymbol{e}_m\| = 0$.

6.2.2 Command Governor Modification

It is proposed in Yucelen and Johnson (2013) that fast transient response with smooth control signals can be achieved by adding a new command governor to the MRAC architecture. Let the command signal in (6.2) and (6.4) be given by,

$$\boldsymbol{c}(t) = \boldsymbol{c}_d(t) + \boldsymbol{G}\boldsymbol{g}(t) \tag{6.12}$$

where $\boldsymbol{c}_d(t) \in \mathbb{R}^q$ is now the given uniformly continuous bounded command and $\boldsymbol{G}\boldsymbol{g}(t) \in \mathbb{R}^{q\times q}$ is the command governor signal with $\boldsymbol{G} \in \mathbb{R}^{q\times p}$ being, the matrix defined by,

$$\boldsymbol{G} = \boldsymbol{K}_2^{-1}\boldsymbol{H}^L = \boldsymbol{K}_2^{-1}(\boldsymbol{H}^T\boldsymbol{H})^{-1}\boldsymbol{H}^T \tag{6.13}$$

The command governor output $\boldsymbol{g}(t) \in \mathbb{R}^{p\times q}$ is generated by,

$$\dot{\boldsymbol{f}}(t) = -\lambda \boldsymbol{f}(t) + \lambda \boldsymbol{e}_m(t), \quad \boldsymbol{f}(0) = \boldsymbol{0}, \quad t \in \bar{\mathbb{R}}_+ \tag{6.14}$$

$$\boldsymbol{g}(t) = \lambda \boldsymbol{f}(t) + \left(\boldsymbol{A}_m - \lambda \boldsymbol{I}_p\right)\boldsymbol{e}_m(t) \tag{6.15}$$

where $\boldsymbol{f}(t)$ is the command governor state vector and $\lambda = \mathbb{R}_+$ is the command governor gain.

Due to the command governor output, (6.2) and (6.10) are respectively modified as,

$$\dot{\boldsymbol{x}}_m(t) = \boldsymbol{A}_m\boldsymbol{x}_m(t) + \boldsymbol{B}_m c_d(t) + \boldsymbol{P}_H\boldsymbol{g}(t) \tag{6.16}$$

$$\dot{\boldsymbol{x}}(t) = \boldsymbol{A}_m\boldsymbol{x}(t) + \boldsymbol{B}_m\boldsymbol{c}_d(t) + \boldsymbol{P}_H\boldsymbol{g}(t) - \boldsymbol{H}\boldsymbol{\Lambda}\left[\tilde{\boldsymbol{W}}_{un}^T\boldsymbol{u}_n(t) + \tilde{\boldsymbol{W}}_{\sigma}^T\boldsymbol{\sigma}(\boldsymbol{x})\right] \tag{6.17}$$

where $\boldsymbol{P}_H = \boldsymbol{H}(\boldsymbol{H}^T\boldsymbol{H})^{-1}\boldsymbol{H}^T$. However this does not change the system error dynamics given by (6.11) as seen by subtracting (6.16) from (6.17). Therefore, the update laws in (6.8) and (6.9) also remain the same.

It has been shown in *Theorem 5.1* in Yucelen and Johnson (2013) using Lyapunov analysis that the system with the command governor is also asymptotically stable with $\lim_{t\to\infty}\|\boldsymbol{e}_m\| = 0$, as well as $\lim_{t\to\infty}\boldsymbol{g}(t) = 0$. From this it can be shown that the modified

reference model in (6.16) asymptotically converge to the ideal reference model given by,

$$\dot{\boldsymbol{x}}_l(t) = \boldsymbol{A}_m \boldsymbol{x}_l(t) + \boldsymbol{B}_m c_d(t) \tag{6.18}$$

where $\boldsymbol{x}_l(t) \in \mathbb{R}^p$ is the ideal reference vector. Therefore, the uncertain dynamical system (6.1) approaches the ideal reference model (6.18) in steady state.

In addition, from *Proposition 6.1* in Yucelen and Johnson (2013), if λ is sufficiently large, the uncertainties $\boldsymbol{H}\boldsymbol{\Lambda}\left[\tilde{\boldsymbol{W}}_{un}^T \boldsymbol{u}_n(t) + \tilde{\boldsymbol{W}}_{\sigma}^T \boldsymbol{\sigma}(\boldsymbol{x})\right]$ in (6.17) are rapidly suppressed in transient time through $\boldsymbol{P}_H \boldsymbol{g}(t)$, and the system approximates the ideal reference model (6.18) in transient time without using high learning rates.

One concern with this method is that at large command governor gain values the noise in system will amplify to the output of the command governor. Therefore, in order to make the control signal less sensitive to measurement noise, the following robustification was proposed in Yucelen and Johnson (2013). Let the command signal $\boldsymbol{c}(t)$ be given by,

$$\boldsymbol{c}(t) = \boldsymbol{c}_d(t) + \boldsymbol{G}\boldsymbol{g}_f(t) \tag{6.19}$$

where $\boldsymbol{g}_f(t) \in \mathbb{R}^{p \times q}$ is the modified command governor output generated through a low-pass filter as given below,

$$\dot{\boldsymbol{g}}_f(t) = -\kappa \boldsymbol{g}_f(t) + \kappa \boldsymbol{g}(t), \;\; \boldsymbol{g}_f(0) = \boldsymbol{0}, \;\; t \in \bar{\mathbb{R}}_+ \tag{6.20}$$

and $\kappa = \mathbb{R}_+$ is the command governor filter gain that should be selected sufficiently small to ensure efficient low pass filtering. This does not affect the steady state performance. However from *Proposition 7.1* in Yucelen and Johnson (2013), in transient time the system (6.1) does not approximates the ideal reference model (6.18), rather approximates the ideal reference model (6.18) modified by a term $\boldsymbol{P}_H\left(\boldsymbol{g}_f(t) - \boldsymbol{g}(t)\right)$, which satisfies $\lim_{t \to \infty} \boldsymbol{P}_H\left(\boldsymbol{g}_f(t) - \boldsymbol{g}(t)\right) = 0$. Therefore, it is expected that there will be deviations from the ideal reference model initially until the modification term has died down. The architecture with the robustification filter is

referred to as RCGAC in this paper.

6.2.3 Weight Filter Modification

In Yucelen and Haddad (2013) a weight filter was introduced to address high-frequency oscillations in MRAC with high gains. Taking $\hat{\boldsymbol{W}}(t) \in \mathbb{R}^{a\times b}$ as a general weight estimate that can represent both $\hat{\boldsymbol{W}}_{un}(t)$ and $\hat{\boldsymbol{W}}_{\sigma}(t)$, a low-pass filtered weight estimate $\hat{\boldsymbol{W}}_f(t) \in \mathbb{R}^{a\times b}$ of $\hat{\boldsymbol{W}}(t)$ is given by

$$\hat{\boldsymbol{W}}_f(t) = \boldsymbol{\Gamma}_f\left[\hat{\boldsymbol{W}}(t) - \hat{\boldsymbol{W}}_f(t)\right],\ \hat{\boldsymbol{W}}_f(0) = \hat{\boldsymbol{W}}_0,\ t \geq 0 \tag{6.21}$$

where $\boldsymbol{\Gamma}_f \in \mathbb{R}^{a\times a}$ is a positive definite filter gain matrix chosen such that $\lambda_{\max}(\boldsymbol{\Gamma}_f) \leq \gamma_{f,\max}$, and where $\gamma_{f,\max} \geq 0$ is a design parameter that needs to be small enough to cut off high frequencies from $\hat{\boldsymbol{W}}(t)$.

For clarity, both (6.8) and (6.9) are represented by a general update law given by,

$$\dot{\hat{\boldsymbol{W}}}(t) = \boldsymbol{\Gamma}\boldsymbol{\beta}(t)\boldsymbol{e}_m{}^T\boldsymbol{P}\boldsymbol{H} \tag{6.22}$$

where $\boldsymbol{\Gamma} = \boldsymbol{\Gamma}_{un}\ or\ \boldsymbol{\Gamma}_{\sigma}$ and $\boldsymbol{\beta}(\mathrm{t}) = \boldsymbol{\sigma}(\boldsymbol{x}(t))\ or\ \boldsymbol{u}_n(t)$. A modification term was added to the update law (6.22) to enforce a distance condition between the trajectories of $\hat{\boldsymbol{W}}(t)$ and $\hat{\boldsymbol{W}}_f(t)$. This leads to a minimization problem of the cost function J given by,

$$J(\hat{\boldsymbol{W}}, \hat{\boldsymbol{W}}_f) = \frac{1}{2}\left\|\hat{\boldsymbol{W}} - \hat{\boldsymbol{W}}_f\right\|_F^2 \tag{6.23}$$

with a negative gradient with respect to $\hat{\boldsymbol{W}}(t)$ given by,

$$\frac{\partial\left[-J(\hat{\boldsymbol{W}}(t), \hat{\boldsymbol{W}}_f(t)\right]}{\partial\hat{\boldsymbol{W}}(t)} = -\left(\hat{\boldsymbol{W}}(t) - \hat{\boldsymbol{W}}_f(t)\right),\ t \geq 0 \tag{6.24}$$

which is also the structure of the proposed modification term. This leads to the modified update law of (6.22) given by,

$$\dot{\hat{\boldsymbol{W}}}(t) = \boldsymbol{\Gamma}\left[\boldsymbol{\beta}(t)\boldsymbol{e}_m{}^T\boldsymbol{P}\boldsymbol{H} - \alpha\left(\hat{\boldsymbol{W}}(t) - \hat{\boldsymbol{W}}_f(t)\right)\right] \tag{6.25}$$

which yield the following modified update laws for (6.8) and (6.9) respectively,

$$\dot{\hat{\boldsymbol{W}}}_{un}(t) = \boldsymbol{\Gamma}_{un}\left[\boldsymbol{u}_n(t)\boldsymbol{e}_m{}^T\boldsymbol{PH} - \alpha\left(\hat{\boldsymbol{W}}_{un}(t) - \hat{\boldsymbol{W}}_{un_f}(t)\right)\right] \tag{6.26}$$

$$\dot{\hat{\boldsymbol{W}}}_{\sigma}(t) = \boldsymbol{\Gamma}_{\sigma}\left[\boldsymbol{\sigma}\left(\boldsymbol{x}(t)\right)\boldsymbol{e}_m{}^T\boldsymbol{PH} - \alpha\left(\hat{\boldsymbol{W}}_{\sigma}(t) - \hat{\boldsymbol{W}}_{\sigma_f}(t)\right)\right] \tag{6.27}$$

where $\alpha > 0$ is a modification gain, and $\hat{\boldsymbol{W}}_{un_f}(t)$ and $\hat{\boldsymbol{W}}_{\sigma_f}(t)$ are the low-pass filtered weight estimate of $\hat{W}_{un}(t)$ and $\hat{W}_{\sigma}(t)$ respectively.

This modification is applied to the update laws for a CGAC system in Yucelen and Johnson (2012c) for the purpose of enabling large domain operations and/or high gain learning rates. The stability of a CGAC system with the modified update laws are proven and presented as *Theorem 3* in Yucelen and Johnson (2012c). Therefore, the previous results for CGAC in section 6.2.2 still hold under the new update laws. In addition, as the robustification filter is no longer applied, the ideal reference model is not modified by the term $\boldsymbol{P}_H\left(\boldsymbol{g}_f(t) - \boldsymbol{g}(t)\right)$. Thus, in transient time the system now directly approximates the ideal reference model (6.18).

Another advantage of using a weight filter apart from filtering high frequency content is shown using a first order example in Yucelen and Haddad (2013). From *Remark 3.2* in Yucelen and Haddad (2013), for $a = b = 1$ and $\boldsymbol{z}(t) \triangleq \boldsymbol{\beta}(t)\boldsymbol{e}_m^T(t)\boldsymbol{PB}$ with $\boldsymbol{\beta}(t) = 1$, $\boldsymbol{\Gamma} = \gamma$, $\boldsymbol{\Gamma}_f = \gamma_f$, $\hat{\boldsymbol{W}}(0) = 0$ and $\hat{\boldsymbol{w}}_f(0) = 0$ we obtain $\dfrac{\hat{W}(s)}{z(s)} = \dfrac{\gamma}{s}$ from (6.22) and $\dfrac{\hat{W}(s)}{z(s)} = \dfrac{\gamma}{s}\left(\dfrac{s+\gamma_f}{s+\gamma_f+\gamma\alpha}\right)$ from (6.25). Thus, it is seen that the modification term adds a phase lead compensator to the original system, which in turn improves the phase margin.

This adaptive control architecture is referred to as WCGAC in this paper and has the capability to;

1) remove high frequency noise due to low pass filtering effect of the weight filter;

2) increase robustness to time-delay due to improved phase margin; and
3) improve transient performance compared to RCGAC due to removal of modification term $\boldsymbol{P}_H\left(\boldsymbol{g}_f(t)-\boldsymbol{g}(t)\right)$

6.2.4 State Predictor Modification

In MRAC described in section 6.2.1, only the system error is used to learn the parameter values. To improve tracking a prediction error can be combined with the system error. Towards this the predictor dynamics is introduced in Lavretsky, Gadient and Gregory (2010) as,

$$\dot{\hat{\boldsymbol{x}}}(\mathrm{t})=\boldsymbol{A}_{prd}(\hat{\boldsymbol{x}}(\mathrm{t})-\boldsymbol{x}(\mathrm{t}))+\boldsymbol{A}_m\boldsymbol{x}(\mathrm{t})+\boldsymbol{B}_m\boldsymbol{c}(\mathrm{t}) \tag{6.28}$$

where $\boldsymbol{A}_{prd}\in\mathbb{R}^{p\times p}$ is a Hurwitz matrix, and $\hat{\boldsymbol{x}}(\mathrm{t})\in\mathbb{R}^p$ is the predictor states vector. This state predictor differs from previous state predictor MRAC schemes in having a closed looped structure as identified in Gibson, Annaswamy and Lavretsky (2013).

The prediction error is defined as $\hat{\boldsymbol{e}}(t)=\hat{\boldsymbol{x}}(t)-\boldsymbol{x}(t)$. The predictor error dynamics can be derived by subtracting (6.10) from (6.28) as

$$\dot{\hat{\boldsymbol{e}}}(t)=\boldsymbol{A}_m\hat{\boldsymbol{e}}(t)+\boldsymbol{H}\boldsymbol{\Lambda}\left[\tilde{\boldsymbol{W}}_{un}{}^T(t)\boldsymbol{u}_n(t)+\tilde{\boldsymbol{W}}_{\sigma}{}^T(t)\boldsymbol{\sigma}(\boldsymbol{x})\right] \tag{6.29}$$

It can be shown by a Lyapunov analysis similar to Lavretsky, Gadient and Gregory (2010) that if the update laws are given as shown in equation (6.30) and (6.31), then,

1) The system error is uniformly ultimately bounded, square integrable, and globally asymptotically stable. i.e. $\lim_{t\to\infty}\|\boldsymbol{e}_m\|=0$
2) The prediction error is uniformly ultimately bounded, square integrable, and globally asymptotically stable. i.e. $\lim_{t\to\infty}\|\hat{\boldsymbol{e}}\|=0$

$$\dot{\hat{\boldsymbol{W}}}_{un}(t)=\boldsymbol{\Gamma}_{un}\boldsymbol{u}_n(t)\left[\boldsymbol{e}_m{}^T\boldsymbol{P}-\hat{\boldsymbol{e}}^T\boldsymbol{P}_{prd}\right]\boldsymbol{H} \tag{6.30}$$

$$\dot{\hat{\boldsymbol{W}}}_{\sigma}(t)=\boldsymbol{\Gamma}_{\sigma}\boldsymbol{\sigma}\left(\boldsymbol{x}(t)\right)\left[\boldsymbol{e}_m{}^T\boldsymbol{P}-\hat{\boldsymbol{e}}^T\boldsymbol{P}_{prd}\right]\boldsymbol{H} \tag{6.31}$$

where $\boldsymbol{P}_{prd}=\boldsymbol{P}_{prd}{}^T>0$ is the solution of the Lyapunov equation

$$\mathbf{0} = \boldsymbol{A}_{prd}{}^{T}\boldsymbol{P}_{prd} + \boldsymbol{P}_{prd}\boldsymbol{A}_{prd} + \boldsymbol{Q}_{prd} \quad \text{for some } \boldsymbol{Q}_{prd} = \boldsymbol{Q}_{prd}{}^{T} > 0.$$

Now if the command governor modification of section 6.2.2 is added it will modify (6.10) to (6.17) and (6.28) as,

$$\dot{\hat{\boldsymbol{x}}}(\mathrm{t}) = \boldsymbol{A}_{prd}\hat{\boldsymbol{e}}(t) + \boldsymbol{A}_{m}\boldsymbol{x}(\mathrm{t}) + \boldsymbol{B}_{m}\boldsymbol{c}_{d}(\mathrm{t}) + \mathbf{P}_{H}\boldsymbol{g}(t). \tag{6.32}$$

However, the addition of the command governor output does not change the predictor error dynamics given by (6.29) as seen by subtracting (6.17) from (6.32). Therefore, the update laws in (6.30) and (6.31) remain the same and the steady state and transient performance guarantees of CGAC will be preserved.

If the weight filter modification is also used, the update laws are now given by,

$$\dot{\hat{\boldsymbol{W}}}_{un}(t) = \boldsymbol{\Gamma}_{un}\left[\boldsymbol{u}_{n}(t)\left(\boldsymbol{e}_{m}{}^{T}\boldsymbol{P} - \hat{\boldsymbol{e}}^{T}\boldsymbol{P}_{prd}\right)\boldsymbol{H} - \alpha\left(\hat{\boldsymbol{W}}_{un}(t) - \hat{\boldsymbol{W}}_{un_{f}}(t)\right)\right] \tag{6.33}$$

$$\dot{\hat{\boldsymbol{W}}}_{\sigma}(t) = \boldsymbol{\Gamma}_{\sigma}\left[\boldsymbol{\sigma}\left(\boldsymbol{x}(t)\right)\left(\boldsymbol{e}_{m}{}^{T}\boldsymbol{P} - \hat{\boldsymbol{e}}^{T}\boldsymbol{P}_{prd}\right)\boldsymbol{H} - \alpha\left(\hat{\boldsymbol{W}}_{\sigma}(t) - \hat{\boldsymbol{W}}_{\sigma_{f}}(t)\right)\right] \tag{6.34}$$

The resulting adaptive control architecture of WCGAC with a composite adaptation based on the closed loop state predictor is shown in Fig. 6.1 and is referred in this paper as Extended CGAC (ECGAC). The stability proof of this method is given in Appendix IV.

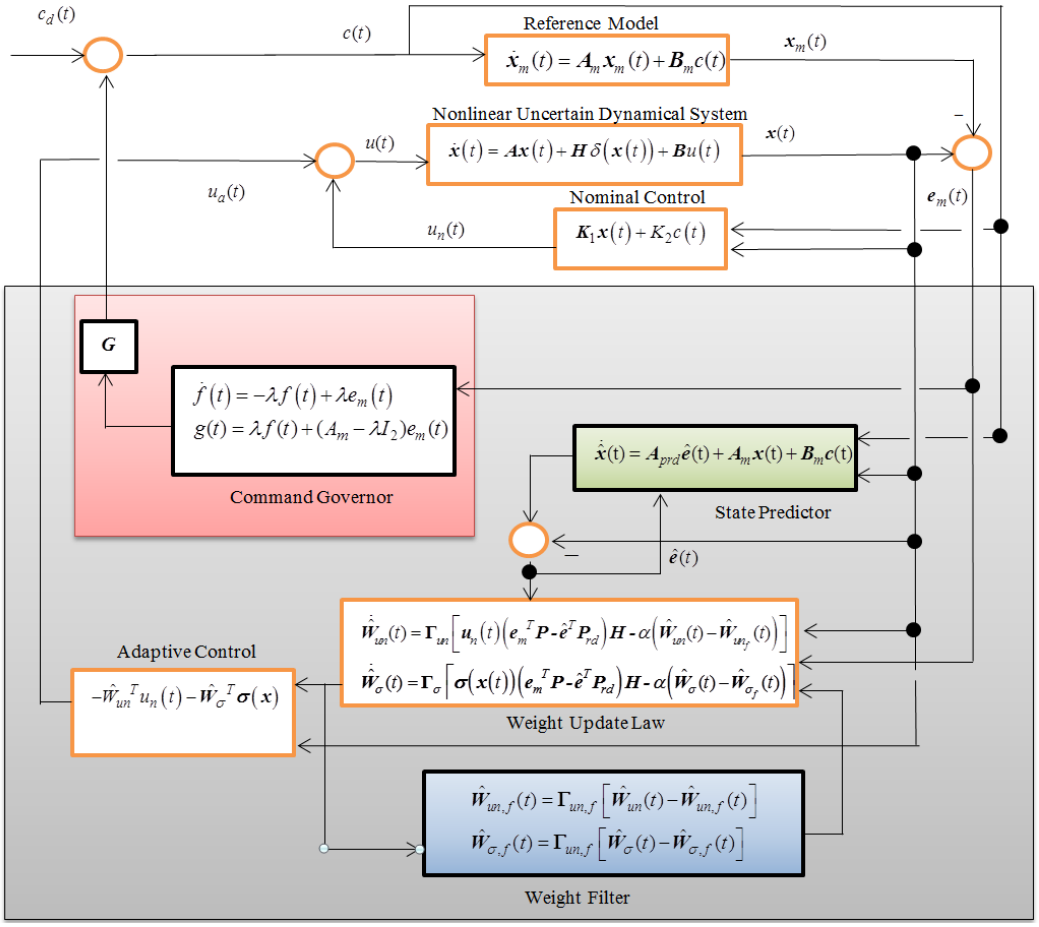

Figure 6. 1: Visualization of the proposed ECGAC architecture

6.3 Mathematical Model

For the purpose of marine control system design a simplified model of the complex 6-DOF kinematics and dynamics must be developed. This CPM is also used as a basis for analytical stability analysis and should capture only the essential features of the system. This section describes the CPM used in this study.

6.3.1 Process Plant Model

The PPM has been described in Chapter 4 section 4.3.1 and for the sake of brevity will not be repeated here.

6.3.2 Control Plant Model for Depth

The CPM has been described in Chapter 4 section 4.3.2 and Chapter 5 section 5B.3.2.1, and for the sake of brevity will not be repeated here.

6.3.3 Reference Model

This reference model has been described in Chapter 3 section 3A.3.2 and for the sake of brevity will not be repeated here.

6.4 Experimental Setup and Test cases

The experimental setup has been described in Chapter 4 section 4.4 and for the sake of brevity will not be repeated here.

6.4.1 Parameter Values

The adaptive control parameters were set as follows. For simplicity, all learning rates were taken as dependent on a single positive constant γ such that $\boldsymbol{\Gamma}_{\sigma} = \gamma \boldsymbol{I}_3$ and $\Gamma_{un} = \gamma$. Unless otherwise specified all controllers used $\gamma = 1$. The command governor gain λ was set to 100 as done in both Makavita et al. (2015a) and Makavita et al. (2017b). The robustification filter gain κ was set to 3 as done in Makavita et al. (2017b). For simplicity, weight filter gains were taken as dependent on a single positive constant γ_f such that $\Gamma_{un,f} = \gamma_f$ and $\boldsymbol{\Gamma}_{\sigma,f} = \gamma_f \mathbf{I}_3$ with $\gamma_f = 1$. The modification gain α was set to 10. For the state predictor from Lavretsky, Gadient and Gregory (2010), it is proposed that $\boldsymbol{A}_{prd} = \mu \boldsymbol{A}_m$ and $\boldsymbol{P}_{prd} = \mu \boldsymbol{P}$ where μ is a positive scalar. The value for μ is set to 10 as done in both Makavita et al. (2016b) and Makavita et al. (2017a).

All the initial values of the CPM parameters were set to zero ($\hat{W}_{un} = 0$ and $\hat{\boldsymbol{W}}_{\sigma} = \begin{bmatrix} 0 & 0 & 0 \end{bmatrix}$), thus assuming no *a priori* knowledge. While this is an extreme assumption considering that some values are known, albeit approximately (e.g. mass), it provides a good basis to test the ability of the controller under severe uncertainty. The reference model parameters were set to $\omega_n = 0.3$ rad/s and $\zeta = 1$, which yields $\boldsymbol{K}_1 = [-0.09 \quad -0.6]$ and $K_2 = 0.09$.

6.4.2 Experimental Scenario

The experiments were conducted for different variants of CGAC including RCGAC, WCGAC and ECGAC under three different phases. The first phase was the comparison between RCGAC and WCGAC for a normal depth change command. The second phase was the comparison of ECGAC with both WCGAC and RCGAC for a normal depth

change command. The final phase was the evaluation of ECGAC performance under a sudden parameter changes represented by the change in control effectiveness due to thrust loss. More details on the experimental scenarios are given below:

6.4.2.1 RCGAC vs WCGAC

RCGAC and WCGAC were applied to a depth change manoeuvre of 150s duration and their performances were compared, with the main objective of comparing tracking performance in the initial 50s. In addition, tracking performance during the next 100s (after the initial 50s), and control signal noise levels and frequency content was also analysed.

6.4.2.2 ECGAC

The vehicle was tested for depth change for ECGAC and compared with WCGAC and RCGAC. The main objective was to counteract the negative effect of weight filtering on tracking and to further improve tracking over RCGAC. Furthermore, the learning rate was increased slightly with the objective of improving the tracking performance to meet the design specification of having rms depth tracking error of 0.02m or lower for the entire run. In addition, control signal noise levels and frequency content was also analysed.

6.4.2.3 Sudden Parameter Variation

This was represented by a 50% loss of thrust in the vertical thruster during operation. This type of partial failure can occur due to an electrical or mechanical malfunction. This situation was created by halving the voltage to the motor controllers. The partial failure was activated at 150s after the start at a depth of 1m. The objective was to ascertain the ability of ECGAC to overcome such a failure and maintain the depth.

6.5 Experimental Results

For the purpose of measuring system performance the system states were compared with the ideal reference states. Thus, the tracking error is defined as $\boldsymbol{e}_l \triangleq \boldsymbol{x} - \boldsymbol{x}_l$. Performance of control methods were measured using six performance indices shown in Table 6.1. The first four indices were based on the tracking errors in depth (e_d) and depth rate (e_w), where $\boldsymbol{e}_l^T = \begin{bmatrix} e_d & e_w \end{bmatrix}$, while the last two are based on the control effort.

These performance indices were designed based on the work of Fossen and Fjellstad (1996).

Table 6. 1: Definition of the Six Performance Indices

Description	Formulae
rms depth error	$d_{e\_rms} = \sqrt{\frac{1}{N}\sum_{i=1}^{N}(e_d)^2}$
rms depth rate error	$w_{e\_rms} = \sqrt{\frac{1}{N}\sum_{i=1}^{N}(e_w)^2}$
maximum depth error	$d_{e\_\max} = \max(\lvert e_d \rvert)$
maximum depth rate error	$w_{e\_\max} = \max(\lvert e_w \rvert)$
rms normalized control effort	$\tilde{\tau}_{w\_rms} = \sqrt{\frac{1}{N}\sum_{i=1}^{N}(\tau_w)^2}$
maximum normalized control effort	$\tilde{\tau}_{w\_\max} = \max(\lvert \tau_w \rvert)$

In addition, other performance indices such as settling time were used as required. The vertical thruster force, when given numerically or graphically, is the value before the dead-zone inverse value is added.

6.5.1 RCGAC vs WCGAC

The experiments were conducted as mentioned in section 4.2. Initially RCGAC (with the robustification filter) was compared with WCGAC (with the weight filter). The results are given in Fig. 6.2, Fig. 6.3 and Table 6.2. As evident in Fig. 6.2, under RCGAC the vehicle depth and depth rate has a significant deviation in the initial 50s. It then settles to a reasonably acceptable tracking performance in the next 100s after the modification term due to the filter has died down. In contrast for WCGAC, tracking in the initial 50s has significantly improved (Fig. 6.3). A more quantitative analysis can be carried out using the performance metrics presented in Table 6.2, in which the RCGAC and WCGAC performance indices are given in three parts: full run, first 50s, and last 100s. Thus, this analysis will look at the first 50s and next 100s separately and compare the performances to capture the clear distinction in performance between first 50s and next 100s.

Table 6. 2: Performance Indices for R-CGAC and W-CGAC

Performance Indices	RCGAC			WCGAC		
	Full run	**First 50s**	**Next 100s**	**Full run**	**First 50s**	**Next 100s**
d_{e_rms} (m)	0.153	0.265	0.018	0.039	0.055	0.028
$d_{e\_\max}$ (m)	0.600	0.600	0.064	0.170	0.170	0.104
w_{e_rms} (deg/s)	0.045	0.075	0.017	0.0187	0.027	0.013
$w_{e\_\max}$ (deg/s)	0.267	0.267	0.067	0.107	0.107	0.049
$\tilde{\tau}_{w\_rms}$	70.588	116.619	25.942	20.752	24.365	18.903
$\tilde{\tau}_{w\_\max}$	334	334	104	112	112	58

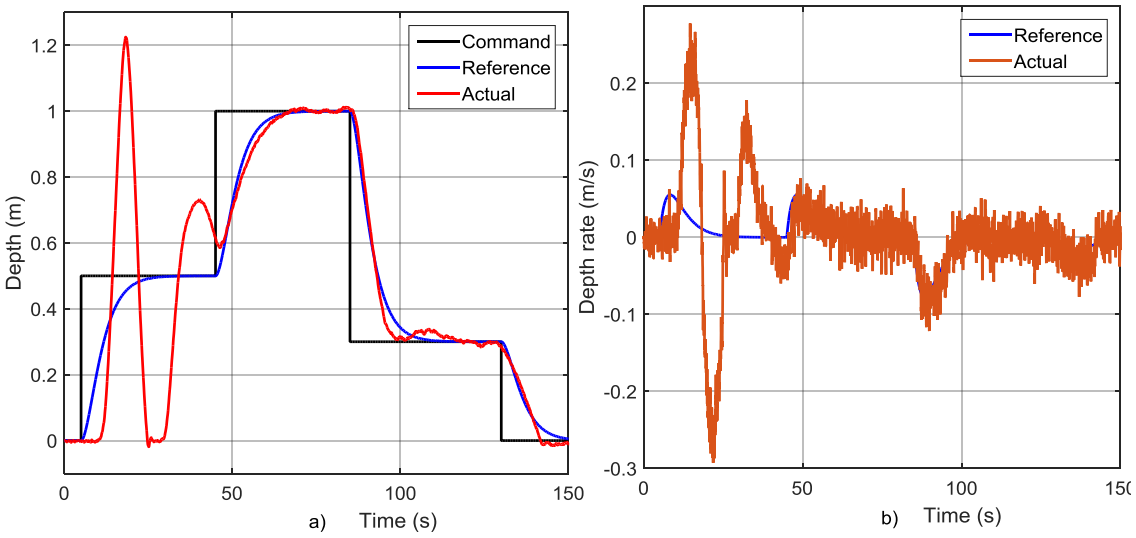

Figure 6. 2: RCGAC a) depth response b) depth rate response

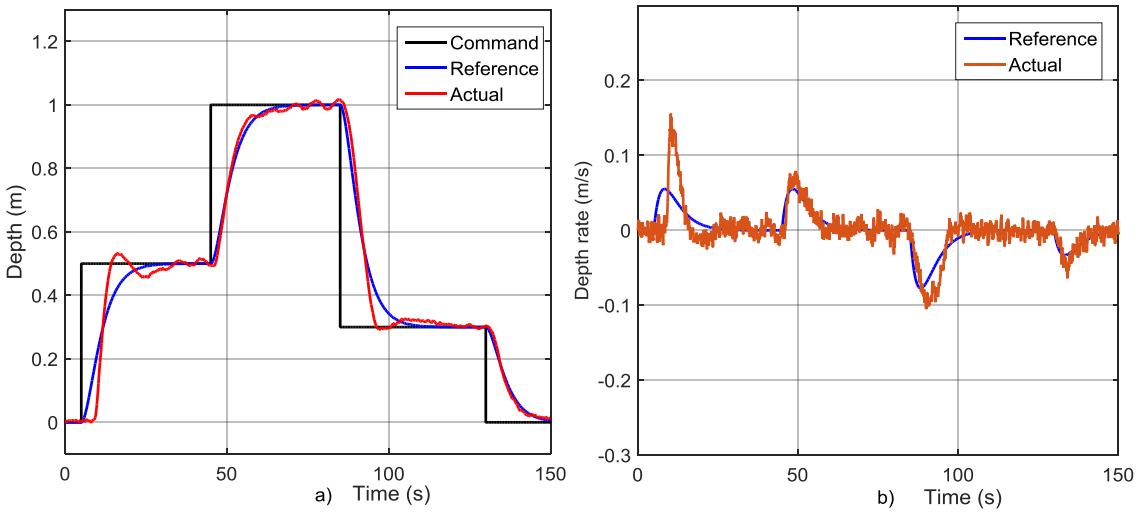

Figure 6. 3: WCGAC a) depth response b) depth rate response

In the first 50s, the first four indices that represent tracking errors, d_{e_rms}, $d_{e\_\max}$, w_{e_rms} and $w_{e\_\max}$ of WCGAC are lower than those of RCGAC by 79% (a factor of 4.8), 72% (a factor of 3.5), 64% (a factor of 2.8), and 60% (a factor of 2.5) respectively. The last two indices that represent control effort, $\tilde{\tau}_{w\_rms}$ and $\tilde{\tau}_{w\_\max}$ of WCGAC are lower than those of RCGAC by 79% (a factor of 4.8) and 66% (a factor of 3) respectively. Thus, there is a clear improvement in all performance metrics for WCGAC over RCGAC.

In the next 100s although w_{e_rms} and $w_{e\_\max}$ of WCGAC are still lower than those of RCGAC by 23% (a factor of 1.3), and 27% (a factor of 1.4) respectively, d_{e_rms} and $d_{e\_\max}$ of WCGAC are higher than those of RCGAC by 55% (a factor of 1.5) and 62% (a factor of 1.6) respectively. Furthermore, $\tilde{\tau}_{w\_rms}$ and $\tilde{\tau}_{w\_\max}$ of WCGAC remains lower than RCGAC by 27% (a factor of 1.4) and 44% (a factor of 1.8) respectively. Thus, although WCGAC improves on depth rate tracking and control effort over RCGAC, it underperforms in the crucial depth tracking metric.

For further analysis of the control signal the discrete rate of change of the control signal $\left(\frac{\Delta u}{\Delta t}\right)$ versus time is provided in Fig. 6.4 and the frequency spectrum is provided in Fig. 6.5. It is clear from these figures that there is a significant reduction in noise levels

and high frequencies in WCGAC compared to RCGAC. This is due to, a) the inherent filtering effect of weight filter and b) the decrease of the cut-off frequency of the input filter from 12rad/s to 6rad/s without instability made possible by the increased robustness to time-delay of the weight filter.

Although, WCGAC has several advantages over RCGAC, the reduced performance of WCGAC in depth tracking after the first 50s should be remedied as it affects the long term tracking performance. An additional concern is that the performance in the first 50s, although much improved, is still much lower than that of the next 100s.

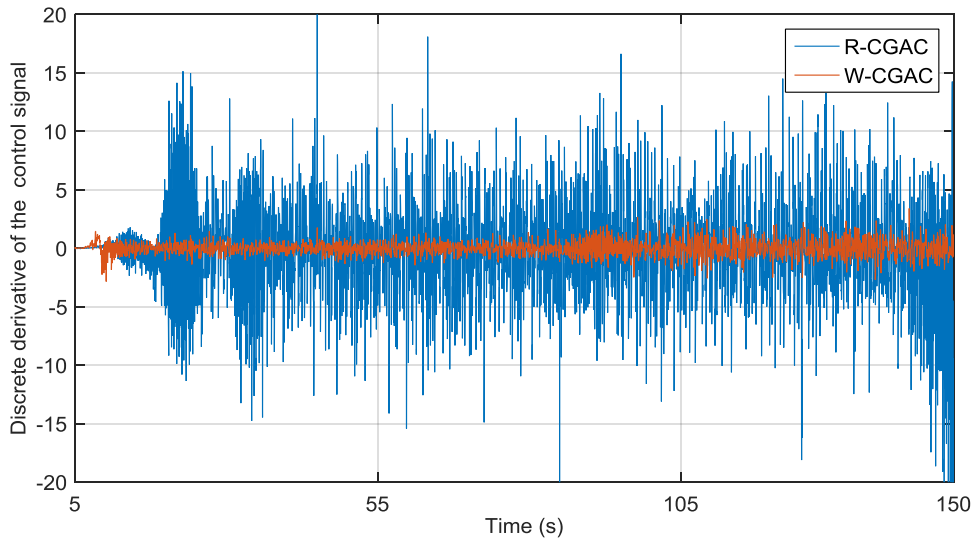

Figure 6. 4: Discrete derivative ($\frac{\Delta u}{\Delta t}$) of RCGAC and WCGAC

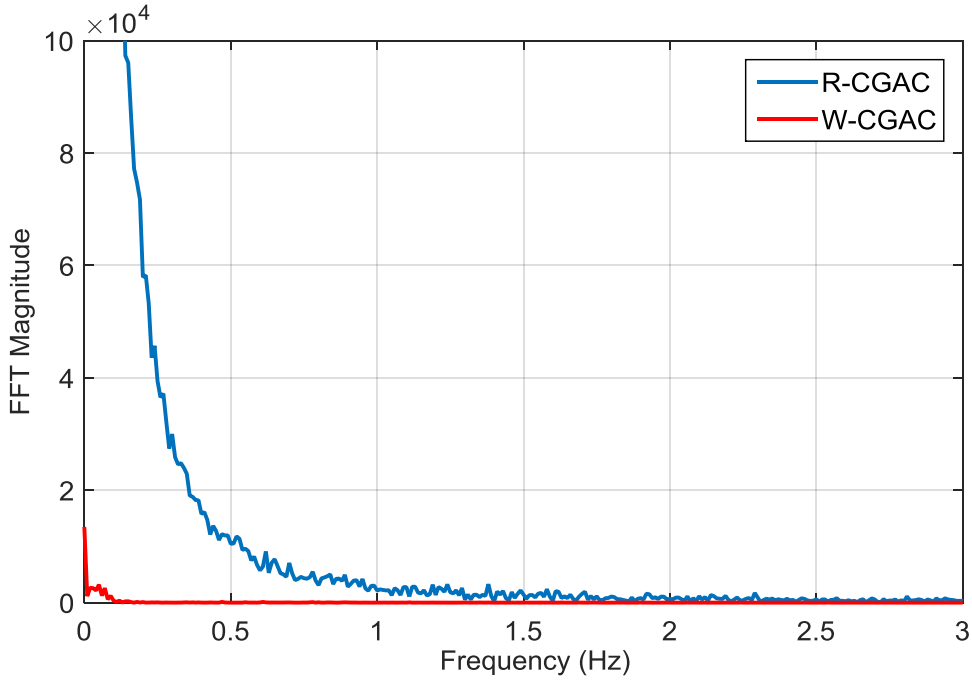

Figure 6. 5: Frequency spectrum of RCGAC and WCGAC

6.5.2 ECGAC

Therefore, a solution was required in which the tracking performance can be increased without increasing learning rates or compromising any of the advantages of WCGAC. As already established by the authors in Makavita et al. (2016b) and Makavita et al. (2017a), PMRAC architecture provides such a solution. As explained in section 6.2.4, WCGAC was combined with state predictor from PMRAC to produce Extended CGAC (ECGAC). The performance of ECGAC is given in Fig. 6.6 and Table 6.3.

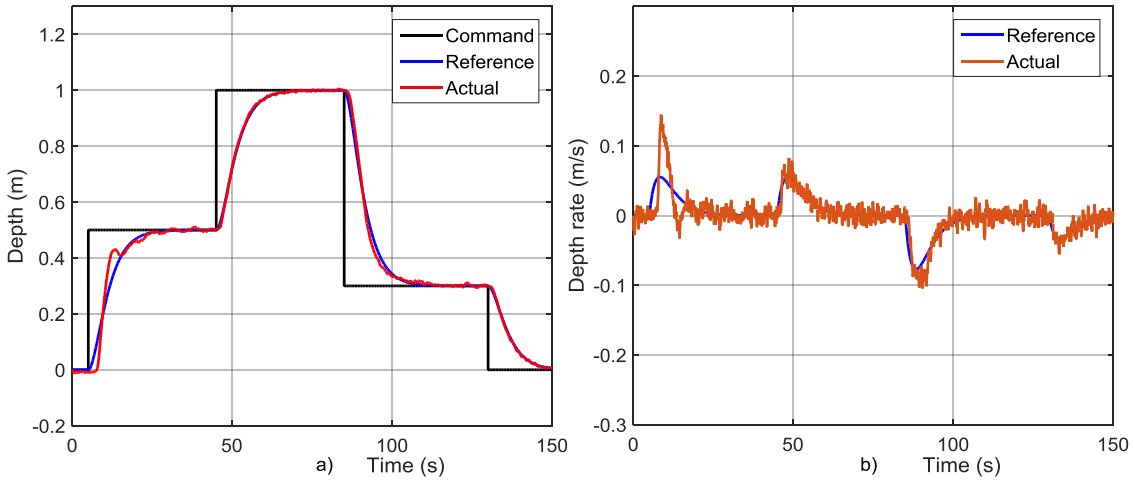

Figure 6. 6: ECGAC a) depth response b) depth rate response

Table 6. 3: Performance Indices for ECGAC at Learning Rates of $\gamma = 1$ and $\gamma = 3$

Performance Indices	ECGAC at $\gamma = 1$			ECGAC at $\gamma = 3$		
	Full run	First 50s	Next 100s	Full run	First 50s	Next 100s
d_{e_rms} (m)	0.020	0.028	0.015	0.016	0.020	0.014
$d_{e\_\max}$ (m)	0.101	0.101	0.060	0.073	0.073	0.051
w_{e_rms} (deg/s)	0.014	0.020	0.011	0.011	0.014	0.010
$w_{e\_\max}$ (deg/s)	0.081	0.081	0.047	0.055	0.054	0.055
$\tilde{\tau}_{w\_rms}$	22.062	25.292	20.44	18.003	17.320	18.303
$\tilde{\tau}_{w\_\max}$	126	126	77	69	46	69

An immediate improvement is seen with the addition of the prediction error at a learning rate $\gamma = 1$. In the first 50s, the first four indices that represent tracking errors, d_{e_rms}, $d_{e\_\max}$, w_{e_rms} and $w_{e\_\max}$ of ECGAC are lower than those of WCGAC by 49% (a factor of 2), 41% (a factor of 1.7), 26% (a factor of 1.4), and 24% (a factor of 1.3) respectively. The last two indices that represent control effort, $\tilde{\tau}_{w\_rms}$ and $\tilde{\tau}_{w\_\max}$ of ECGAC are increased in comparison with those of WCGAC by 4% (a factor of ~1) and 11% (a factor of 1.1) respectively. Thus, ECGAC improves its tracking performance with only a slight increase in control effort.

In the next 100s d_{e_rms}, $d_{e\_\max}$, w_{e_rms} and $w_{e\_\max}$ of ECGAC are lower than those of WCGAC by 46% (a factor of 1.9), 42% (a factor of 1.7), 15% (a factor of 1.2), and 4% (a factor of ~1) respectively. In addition, they are also lower than those of RCGAC by 16% (a factor of 1.2), 6% (a factor of 1.1), 35% (a factor of 1.5) and 30% (a factor of 1.4) respectively. Furthermore, $\tilde{\tau}_{w\_rms}$ and $\tilde{\tau}_{w\_\max}$ of ECGAC while increased from WCGAC by 8% (a factor of 1.1) and 33% (a factor of 1.5) respectively, are lower than RCGAC by 21% (a factor of 1.3) and 26% (a factor of 1.4) respectively.

Thus, ECGAC has better tracking than WCGAC and remedies the reduced depth tracking performance of WCGAC for a marginal increase in control effort. Furthermore, this analysis clearly shows that ECGAC outperforms RCGAC in every single performance index. In addition, if we compare the performances of each individual method in the first 50s with the next 100s, ECGAC has the more homogeneous response compared to RCGAC.

While the performance of ECGAC at $\gamma = 1$ (now denoted by $ECGAC_1$) was quite satisfactory it was decided to see if any additional improvements can be made by increasing the learning rate to improve depth tracking such that $d_{e\_rms} \leq 0.02m$ for both the first 50s and the next 100s of the run. This specification was achieved by a small increase in learning rate to $\gamma = 3$, denoted by $ECGAC_3$. The performance indices for this condition are also given in Table 3.

Comparing these with $ECGAC_1$ in the first 50s d_{e_rms}, $d_{e\_\max}$, w_{e_rms} and $w_{e\_\max}$ of $ECGAC_3$ are lower than those E-$CGAC_1$ by 29% (a factor of 1.4) , 28% (a factor of 1.4), 30% (a factor of 1.4), and 33% (a factor of 1.5) respectively. In addition, the control effort indices of $\tilde{\tau}_{w\_rms}$ and $\tilde{\tau}_{w\_\max}$ of E-$CGAC_3$ are lower than those of $ECGAC_1$ by 32% and 63% respectively.

In the next 100s the tracking performance indices of $ECGAC_3$ is approximately equal to the performance indices of $ECGAC_1$ while the control effort indices have reduced slightly.

It is important to ensure that these performance improvements are not at the expense of noise or high frequencies in the control signal. To verify this, the discrete derivative and the frequency spectrum of the control signal for WCGAC, $ECGAC_1$, and $ECGAC_3$ are

given in Figs. 6.7 and 6.8. From both figures it is clearly seen that the noise levels and frequency distributions are approximately the same. A closer analysis show, though there is a slight increase in high frequencies and noise for $ECGAC_1$ over WCGAC, this decreases at $ECGAC_3$.

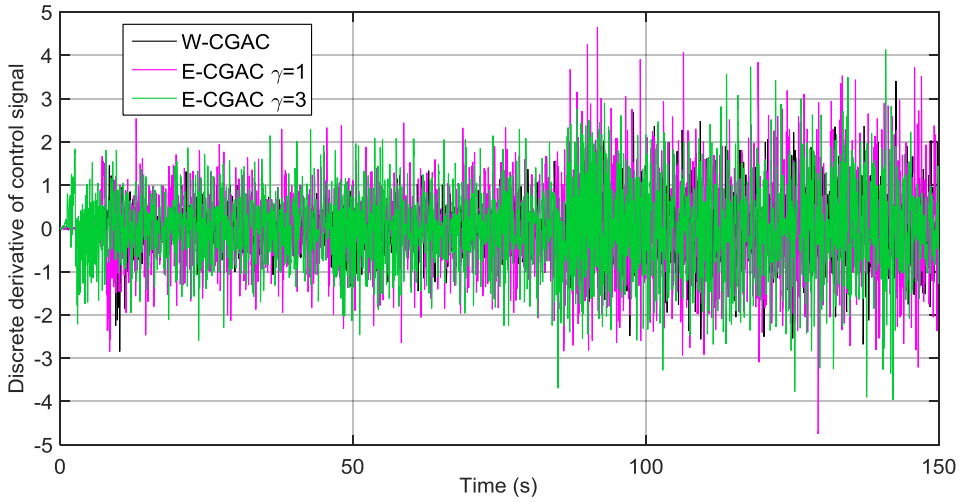

Figure 6. 7: Discrete derivative of control signal for WCGAC, $ECGAC_1$, and $ECGAC_3$

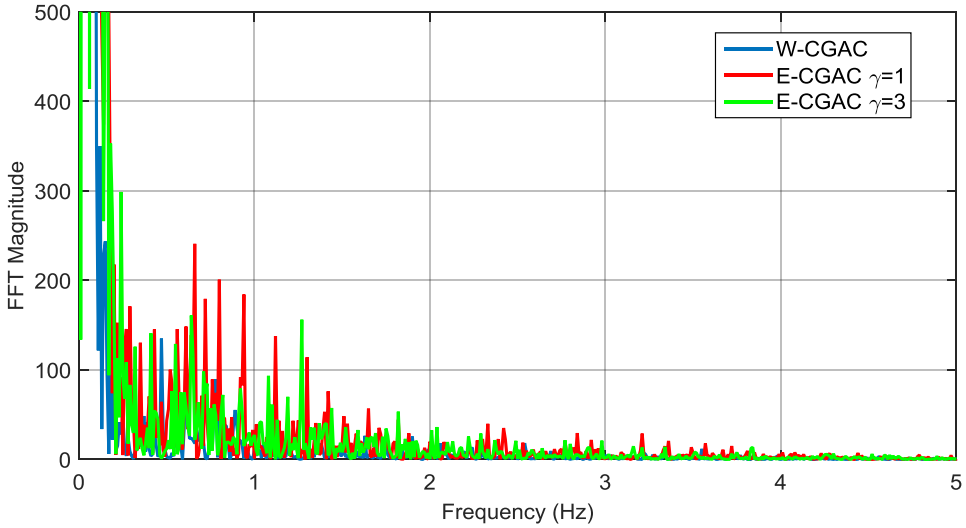

Figure 6. 8: Frequency spectrum of the control signal for WCGAC, $ECGAC_1$, $ECGAC_3$

6.5.3 Sudden Parameter Variations

A further experiment was carried out to verify the capability of $ECGAC_3$ by comparing it with RCGAC for a thrust loss anomaly. A thrust loss manifests itself as a sudden variation of the control effectiveness parameter and is a good candidate to check the

ability of the controller to perform under such a variation. The results for 50% thrust loss while holding constant depth is given in Table 6.4, while the results for changing depth after the thrust loss is given in Fig. 6.9 and Table 6.5.

From Table 6.4 it is seen that both methods have similar performances in tracking before and after thrust loss. $ECGAC_3$ has an advantage in terms of maximum deviation which is 40% (a factor of 1.7) less than RCGAC and only 0.001m outside the 2% settling time band of ± 0.02m. As this difference is within the resolution of the depth sensor it is negligible and thus settling time is not applicable for $ECGAC_3$. In addition, the advantage of having a reduced control effort is carried through even after thrust loss, although the control magnitudes have increased to accommodate the reduced thrust.

Table 6. 4: Performance indices for 50% thrust loss for RCGAC and $ECGAC_3$

Performance Indices	**RCGAC**	**$ECGAC_3$**
d_{e_rms} before thrust loss (m)	0.006	0.005
d_{e_rms} after thrust loss (m)	0.014	0.012
$d_{e\_\max}$ after thrust loss (m)	0.035	0.021
Time to depth response to settle to final value (s)	22	N/A
$\tilde{\tau}_{w\_rms}$ before thrust loss	21.04	17.24
$\tilde{\tau}_{w\_rms}$ after thrust loss	34.49	29.39
$\tilde{\tau}_{w\_\max}$ before thrust loss	77	61
$\tilde{\tau}_{w\_\max}$ after thrust loss	82	64

From Table 6.5 it is seen that when a depth change is done after thrust loss at 120s, $ECGAC_3$ has better performance in all performance indices other than the maximum thrust which is equal for the two. Further insight can be had by observing the plots in Fig. 6.10. It is seen that $ECGAC_3$ has increased oscillations in comparison to RCGAC just after thrust loss. In addition, RCGAC in contrast to $ECGAC_3$ undershoots the command in first down step with a peak undershoot of 8.6% and in the second step it is prevented from undershooting only by the physical constraint of hitting the water surface.

Thus, after partial thrust loss both RCGAC and ECGAC$_3$ perform well, but ECGAC$_3$ does have an advantage in both maintaining and changing depth.

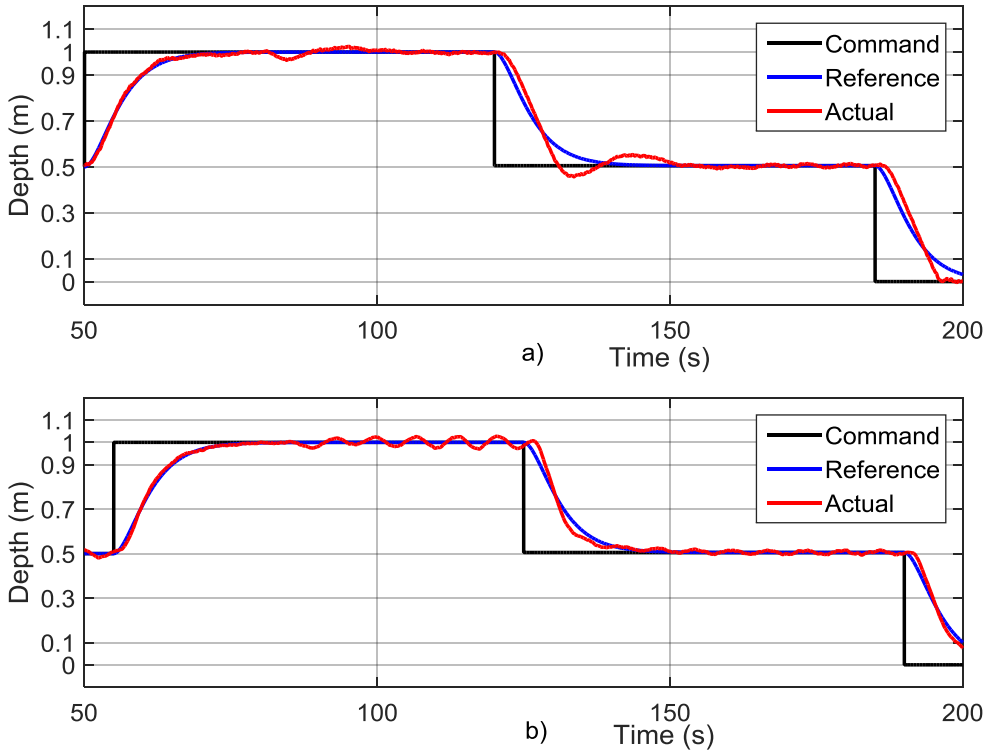

Figure 6. 9: Depth response of a) R-CGAC b) ECGAC$_3$ for a 50% thrust loss at 85s

Table 6. 5: Performances indices for depth change after thrust loss

Performance Indices	**RCGAC**	**ECGAC$_3$**
d_{e_rms} (m)	0.029	0.019
$d_{e\_\max}$ (m)	0.099	0.071
w_{e_rms} (deg/s)	0.019	0.015
$w_{e\_\max}$ (deg/s)	0.070	0.054
$\tilde{\tau}_{w\_rms}$	43.441	34.092
$\tilde{\tau}_{w\_\max}$	100	100

Overall the results indicate that the proposed method of ECGAC, which is an extension of RCGAC by replacing the robustification filter with the weight filter and adding the closed loop state predictor, has the following advantages over RCGAC.

a) Resolves the initial deviation problem of RCGAC
b) Better tracking
c) Lower control effort
d) Less noise and high frequencies in the control signal and
e) Handles sudden changes in parameters better.

Therefore, ECGAC is a viable solution to achieve accurate manoeuvring without using high learning rates.

6.6 Conclusion

This paper proposes an extension to the command governor adaptive control to enhance the initial tracking performance of UUVs intended to use in advanced applications that require precise manoeuvring. The proposed ECGAC replaces the robustification filter with a weight filter and adds a closed loop state predictor. Experimental results and analysis indicate that the weight filter alone produces better tracking performance at the start with substantial improvement in reducing control effort, control signal noise and high frequencies. However, its overall depth tracking performance is reduced compared to that of RCGAC. The subsequent addition of the closed loop state predictor has resolved this issue and improved the overall tracking performance while retaining lower control effort, lower control signal noise and lower high frequencies. A further increase of the learning rate from 1 to 3 enabled the achievement of a specific design specification for depth tracking. In addition, ECGAC outperformed RCGAC under a 50% partial thruster failure in the vertical thruster.

Thus, ECGAC has an overall improvement over RCGAC and has highly promising performance metrics without using high learning rates. Therefore, it is concluded that ECGAC is a viable candidate for underwater missions that require precise manoeuvres. Future work should extend these findings to quantitatively analyse the robustness improvements of ECGAC.

Chapter 7:

Summary, Conclusions and Future Work

This chapter provides a summary of the thesis and brings together the findings reported in each of the chapters. It also presents the conclusions drawn from the findings and discusses the implications of the findings. Limitations of the proposed control solutions and recommendations for future research are also presented at the end of the chapter.

7.1 Summary of Work Performed

This thesis is an effort to answer the question, "What modifications or additions to adaptive control systems provide good transient tracking with smooth control signals under model parameter variation and external disturbances at low adaptation gains for UUV applications?" As the first step in addressing this question, it was required to identify which adaptive control algorithms enabled good transient tracking at low learning rates. Once the suitable control algorithms were identified, the next step was to determine how well these algorithms improved transient tracking under model uncertainty, followed by the assessment of their performance under model parameter variations and external disturbances. The final step was to determine which methods, singularly or as a combination, are the most viable adaptive control solutions for current and future UUV applications. In addition, further modifications to improve performances were also envisaged in this step.

In the first step, three methods were identified based on a comprehensive literature study. Two of them are based on composite adaptation and the third one is based on command modification to improve transient tracking. The two composite methods are CMRAC and PMRAC, while the command modification based method is CGAC.

In the second stage, the composite methods were tested using simulations for both heading and depth control and compared with standard MRAC. The simulations were carried out for three different learning rates for normal operations without disturbances or sudden parameter variations. In order to emulate a severe model uncertainty scenario, initial values of the adaptive parameters were set to zero. After simulating the normal operations, both methods were tested for external impact disturbances in the vertical direction and also for a sudden thrust loss in the vertical thruster while holding depth against positive buoyancy. After the simulations, both methods were validated experimentally for the same scenarios using the UUV developed at AMC and compared with MRAC. Based on their performances, PMRAC was selected and tested under both a persistent wave disturbance for heading and vertical impact disturbance for depth. In addition, it was also tested for horizontal and vertical thrust loss.

The third method CGAC was also tested in simulations for both heading and depth control with low gain and compared with the standard MRAC having low and high

gains. Initial testing of CGAC was carried out for normal operations (without disturbances or thrust loss) and under a sinusoidal disturbance. Simulations were also carried out for heading control under severe measurement noise and a possible solution for it by using a robustification filter, which consists of a low pass filter to filter out the noise in the command governor signal. Furthermore, input filtering of the noisy measured signal that injects time-delay to the system was also simulated, separately and in conjunction with the robustification filter. Moreover, CGAC with the robustification filter (RCGAC) was also tested with dead-zones in both horizontal thrusters without a dead-zone inverse and compared against MRAC. RCGAC was then experimentally tested for normal operations in heading and depth, horizontal and vertical impact disturbances, a tether snag disturbance, horizontal and vertical partial thruster failures, thruster dead-zone effects and robustification filter effects.

Furthermore, a new extension to CGAC, named as Extended CGAC (ECGAC), that a) replaces the robustification filter with a weight filter to improve the robustness to measurement noise and input time-delay and b) using the closed-loop state predictor from PMRAC to improve transient tracking was also proposed. This was experimentally tested for its tracking performance under normal operations and sudden parameter variations represented by a partial thrust loss. Further analysis was conducted to verify the improved robustness by comparing the noise in the control signal of ECGAC with RCGAC.

Overall, comprehensive simulation and experimental results for CMRAC, PMRAC, CGAC/RCGAC and ECGAC were provided both qualitatively using plots of output, control signal and frequency spectrum, and quantitatively using six performance metrics and several other performance specifications for reference tracking and control signal behaviour. These allowed for an extensive analysis of the tracking performance, control efforts, disturbance rejection, effect of sudden parameter variation and effect of measurement noise and time-delay that led to the findings and conclusions given below.

7.2 Findings

The major findings of the research are listed below.

7.2.1 Transient Tracking

- All four modifications, CMRAC, PMRAC, CGAC and ECGAC, introduced in this thesis improve transient tracking over the standard MRAC.
- CMRAC does not improve transient tracking substantially, while both PMRAC and CGAC substantially improve transient tracking over MRAC.
- CGAC has better transient tracking than PMRAC at the same learning rate.
- Overall, ECGAC has the best tracking performance of all methods at the same learning rate.
- Effect of the robustification filter is detrimental for the transient tracking performance of RCGAC for a short period at the beginning of each run.
- ECGAC substantially improves performance in the initial period of a run compared to RCGAC.
- CMRAC is difficult to implement for real-time operations compared to PMRAC and CGAC.

7.2.2 Control Signal Behaviour

- While CMRAC has inconsistent variation in control effort compared to MRAC, PMRAC has significantly reduced control effort compared to both MRAC and CMRAC.
- While both CMRAC and PMRAC reduce high frequency oscillations in the control signal, CMRAC is marginally better than PMRAC for a given learning rate.
- CGAC requires a lower control effort compared to MRAC, which is approximately equal to PMRAC.
- CGAC reduces high frequency oscillations in the control signal compared to high gain MRAC while maintaining the same tracking performance.
- ECGAC has the best control signal behaviour (lower control effort and lower high frequency oscillations) at base learning rate of all methods.

7.2.3 Robustness to Noise and Time-delay

- Both CMRAC and PMRAC are robust to noise and time-delay at low learning rates.
- PMRAC is less robust to time-delay compared to CMRAC and MRAC and should be used cautiously at higher learning rates.
- CGAC without robustification filter is susceptible to high measurement noise and cannot be used in applications under such conditions.
- The robustification filter improves robustness to measurement noise and time-delay in RCGAC.
- RCGAC has significant deviations in tracking for an initial time duration until the effect of the filter has died down. This compromise between robustness and performance increases as the filter gain value decreases.
- ECGAC has much improved robustness to noise and time-delay over RCGAC and does not sacrifice performance for robustness.

7.2.4 Thrust Loss Anomaly

- PMRAC and RCGAC have better ability to recover from a thrust loss compared to MRAC at a given learning rate.
- RCGAC has better recovery from thrust loss than PMRAC at the base learning rate.
- ECGAC has the best performance under thrust loss anomaly among all the methods tested.

7.2.5 External Disturbances

- PMRAC and RCGAC have better disturbance rejection for an impact disturbance compared to MRAC. Thus, they will provide a better capability to deal with impacts that could occur in a cluttered environment.
- PMRAC has better disturbance rejection of persistent disturbances as it is less affected while holding and changing position. Thus, it can provide a better capability for the vehicle to carry out observations and imaging in shallow water bodies.

- RCGAC has better disturbance rejection under sustained disturbances such as tether snag effect and sinusoidal disturbance. Thus, it can provide a better capability to deal with tether disturbance that affects ROVs.

7.2.6 Actuator Dead-zone

- Command governor used in RCGAC and ECGAC can overcome an actuator dead-zone, which is quite common in marine thrusters without an additional dead-zone inverse.
- RCGAC and ECGAC can adjust to changes in the dead-zone that occur over time or across different thrusters without any adaptive mechanism as in an additional dead-zone inverse.
- Tracking performance of RCGAC and ECGAC are not affected by the absence of and additional dead-zone inverse.
- CMRAC and PMRAC require an additional dead-zone inverse to provide required tracking performance under an actuator dead-zone.

7.3 Conclusions and Implications of the Research

In this study, PMRAC has been tested and analysed comprehensively with low learning rates and its superiority over MRAC and CMRAC under tracking, control effort, disturbance, and thrust loss has been demonstrated. This has filled an existing knowledge gap regarding the performance of PMRAC under low learning rates, especially with experimental validation. As the PMRAC method is also a relatively simple extension of MRAC, this work implies that PMRAC extension should definitely be considered for systems that use MRAC with low adaptive gains. Nevertheless, care must be taken at high adaptive gains if there are significant time-delay effects in the system.

CGAC has also been tested and analysed comprehensively using low learning rates and shown to have the best tracking performance compared to MRAC, CMRAC and PMRAC. It also shows good control effort, disturbance rejection, thrust loss recovery and ability to overcome a thruster dead-zone. Therefore, this work adds important quantitative results to a field of work with relatively few published data and even less experimental data. It is also implied that CGAC is a very good candidate for underwater

vehicle applications, especially if measurement noise is low as demonstrated in heading control. It also has the additional advantage of being able to overcome actuator dead-zone without relying on an additional dead-zone inverse.

The main drawback of CGAC is its susceptibility to noise. The robustification filter solution is effective only at low noise conditions. Specifically, this work contributes an experimental validation of the adverse effects of the filter on tracking and also its inability to reduce noise to acceptable levels under high noise conditions. To find a more effective solution, this work proposed an extension to CGAC that uses a weight filter derived from literature and combining with the PMRAC extension to create ECGAC. This method has the best tracking performance of all methods and considerably low noise compared to CGAC. Thus, this work has introduced a new extension to MRAC, with the implications that it could be a viable low gain adaptive controller for applications with significant measurement noise.

The final and most important implication of this thesis is the applicability of low gain adaptive controllers for current and future underwater vehicle applications. In addition to the above mentioned tracking performance improvement, there are several other factors that were illuminated by this study that make this a real possibility. These include reduced average control effort that allows autonomous vehicles with these controllers to carry out longer missions and lower maximum control effort that reduces the risk of saturation. Furthermore, the control signals remain less in the saturation region thus preventing damage to actuators and nonlinear effect on adaptive learning. Moreover, the proposed methods are better compared to MRAC in disturbance rejection, i.e. they have a better capability to manoeuvre the vehicle as required under the numerous disturbances that can occur in a real application. These methods are also better equipped to recover from sudden parameter changes such as thrust loss, thus preventing large deviations. Therefore, it can be concluded that low gain adaptive controllers with proper modifications as proposed in this thesis enhance the control performance without scarifying the stability, smoother control signals and robustness.

7.4 Limitations & Future Work

Although much has been accomplished in this work, there are areas that could not be fully covered due to time and scope limitations that would be interesting frontiers for future researchers to explore. These have been succinctly described below.

One important factor that was looked at in this work is the robustness of the proposed controllers against time-delay. While it was shown that these controllers are robust to time-delay, the study does not delve deeply into calculating the stability margins available. In addition, while the analysis of stability margins is well established for linear time invariant (LTI) systems, the nonlinearity of the adaptive controllers makes it a non-trivial task. Therefore, a future extension of this work would be to do a comprehensive stability analysis that would provide a better understanding of the trade-off between robustness and performance for these methods.

Another important focus of this work was the disturbance rejection capability of the proposed controllers for several different types of disturbances that could be applied to UUVs in an actual underwater environment. Although, this approach provided a number of insights from an application viewpoint it would have been more interesting from a control viewpoint to analyse the disturbance rejection capability of the controllers in the frequency domain. Therefore, a further extension of this work would be to do such an analysis that would provide a better understanding of the disturbances rejection capability of the controllers at different frequencies.

ECGAC has been introduced in this work and showed promising results. While it was experimentally tested, further simulations and experiments have to be carried out to obtain further insight into its operations. These tests should include operation under disturbances, test to determine how the different parameters of adaptive gains, state predictor gains and weight filter gains interact and their effect on performance and robustness. Therefore, a future extension of this work would be to do such simulations and experiments to have a better evaluation of capabilities and limitations of ECGAC.

As this work was a pioneering effort in low gain adaptive control, the experiments were carried out in a controlled environment. While this allowed investigation into the operation of these methods, for practical implementation these have to be tested in an

uncontrolled environment. Therefore, a future extension of this work would be to first carry out experiments in natural fresh water bodies such as lakes and rivers and follow it up with a series of sea trials.

In this work, the controllers are only developed for heading and depth control considering the dynamics to be decoupled. Therefore, a future extension of this work would be to first implement controllers for other DOFs and then develop a controller for a full 6-DOF coupled system. Although this would be computationally intensive and require much more resources, it would perhaps provide the best path for eventual implementation of these control methods in UUVs used in advanced and demanding applications.

References

Anderson, BDO 2005, 'Failures of adaptive control theory and their resolution', *Communications in Information and Systems*, vol. 5, no. 1, pp. 1-20.

Antonelli, G, Caccavle, F, Chiaverini, S & Fusco, G 2003, 'A novel adaptive control law for underwater vehicles', *IEEE Transactions on Control Systems Technology*, vol. 11, no. 2, pp. 221-232.

Antonelli, G, Chiaverini, S, Sarkar, N & West, M 2001, 'Adaptive control of an autonomous underwater vehicle: experimental results on ODIN', *IEEE Transactions on Control Systems Technology*, vol. 9, no. 5, pp. 756-765.

Antonelli, G, Fossen, TI & Yoerger, DR 2016, 'Modeling and control of underwater robots', in B Siciliano & O Khatib (eds), *Springer Handbook of Robotics*, Springer International Publishing, Cham, pp. 1285-1306.

Åström, KJ & Wittenmark, B 1995, *Adaptive control*, 2 edn, Addison-Wesley, Reading Massachusetts.

Avila, JPJ, Adamowski, JC, Maruyama, N, Takase, FK & Saito, M 2012, 'Modeling and identification of an open-frame underwater vehicle: the yaw motion dynamics', *Journal of Intelligent & Robotic Systems*, vol. 66, no. 1, pp. 37-56.

Avila, JPJ, Donha, DC & Adamowski, JC 2013, 'Experimental model identification of open-frame underwater vehicles', *Ocean Engineering*, vol. 60, pp. 81-94.

Avila, JPJ, Nishimoto, K, Sampaio, CM & Adamowski, JC 2011, 'Experimental investigation of the hydrodynamic coefficients of a remotely operated vehicle using a planar motion mechanism', *Journal of Offshore Mechanics and Arctic Engineering*, vol. 134, no. 2, p. 021601.

Bagheri, A, Karimi, T & Amanifard, N 2010, 'Tracking performance control of a cable communicated underwater vehicle using adaptive neural network controllers', *Applied Soft Computing*, vol. 10, no. 3, pp. 908-918.

Bessa, W, Dutra, M & Kreuzer, E 2013, 'Dynamic positioning of underwater robotic vehicles with thruster dynamics compensation', *International Journal of Advanced Robotic Systems*, vol. 10, no. 325, pp. 1-8.

Bessa, W & Kreuzer, E 2011, 'Sliding mode control of a remotely operated underwater vehicle with adaptive fuzzy dead-zone compensation', *Proceedings in Applied Mathematics and Mechanics*, vol. 11, no. 1, pp. 803-804.

BlueRobotics 2016, *Bar30 high-resolution 300m depth/pressure sensor*, Blue Robotics Inc., viewed 30 December 2016, <https://www.bluerobotics.com/store/electronics/bar30-sensor-r1/>.

Bowen, AD, Yoerger, DR, Taylor, C, McCabe, R, Howland, J, Gomez-Ibanez, D, Kinsey, JC, Heintz, M, McDonald, G, Peters, D, Young, C, Buescher, J, Fletcher, B, Whitcomb, LL, Martin, SC, Webster, SE & Jakuba, MV 2009, 'The Nereus hybrid underwater robotic vehicle', *Underwater Technology*, vol. 28, no. 3, pp. 79-89.

Brun, L 2012, 'ROV/AUV trends market and technology', *Marine Technology Reporter*, September, pp. 48-51.

Budiyono, A 2011, 'Model predictive control for autonomous underwater vehicle', *Indian Journal of Geo-Marine Sciences*, vol. 40, no. 2, pp. 191-199.

Caccia, M, Indiveri, G & Veruggio, G 2000, 'Modeling and identification of open-frame variable configuration unmanned underwater vehicles', *IEEE Journal of Oceanic Engineering*, vol. 25, no. 2, pp. 227-240.

Campbell, S & Kaneshige, J 2010, 'A nonlinear dynamic inversion Predictor-Based Model Reference Adaptive Controller for a Generic Transport Model', in *Proceedings of the 2010 American Control Conference*, Baltimore, MD, pp. 868-873.

Campbell, S, Kaneshige, J, Nguyen, N & Krishnakumar, K 2010a, 'An Adaptive Control Simulation Study using Pilot Handling Qualities Evaluations', in *Proceedings of the AIAA Guidance, Navigation, and Control Conference*, Toronto, Ontario Canada, pp. AIAA-2010-8013.

—— 2010b, 'Implementation and Evaluation of Multiple Adaptive Control Technologies for a Generic Transport Aircraft Simulation', in *Proceedings of the AIAA Infotech@Aerospace 2010*, Atlanta, Georgia.

Cao, C & Hovakimyan, N 2006a, 'Design and analysis of a novel L1 adaptive controller, Part I: Control signal and asymptotic stability', in *Proceedings of the 2006 American Control Conference*, Minneapolis, MN, pp. 3397-3402.

—— 2006b, 'Design and analysis of a novel L1 adaptive controller, Part II: Guaranteed transient performance', in *2006 American Control Conference*, Minneapolis, MN, pp. 3403-3408.

—— 2008, 'Design and analysis of a novel adaptive control architecture with guaranteed transient performance', *IEEE Transactions on Automatic Control*, vol. 53, no. 2, pp. 586-591.

Carreras, M, Yuh, J & Batlle, J 2002, 'High-Level control of autonomous robots using a behavior-based scheme and reinforcement learning', in *Proceedings of the 15th IFAC World Congress*, Barcelona, Spain, pp. 469-474.

Cavalletti, M, Ippoliti, G & Longhi, S 2006, 'Lyapunov-based switching control for a remotely operated vehicle', in *Proceedings of the 9th International Conference on Control, Automation, Robotics and Vision*, Singapore, pp. 2016-2021.

—— 2007, 'Switching adaptive control for a remotely operated vehicle', in *Proceedings of the American Control Conference, 2007.* , New York, USA, pp. 2799-2806.

—— 2011, 'A comparative study between switching and adaptive controllers for a remotely operated vehicle', *Proceedings of the Institution of Mechanical Engineers, Part M: Journal of Engineering for the Maritime Environment*, vol. 225, no. 3, pp. 191-205.

Chang, W-J, Chang, W & Liu, H-H 2003, 'Model-based fuzzy modeling and control for autonomous underwater vehicles in the horizontal plane', *Journal of Marine Science and Technology*, vol. 11, no. 3, pp. 155-163.

Chen, H, Stavinoha, S, Walker, M, Zhang, B & Fuhlbrigge, T 2014, 'Opportunities and challenges of robotics and automation in offshore oil and gas industry', *Intelligent Control and Automation*, vol. 05, no. 03, pp. 136-145.

Chin, C & Lau, M 2012, 'Modeling and testing of hydrodynamic damping model for a complex-shaped remotely-operated vehicle for control', *Journal of Marine Science and Application*, vol. 11, no. 2, pp. 150-163.

Chowdhary, GV & Johnson, E 2011, 'Theory and flight-test validation of a concurrent-learning adaptive controller', *Journal of Guidance, Control, and Dynamics*, vol. 34, no. 2, pp. 592-607.

Crespo, L, Matsutani, M & Annaswamy, A 2010, 'Design of a Model Reference Adaptive Controller for an Unmanned Air Vehicle', in *Proceedings of the AIAA*

Guidance, Navigation, and Control Conference, Toronto, Ontario, Canada, pp. AIAA 2010-8049.

De La Torre, G, Yucelen, T & Johnson, EN 2016, 'A new model reference control architecture: Stability, performance, and robustness', *International Journal of Robust and Nonlinear Control*, vol. 26, no. 11, pp. 2355-2377.

DeMarco, KJ, West, ME & Howard, AM 2014, 'Autonomous robot-diver assistance through joint intention theory', in *Proceedings of the IEEE/MTS 2014 Oceans - St. John's*, St. John's, NL, Canada.

Duarte-Mermoud, MA & Narendra, KS 1989, 'Combined direct and indirect approach to adaptive control', *IEEE Transactions on Automatic Control*, vol. 34, no. 10, pp. 1071-1075.

Duarte-Mermoud, MA, Rioseco, JS & González, RI 2005, 'Control of longitudinal movement of a plane using combined model reference adaptive control', *Aircraft Engineering and Aerospace Technology*, vol. 77, no. 3, pp. 199-213.

Duarte-Mermoud, MA, Rojo, FA & Pérez, R 2002, 'Experimental evaluation of combined model reference adaptive controller in a pH regulation process', *International Journal of Adaptive Control and Signal Processing*, vol. 16, no. 2, pp. 85-106.

Dukan, F 2014, 'ROV Motion Control Systems', PhD thesis, Norwegian University of Science and Technology.

Dydek, ZT, Annaswamy, AM & Lavretsky, E 2013, 'Adaptive control of quadrotor UAVs: a design trade study with flight evaluations', *IEEE Transactions on Control Systems Technology*, vol. 21, no. 4, pp. 1400-1406.

Dydek, ZT, Annaswamy, AM, Slotine, JJE & Lavretsky, E 2010, 'High performance adaptive control in the presence of time delays', in *Proceedings of the 2010 American Control Conference*, Baltimore, MD, pp. 880-885.

Eidsvik, OA 2015, 'Identification of Hydrodynamic Parameters for Remotely Operated Vehicles', M.Sc. thesis, Norwegian University of Science and Technology.

El-Fakdi, A & Carreras, M 2008, 'Policy gradient based Reinforcement Learning for real autonomous underwater cable tracking', in *Proceedings of the 2008 IEEE/RSJ International Conference on Intelligent Robots and Systems*, Nice, France, pp. 3635-3640.

Eng, YH, Chin, CS & Lau, M 2014, 'Added mass computation for control of an open-frame remotely-operated vehicle: Application using WAMIT and MATLAB', *Journal of Marine Science and Technology*, vol. 22, no. 4, pp. 405-416.

Eng, YH, Teo, KM, Chitre, M & Ng, KM 2016, 'Online system identification of an autonomous underwater vehicle via in-field experiments', *IEEE Journal of Oceanic Engineering*, vol. 41, no. 1, pp. 5-17.

Evers, G, Vervoort, JHAM, Engelaar, RC, Nijmeijer, H, Jager, AGd, Chen, XQ & Wang, WH 2009, 'Modeling and simulated control of an under actuated autonomous underwater vehicle', in *Proceedings of the 2009 IEEE International Conference on Control and Automation*, Christchurch, New Zealand, pp. 343-348.

Falconí, GP, Schatz, SP & Holzapfel, F 2016, 'Fault tolerant control of a hexarotor using a command governor augmentation', in *Proceedings of the 24th Mediterranean Conference on Control and Automation (MED)*, Athens, Greece, pp. 182-187.

Fernandes, DdA, Dukan, F & Sørensen, AJ 2012, 'Reference model for high performance and low energy consumption motions', in *Proceedings of the 3rd IFAC Workshop on Navigation, Guidance and Control of Underwater Vehicles*, Porto, Portugal, pp. 217-222.

Fjellstad, O-E, Fossen, TI & Egeland, O 1992 'Adaptive control of ROVs with actuator dynamics and saturation', *Modeling, Identification and Control*, vol. 13, no. 3, pp. 175-188.

Fossen, TI 1994, *Guidance and control of ocean vehicles*, John Wiley & Sons, Chichester.

—— 2011, *Handbook of marine craft hydrodynamics and motion control*, John Wiley & Sons, Chichester.

Fossen, TI & Fjellstad, O-E 1996, 'Robust adaptive control of underwater vehicles: A comparative study', *Modeling, Identification and Control*, vol. 17, no. 1, pp. 47-62.

Fossen, TI & Sagatun, SI 1991, 'Adaptive control of nonlinear underwater robotic systems', in *Proceedings.of the 1991 IEEE International Conference onRobotics and Automation* pp. 1687-1694

Frost, AR, McMaster, AP, Saunders, KG & Lee, SR 1996, 'The development of a remotely operated vehicle (ROV) for aquaculture', *Aquacultural Engineering*, vol. 15, no. 6, pp. 461-483.

Garcia-Valdovinos, LG, Salgado-Jiménez, T & Torres-Rodríguez, H 2009, 'Model-free high order sliding mode control for ROV: Station-keeping approach', in *Proceedings of the IEEE/MTS 2009 OCEANS- Biloxi*, Biloxi, MS, USA.

Georgiou, TT & Smith, MC 1997, 'Robustness analysis of nonlinear feedback systems: an input-output approach', *IEEE Transactions on Automatic Control*, vol. 42, no. 9, pp. 1200-1221.

Gibson, TE, Annaswamy, AM & Lavretsky, E 2013, 'Adaptive systems with closed-loop reference-models, part I: Transient performance', in *Proceedings of the 2013 American Control Conference*, Washington, DC, pp. 3376-3383.

Gregory, I, Gadient, R & Lavretsky, E 2011, 'Flight test of composite model reference adaptive control (CMRAC) augmentation using NASA AirSTAR infrastructure', in *AIAA Guidance, Navigation, and Control Conference*, Portland, Oregon.

Hallin, NJ, Egbo, H, Ray, P, Soule, T, Rourke, MO & Edwards, D 2009, 'Enabling autonomous underwater vehicles to reason hypothetically', in *Proceedings of the IEEE/MTS 2009 OCEANS- Biloxi*, Biloxi, MS, USA.

Han, C, Yang, L & Zhang, J 2013, 'A predictor-based model reference adaptive controller for aircraft with center of gravity variations', in *Proceedings of the 32nd Chinese Control Conference*, Xi'an, pp. 3079-3082.

Hanai, A, Choi, HT, Choi, SK & Yuh, J 2003, 'Minimum energy based fine motion control of underwater robots in the presence of thruster nonlinearity', in *Proceedings of the 2003 IEEE/RSJ International Conference onIntelligent Robots and Systems*, Las Vegas, NV, USA, vol. 1, pp. 559-564

Healey, AJ & Lienard, D 1993, 'Multivariable sliding mode control for autonomous diving and steering of unmanned underwater vehicles', *IEEE Journal of Oceanic Engineering*, vol. 18, no. 3, pp. 327-339.

Ho, G, Pavlovic, N & Arrabito, R 2011, 'Human Factors Issues with Operating Unmanned Underwater Vehicles', *Proceedings of the Human Factors and Ergonomics Society Annual Meeting*, vol. 55, no. 1, pp. 429-433.

Honeywell 2006, *Digital Compass Solution HMC6352* viewed 10/02/2017, <https://www.sparkfun.com/datasheets/Components/HMC6352.pdf>.

Hovakimyan, N & Cao, C 2010, *L1 adaptive control theory: guaranteed robustness with fast adaptation*, Society for Industrial and Applied Mathematics, Philadelphia.

Hsu, L, Battistel, A & Nunes, EVL 2014, 'Extended binary model reference adaptive control overcomes limitations of L1 adaptive control', in *Proceedings of the 19th IFAC World Congress*, Cape Town, South Africa, pp. 6920-6925.

InvenSense 2016, *MPU-9250 Product Specification Revision 1.1*, viewed 10/02/2017, <https://www.invensense.com/wp-content/uploads/2015/02/PS-MPU-9250A-01-v1.1.pdf>.

Ioannou, P, Annaswamy, AM, Narendra, KS, Jafari, S, Rudd, L, Ortega, R & Boskovic, J 2014, 'L1-adaptive control: stability, robustness, and interpretations', *IEEE Transactions on Automatic Control*, vol. 59, no. 11, pp. 3075-3080.

Ioannou, P & Fidan, B 2006, *Adaptive control tutorial*, Society for Industrial and Applied Mathematics, Philadelphia.

Ippoliti, G, Jetto, L & Longhi, S 2006, 'Switching-based supervisory control of underwater vehicles', in GN Roberts & R Sutton (eds), *Advances in Unmanned Marine Vehicles*, Institution of Engineering and Technology, London, UK, pp. 105-126.

Ippoliti, G, Longhi, S & Radicioni, A 2002, 'Modelling and identification of a remotely operated vehicle', *Proceedings of the Institute of Marine Engineering, Science and Technology. Part A, Journal of Marine Engineering and Technology*, vol. 1, no. 1, pp. 48-56.

Jessup, ME 2014, 'Mesophotic coral ecosystems: tools and techniques for scientific exploration', in G Eckert, S Keller & S Tamone (eds), *Diving for Science 2014: Proceedings of the AAUS 33rd Scientific Symposium*, Sitka, Alaska, pp. 14-21.

Jin-Yeong, P, Bong-Huan, J, Pan-Mook, L, Yong-Kon, L & Jun-Ho, O 2011, 'Docking problem and guidance laws considering drift for an underactuated AUV', in *Proceedings of the IEEE/MTS 2011 OCEANS- Spain*, Santander, Spain.

Jonathan, M & Anthony, C 2010, 'Adaptive Control for Systems with Slow Reference Models', in *Proceedings of the AIAA Infotech@Aerospace 2010*, Atlanta, Georgia.

Jun, SW, Kim, DW & Lee, HJ 2011, 'Design of T-S fuzzy-model-based controller for depth control of autonomous underwater vehicles with parametric uncertainties', in *Proceedings of the 11th International Conference on Control, Automation and Systems*, pp. 1682-1684.

Karras, GC, Loizou, SG & Kyriakopoulos, KJ 2010, 'A visual-servoing scheme for semi-autonomous operation of an underwater robotic vehicle using an IMU and a laser vision system', in *Proceedings of the 2010 IEEE International Conference on Robotics and Automation*, pp. 5262-5267.

Kawaguchi, K, Araki, E, Kaneko, S, Nishida, T & Komine, T 2011, 'Subsea engineering ROV and seafloor observatory construction', in *Proceedings of the 2011 IEEE Symposium on Underwater Technology and Workshop on Scientific Use of Submarine Cables and Related Technologies* Tokyo, Japan.

Kemna, S, Hamilton, MJ, Hughes, DT & LePage, KD 2011, 'Adaptive autonomous underwater vehicles for littoral surveillance', *Intelligent Service Robotics*, vol. 4, no. 4, pp. 245-258.

Khosravi, A, Lachini, Z & Sarhadi, P 2015, 'Predictor-based model reference adaptive control for a vehicle lateral dynamics considering uncertainties', *Proceedings of the Institution of Mechanical Engineers, Part I: Journal of Systems and Control Engineering*, vol. 229, no. 9, pp. 797-807.

Kim, TW & Yuh, J 2004, 'Development of a real-time control architecture for a semi-autonomous underwater vehicle for intervention missions', *Control engineering practice*, vol. 12, no. 12, pp. 1521-1530.

Koh, TH, Lau, MWS, Seet, G & Low, E 2006, 'A Control Module Scheme for an Underactuated Underwater Robotic Vehicle', *Journal of Intelligent and Robotic Systems*, vol. 46, no. 1, pp. 43-58.

Kukulya, A, Plueddemann, A, Austin, T, Stokey, R, Purcell, M, Allen, B, Littlefield, R, Freitag, L, Koski, P, Gallimore, E, Kemp, J, Newhall, K & Pietro, J 2010, 'Under-ice operations with a REMUS-100 AUV in the Arctic', in *Proceedings of the 2010 IEEE/OES Autonomous Underwater Vehicles*, Monterey, CA, USA, pp. 1-8.

L'Hour, M & Creuze, V 2016, 'French Archaeology's Long March to the Deep—The Lune Project: Building the Underwater Archaeology of the Future', in MA Hsieh, O Khatib & V Kumar (eds), *Experimental Robotics: The 14th International*

Symposium on Experimental Robotics, Springer International Publishing, Cham, pp. 911-927.

Lavretsky, E 2009, 'Combined / Composite Model Reference Adaptive Control', in *Proceedings of the 2009 AIAA Guidance, Navigation, and Control Conference*, Chicago, Illinois.

Lavretsky, E, Gadient, R & Gregory, IM 2010, 'Predictor-based model reference adaptive control', *Journal of Guidance, Control, and Dynamics*, vol. 33, no. 4, pp. 1195-1201.

Lavretsky, E & Gibson, TE 2011, 'Projection Operator in Adaptive Systems', *arXiv:1112.4232*.

Le, KD, Nguyen, HD & Ranmuthugala, D 2013, 'Development and modelling of a three-thurster remotely operated vehicle using open source hardware', in *Proceedings of the 17th International Conference On Mechatronics Technology*, Jeju Island, Korea.

Leong, ZQ 2014, 'Effects of Hydrodynamic Interaction on an AUV Operating Close to a Moving Submarine', PhD thesis, University of Tasmania.

Leong, ZQ, Ranmuthugala, D, Penesis, I & Nguyen, HD 2015, 'Quasi-static analysis of the hydrodynamic interaction effects on an autonomous underwater vehicle operating in proximity to a moving submarine', *Ocean Engineering*, vol. 106, pp. 175-188.

Liu, H, Costa, RR, Lizarralde, F & Cunha, JPVSD 2000, 'Dynamic positioning of remotely operated underwater vehicles', *IEEE Robotics & Automation Magazine*, vol. 7, no. 3, pp. 21-31.

TE Connectivity 2015, *MS5837-30BA ultra small gel filled pressure sensor datasheet*, TE Connectivity Ltd., Schaffhausen, Switzerland, viewed 30/12/2016, <http://www.te.com/commerce/DocumentDelivery/DDEController?Action=showdoc&DocId=Data+Sheet%7FMS583730BA%7FB1%7Fpdf%7FEnglish%7FENG_DS_MS5837-30BA_B1.pdf%7FCAT-BLPS0017>.

Lygouras, JN 1999, 'DC Thruster Controller Implementation with Integral Anti-wind up Compensator for Underwater ROV', *Journal of Intelligent and Robotic Systems*, vol. 25, no. 1, pp. 79-94.

Lynn, DC & Bohlander, GS 1999, 'Performing ship hull inspections using a remotely operated vehicle', in *Proceedings of the IEEE/MTS 1999 OCEANS*, Seattle, WA, USA, vol. 2, pp. 555-562

Maalouf, D 2013, 'Contributions to Nonlinear Adaptive Control of Low Inertia Underwater Robots', PhD thesis, University of Montpellier.

Maalouf, D, Chemori, A & Creuze, V 2015, 'Adaptive depth and pitch control of an underwater vehicle with real-time experiments', *Ocean Engineering*, vol. 98, pp. 66-77.

Maalouf, D, Creuze, V & Chemori, A 2012a, 'A novel application of multivariable L1 adaptive control: From design to real-time implementation on an underwater vehicle', in *Proceedings of the 2012 IEEE/RSJ International Conference on Intelligent Robots and Systems*, Vilamoura, Portugal, pp. 76-81.

—— 2012b, 'State feedback control of an underwater vehicle for wall following', in *Proceedings of the 20th Mediterranean Conference on Control & Automation (MED)*, Barcelona, Spain, pp. 542-547.

—— 2013, 'A new extension of the L1 adaptive controller to drastically reduce the tracking time lags', in *Proceedings of the 9th IFAC Symposium on Nonlinear Control Systems*, Toulouse, France, pp. 481-486.

Maalouf, D, Creuze, V, Chemori, A, Tamanaja, IT, Mercado, EC, Muñoz, JT, Lozano, R & Tempier, O 2015, 'Real-time experimental comparison of two depth control schemes for underwater vehicles', *International Journal of Advanced Robotic Systems*, vol. 12, no. 2, pp. 1-15.

Maalouf, D, Tamanaja, I, Campos, E, Creuze, V, Chemori, A, Torres, J & Rogelio, L 2013, 'From PD to Nonlinear Adaptive Depth-Control of a Tethered Autonomous Underwater Vehicle', in *Proceedings of the 5th Symposium on System Structure and Control*, Grenoble, France, pp. 743-748.

Magree, D, Yucelen, T & Johnson, E 2012, 'Command Governor-Based Adaptive Control of an Autonomous Helicopter', in *AIAA Guidance, Navigation, and Control Conference*, Minneapolis, Minnesota.

Makavita, CD, Nguyen, HD, Jayasinghe, SG & Ranmuthugala, D 2016a, 'Command Governor Adaptive Control for Unmanned Underwater Vehicles with measurement noise and actuator dead-zone', in *Proceedings of the 2016*

Moratuwa Engineering Research Conference (MERCon), Moratuwa, Sri Lanka, pp. 379-384.

—— 2016b, 'Predictor-based model reference adaptive control of an unmanned underwater vehicle', in *Proceedings of the 14th International Conference on Control, Automation, Robotics and Vision (ICARCV)*, Phuket, Thailand.

—— 2017a, 'Experimental Comparison of Two Composite MRAC methods for UUV Operations under Low Adaptation Gains ', *Unpublished*.

—— 2017b, 'Experimental Study of an Command Governor Adaptive Depth Controller for an Unmanned Underwater Vehicle ', *Unpublished*.

—— 2017c, 'Experimental Study of Command Governor Adaptive Control for Unmanned Underwater Vehicles', *IEEE Transactions on Control Systems Technology*.

Makavita, CD, Nguyen, HD & Ranmuthugala, D 2014, 'Fuzzy gain scheduling based optimally tuned PID controllers for an unmanned underwater vehicle', *International Journal of Conceptions on Electronics and Communications Engineering*, vol. 2, pp. 7-13.

Makavita, CD, Nguyen, HD, Ranmuthugala, D & Jayasinghe, SG 2015a, 'Command governor adaptive control for an unmanned underwater vehicle', in *Proceedings of the 2015 IEEE Conference on Control Applications (CCA)*, Sydney, Australia, pp. 1096-1102.

—— 2015b, 'Composite model reference adaptive control for an unmanned underwater vehicle', *Underwater Technology*, vol. 33, no. 2, pp. 81-93.

Martin, SC & Whitcomb, LL 2014, 'Experimental identification of six-degree-of-freedom coupled dynamic plant models for underwater robot vehicles', *IEEE Journal of Oceanic Engineering*, vol. 39, no. 4, pp. 662-671.

MathWorks 2017, *How the Optimization Algorithm Formulates Minimization Problems*, Mathworks, viewed 8/8/2017 2017, <https://au.mathworks.com/help/sldo/ug/how-the-optimization-algorithm-formulates-minimization-problems.html>.

McFarland, CJ & Whitcomb, LL 2014, 'Experimental evaluation of adaptive model-based control for underwater vehicles in the presence of unmodeled actuator

dynamics', in *Proceedings of the 2014 IEEE International Conference on Robotics and Automation (ICRA), ,* pp. 2893-2900.

McLain, T & Rock, S 1992, 'Experimental measurement of rov tether tension', in *Proceedings of Intervention/ROV '92*, San Diego, CA.

Medagoda, L & Williams, SB 2012, 'Model predictive control of an autonomous underwater vehicle in an in situ estimated water current profile', in *IEEE/MTS OCEANS 2012- Yeosu*, Yeosu, South Korea.

Meinecke, G, Ratmeyer, V & Renken, J 2011, 'HYBRID-ROV - Development of a new underwater vehicle for high-risk areas', in *Proceedings of the IEEE/MTS OCEANS 2011- KONA*, Waikoloa, HI, USA.

Miskovic, N, Vukic, Z, Barisic, M & Tovornik, B 2006, 'Autotuning Autopilots for Micro-ROVs', in *Proceedings of the 14th Mediterranean Conference on Control and Automation*, Ancona, Italy.

Mrad, FT & Majdalani, AS 2003, 'Composite adaptive control of astable UUVs', *IEEE Journal of Oceanic Engineering*, vol. 28, no. 2, pp. 303-307.

Na, J, Herrmann, G & Zhang, K 2017, 'Improving transient performance of adaptive control via a modified reference model and novel adaptation', *International Journal of Robust and Nonlinear Control*, vol. 27, no. 8, pp. 1351-1372.

Narendra, KS & Annaswamy, AM 2005, *Stable adaptive systems*, Dover Publications, New York.

Nguyen, HD, Pienaar, R, Ranmuthugala, D & West, W 2011, 'Modeling, simulation and control of underwater vehicles', in *Proceedings of the 1st Vietnam Conference on Control and Automation*, Hanoi, Vietnam, pp. 150-159.

Nguyen, N & Summers, E 2011, 'On Time Delay Margin Estimation for Adaptive Control and Robust Modification Adaptive Laws', in *AIAA Guidance, Navigation, and Control Conference*, Portland, Oregon.

Nomoto, M & Hattori, M 1986, 'A deep ROV "DOLPHIN 3K": Design and performance analysis', *IEEE Journal of Oceanic Engineering*, vol. 11, no. 3, pp. 373-391.

Oktafianto, K, Herlambang, T, Mardlijah & Nurhadi, H 2015, 'Design of Autonomous Underwater Vehicle motion control using Sliding Mode Control method', in

Proceedings of the 2015 International Conference on Advanced Mechatronics, Intelligent Manufacture, and Industrial Automation (ICAMIMIA), pp. 162-166.

OpenROV 2016, viewed 25 June 2016, <http://www.openrov.com/>.

Ortega, R & Panteley, E 2014, 'Comments on -adaptive control: stabilisation mechanism, existing conditions for stability and performance limitations', *International Journal of Control*, vol. 87, no. 3, pp. 581-588.

Pacunski, RE, Palsson, WA, Greene, HG & Gunderson, D 2008, 'Conducting visual surveys with a small ROV in shallow water', in JR Reynolds & HG Greene (eds), *Marine Habitat Mapping Technology for Alaska*, Alaska Sea Grant for North Pacific Research Board, University of Alaska Fairbanks, pp. 109-128.

Pascoal, A, Oliveira, P, Silvestre, C, Bjerrum, A, Ishoy, A, Pignon, JP, Ayela, G & Petzelt, C 1997, 'MARIUS: an autonomous underwater vehicle for coastal oceanography', *IEEE Robotics & Automation Magazine*, vol. 4, no. 4, pp. 46-59.

Pascoal, A, Silvestre, C & Oliveira, P 2006, 'Vehicle and mission control of single and multiple autonomous marine robots', in GN Roberts & R Sutton (eds), *Advances in Unmanned Marine Vehicles*, Institution of Engineering and Technology, London, UK, pp. 353-386.

Perez, T & Fossen, TI 2005, 'Kinematics of Ship Motion', in *Ship Motion Control: Course Keeping and Roll Stabilisation Using Rudder and Fins*, Springer, London, pp. 45-58.

Perrier, M & Canudas-De-Wit, C 1996, 'Experimental comparison of PID vs. PID plus nonlinear controller for subsea robots', *Autonomous Robots*, vol. 3, no. 2, pp. 195-212.

Pisano, A & Usai, E 2004, 'Output-feedback control of an underwater vehicle prototype by higher-order sliding modes', *Automatica*, vol. 40, no. 9, pp. 1525-1531.

Pivano, L 2008, 'Thrust Estimation and Control of Marine Propellers in FourQuadrant Operations', PhD thesis, Norwegian University of Science and Technology.

Proctor, AA, Buchanan, A, Buckham, B & Bradley, C 2015, 'ROVs with semi-autonomous capabilities for use on renewable energy platforms', in *The Twenty-fifth International Offshore and Polar Engineering Conference*, Kona, Hawaii, USA.

Qin, SJ & Badgwell, TA 2003, 'A survey of industrial model predictive control technology', *Control engineering practice*, vol. 11, no. 7, pp. 733-764.

Refsnes, JE 2007, 'Nonlinear model-based control of slender body AUVs', Ph.D. dissertation thesis, Nowergian University of Science and Technology.

Roche, E, Sename, O, Simon, D & Varrier, S 2011, 'A hierarchical varying sampling H∞ control of an AUV', in *Proceedings of the 18th IFAC World Congress*, pp. 14729-14734.

Rodgers, J, Wharington, J, Tynan, A & Coxhead, M 2008, 'A concept for the deployment of unmanned maritime systems from submarines: MURULA integration impact modelling and results', in *Undersea Defence Technology Pacific Conference*, Sydney, Australia.

Rubin, S 2013, 'Mini-ROVs, going where no ROV has gone before', in *Proceedings of the IEEE/MTS 2013 Oceans - San Diego*, San Diego, CA, USA.

Sayer, P 1996, 'Hydrodynamic Forces On ROVs Near the Air-Sea Interface', *International Journal of Offshore and Polar Engineering*, vol. 6, no. 3, pp. 177-183.

Schatz, SP, Yucelen, T & Johnson, EN 2013, 'Constrained adaptive control with transient and steady-state performance guarantees', in *CEAS EuroGNC, Delft, Netherlands*, Delft, Netherlands.

Schatz, SP, Yucelen, T, Johnson, EN & Holzapfel, F 2013, 'Constraint Enforcement Methods for Command Governor based Adaptive Control of Uncertain Dynamical Systems', in *AIAA Guidance, Navigation, and Control (GNC) Conference*, Boston, MA, USA.

SeaBotix, 2015, *BTD150 AUV/ROV Thruster Datasheet*, San Diego, USA.

Selbe, S 2014, *Exploration to Conservation Through Underwater Robotics*, National Geographic, viewed 25 June 2016, <http://voices.nationalgeographic.com/2014/12/10/exploration-to-conservation-through-underwater-robotics/>.

Slotine, JJE & Li, W 1989, 'Composite adaptive control of robot manipulators', *Automatica*, vol. 25, no. 4, pp. 509-519.

Smallwood, DA & Whitcomb, LL 2002, 'The effect of model accuracy and thruster saturation on tracking performance of model based controllers for underwater

robotic vehicles: experimental results', in *Proceedings of the 2002 IEEE International Conference on Robotics and Automation*, vol. 2, pp. 1081-1087.

—— 2003, 'Adaptive identification of dynamically positioned underwater robotic vehicles', *IEEE Transactions on Control Systems Technology*, vol. 11, no. 4, pp. 505-515.

—— 2004, 'Model-based dynamic positioning of underwater robotic vehicles: theory and experiment', *IEEE Journal of Oceanic Engineering*, vol. 29, no. 1, pp. 169-186.

SNAME 1950, *Nomenclature for Treating the Motion of a Submerged Body Through a Fluid: Report of the American Towing Tank Conference*, Society of Naval Architects and Marine Engineers.

Solvang, B, Deng, Z & Lien, TK 2001, 'A methodological framework for developing ROV-manipulator systems for underwater unmanned intervention', in *Proceedings of the IEEE/MTS Oceans 2001. An Ocean Odyssey.* , vol. 2, pp. 1085-1091

Sørensen, AJ 2005, 'Structural issues in the design and operation of marine control systems', *Annual Reviews in Control*, vol. 29, no. 1, pp. 125-149.

Sørensen, MEN & Breivik, M 2015, 'Comparing Nonlinear Adaptive Motion Controllers for Marine Surface Vessels', in R Galeazzi & M Blanke (eds), *Proceedings of the 10th IFAC Conference on Manoeuvring and Control of Marine Craft* Copenhagen, vol. 48, pp. 291-298.

Steenson, LV, Phillips, AB, Turnock, SR, Furlong, ME & Rogers, E 2012, 'Effect of measurement noise on the performance of a depth and pitch controller using the model predictive control method', in *2012 IEEE/OES Autonomous Underwater Vehicles (AUV)*, Southampton, UK, pp. 1-8.

Steenson, LV, Turnock, SR, Phillips, AB, Harris, C, Furlong, ME, Rogers, E, Wang, L, Bodles, K & Evans, DW 2014, 'Model predictive control of a hybrid autonomous underwater vehicle with experimental verification', *Proceedings of the Institution of Mechanical Engineers, Part M: Journal of Engineering for the Maritime Environment*, vol. 228, no. 2, pp. 166-179.

Stepanyan, V & Krishnakumar, K 2010, 'MRAC Revisited: Guaranteed performance with reference model modification', in *Proceedings of the 2010 American Control Conference*, pp. 93-98.

—— 2012a, 'Adaptive Control with Reference Model Modification', *Journal of Guidance, Control, and Dynamics*, vol. 35, no. 4, pp. 1370-1374.

—— 2012b, 'Indirect M-MRAC for systems with time varying parameters and bounded disturbances', in *Proceedings of the 2012 IEEE International Symposium on Intelligent Control*, pp. 1232-1237.

Stewart, K 2013, *NPS, NASA Collaborate on Human-Robot Interaction in Extreme Environments*, NPS, viewed 25 June 2016, <http://www.nps.edu/About/News/NPS-NASA-Collaborate-on-Human-Robot-Interaction-in-Extreme-Environments.html>.

Stilinović, N, Nađ, Đ & Mišković, N 2015, 'AUV for diver assistance and safety: Design and implementation', in *IEEE/MTS OCEANS 2015 - Genova*, p. 4.

Tyagi, A & Sen, D 2006, 'Calculation of transverse hydrodynamic coefficients using computational fluid dynamic approach', *Ocean Engineering*, vol. 33, no. 5, pp. 798-809.

Valladarez, LND 2015, 'An adaptive approach for precise underwater vehicle control in combined robot-diver operations', M.Sc thesis, Naval Postgraduate School.

Valladarez, LND & Toit, NED 2015, 'Robust adaptive control of Underwater Vehicles for precision operations', in *MTS/IEEE OCEANS 2015* Washington, pp. 1-7.

Vazquez, S, Leon, JI, Franquelo, LG, Rodriguez, J, Young, HA, Marquez, A & Zanchetta, P 2014, 'Model predictive control: a review of its applications in power electronics', *IEEE Industrial Electronics Magazine*, vol. 8, no. 1, pp. 16-31.

Wang, X-S, Su, C-Y & Hong, H 2004, 'Robust adaptive control of a class of nonlinear systems with unknown dead-zone', *Automatica*, vol. 40, no. 3, pp. 407-413.

Whitworth, M & Cohan, S 2011, 'Advances in ROV automation', *Ocean News & Technology*, vol. 17, no. 6, July, pp. 22-23.

Williams, SB, Pizarro, O, Mahon, I & Johnson-Roberson, M 2009, 'Simultaneous Localisation and Mapping and Dense Stereoscopic Seafloor Reconstruction Using an AUV', in O Khatib, V Kumar & GJ Pappas (eds), *Experimental Robotics: The Eleventh International Symposium*, Springer-Verlag Berlin Heidelberg, Berlin, Heidelberg, pp. 407-416, DOI 10.1007/978-3-642-00196-3_47.

Willy, CJ 1994, 'Attitude control of an underwater vehicle subjected to waves', M.Sc thesis, Massachusetts Institute of Technology and Woods Hole Oceanographic Institution.

Wu, J, Liu, J & Xu, H 2014, 'A variable buoyancy system and a recovery system developed for a deep-sea AUV Qianlong I', in *IEEE/MTS OCEANS 2014 - TAIPEI*, p. 4.

Wynn, RB, Huvenne, VAI, Le Bas, TP, Murton, BJ, Connelly, DP, Bett, BJ, Ruhl, HA, Morris, KJ, Peakall, J, Parsons, DR, Sumner, EJ, Darby, SE, Dorrell, RM & Hunt, JE 2014, 'Autonomous Underwater Vehicles (AUVs): Their past, present and future contributions to the advancement of marine geoscience', *Marine Geology*, vol. 352, pp. 451-468.

Yoerger, DR, Jakuba, M, Bradley, AM & Bingham, B 2007, 'Techniques for Deep Sea Near Bottom Survey Using an Autonomous Underwater Vehicle', *The International Journal of Robotics Research*, vol. 26, no. 1, pp. 41-54.

Yoerger, DR & Slotine, JJE 1991, 'Adaptive sliding control of an experimental underwater vehicle', in *Proceedings of the 1991 IEEE International Conference on Robotics and Automation*, vol. 3, pp. 2746-2751.

Yoerger, DR, Slotine, JJE, Newman, J & Schempf, H 1985, 'Robust trajectory control of underwater vehicles', in *Proceedings of the 1985 4th International Symposium on Unmanned Untethered Submersible Technology*, vol. 4, pp. 184-197.

Yu, H & Lloyd, S 1997, 'Combined direct and indirect adaptive control of constrained robots', *International Journal of Control*, vol. 68, no. 5, pp. 955-970.

Yucelen, T & Calise, AJ 2011, 'Derivative-free model reference adaptive control', *Journal of Guidance, Control, and Dynamics*, vol. 34, no. 4, pp. 933-950.

Yucelen, T & Haddad, WM 2012, 'A robust adaptive control architecture for disturbance rejection and uncertainty suppression with L∞ transient and steady-state performance guarantees', *International Journal of Adaptive Control and Signal Processing*, vol. 26, no. 11, pp. 1024-1055.

Yucelen, T & Haddad, WM 2013, 'Low-frequency learning and fast adaptation in model reference adaptive control', *IEEE Transactions on Automatic Control*, vol. 58, no. 4, pp. 1080-1085.

Yucelen, T & Johnson, E 2012a, 'Command governor-based adaptive control', in *AIAA Guidance, Navigation, and Control Conference*, Minneapolis, Minnesota, pp. 1-18.

—— 2012b, 'Design and analysis of a novel command governor architecture for shaping the transient response of nonlinear uncertain dynamical systems', in *Proceedings of the IEEE 51st Annual Conference on Decision and Control (CDC)*, pp. 2890-2895.

—— 2012c, 'On achieving predictable adaptive control response for uncertain dynamical systems with large domains of operation', in *AIAA Guidance, Navigation, and Control Conference*, Minneapolis, Minnesota, pp. 1-18.

—— 2013, 'A new command governor architecture for transient response shaping', *International Journal of Adaptive Control and Signal Processing*, vol. 27, no. 12, pp. 1065-1085.

Yucelen, T, Torre, GDL & Johnson, E 2013, 'Frequency-limited adaptive control architecture for transient response improvement', in *Proceedings of the 2013 American Control Conference*, pp. 6631-6636.

Yuh, J, Nie, J & Lee, CSG 1999, 'Experimental study on adaptive control of underwater robots', in *Proceedings of the1999 IEEE International Conference onRobotics and Automation*, vol. 1, pp. 393-398

Zang, Z & Bitmead, RR 1990, 'Transient bounds for adaptive control systems', in *Proceedings of the 29th IEEE Conference on Decision and Control*, vol. 5, pp. 2724-2729

—— 1994, 'Transient bounds for adaptive control systems', *IEEE Transactions on Automatic Control*, vol. 39, no. 1, pp. 171-175.

Zanoli, SM & Conte, G 2003, 'Remotely operated vehicle depth control', *Control engineering practice*, vol. 11, no. 4, pp. 453-459.

Zhao, S & Yuh, J 2005, 'Experimental study on advanced underwater robot control', *IEEE Transactions on Robotics*, vol. 21, no. 4, pp. 695-703.

Zhou, J, Wen, C & Zhang, Y 2006, 'Adaptive output control of nonlinear systems with uncertain dead-zone nonlinearity', *IEEE Transactions on Automatic Control*, vol. 51, no. 3, pp. 504-511.

Appendix 1 has been removed for copyright or proprietary reasons.

Appendix I:

Fuzzy Gain Scheduled based Optimally Tuned PID Controllers for an Unmanned Underwater Vehicle

This appendix has been published in the International Journal of Conceptions on Electronics and Communications Engineering. The citation for the research article is:

Makavita, CD, Nguyen, HD, & Ranmuthugala, D 2014, Fuzzy Gain Scheduled based Optimally Tuned PID Controllers for an Unmanned Underwater Vehicle, *International Journal of Conceptions on Electronics and Communications Engineering*,*2*, (1)pp.7-13. ISSN 2357-2809 [Refereed Article].

In this appendix, a number of PID controllers are designed for different operating regions of a UUV using a mathematical model with the gain values obtained using an optimisation algorithm. Then these controllers are gained scheduled using fuzzy logic and tested using computer simulations. While this method alowes some form of uncertanity handling it was determined that it was not as suitable as adaptive control for the required applications and therefore not included in the main body of this thesis.

Appendix II:

Simulation Setup

This appendix describes the Simulink models used in simulating the control algorithms

To obtain simulation results the MATLAB/Simulink model shown in Fig. AII.1 was used. In this model the main blocks are 6 DOF ROV Model represented by "AMC ROV" block, transformation of body fixed velocities to earth fixed positions represented by "Euler Transformation" block, conversion of forces to input voltages and input voltages to thrust of each thruster represented by "Thruster Allocation" block, depth controller represented by "Depth" block, and heading controller represented by the "Heading" block.

The three blocks "AMC ROV", "Euler Transformation" and Thruster Allocation" have the same functionality for all simulations. The internal structures of these three blocks are given in Figs. AII.2, AII.3, and AII.4. In addition the internal structure of the "Depth" block used for CGAC is given in Fig. AII.5. The "Depth" block for other controllers and "Heading" block have a similar structure to Fig. AII.5 with variations to accommodate the differences and is omitted for brevity.

In addition to these blocks there are few other blocks such as signal generator used to generate the reference signal given by "50sec Signal" block, the dead-zone inverse used for heading control given by "Dead-zone Inverse" block, and the noise generator represented by the "Band-Limited White Noise" blocks.

The simulation parameters where set as shown in Fig. AII.6.

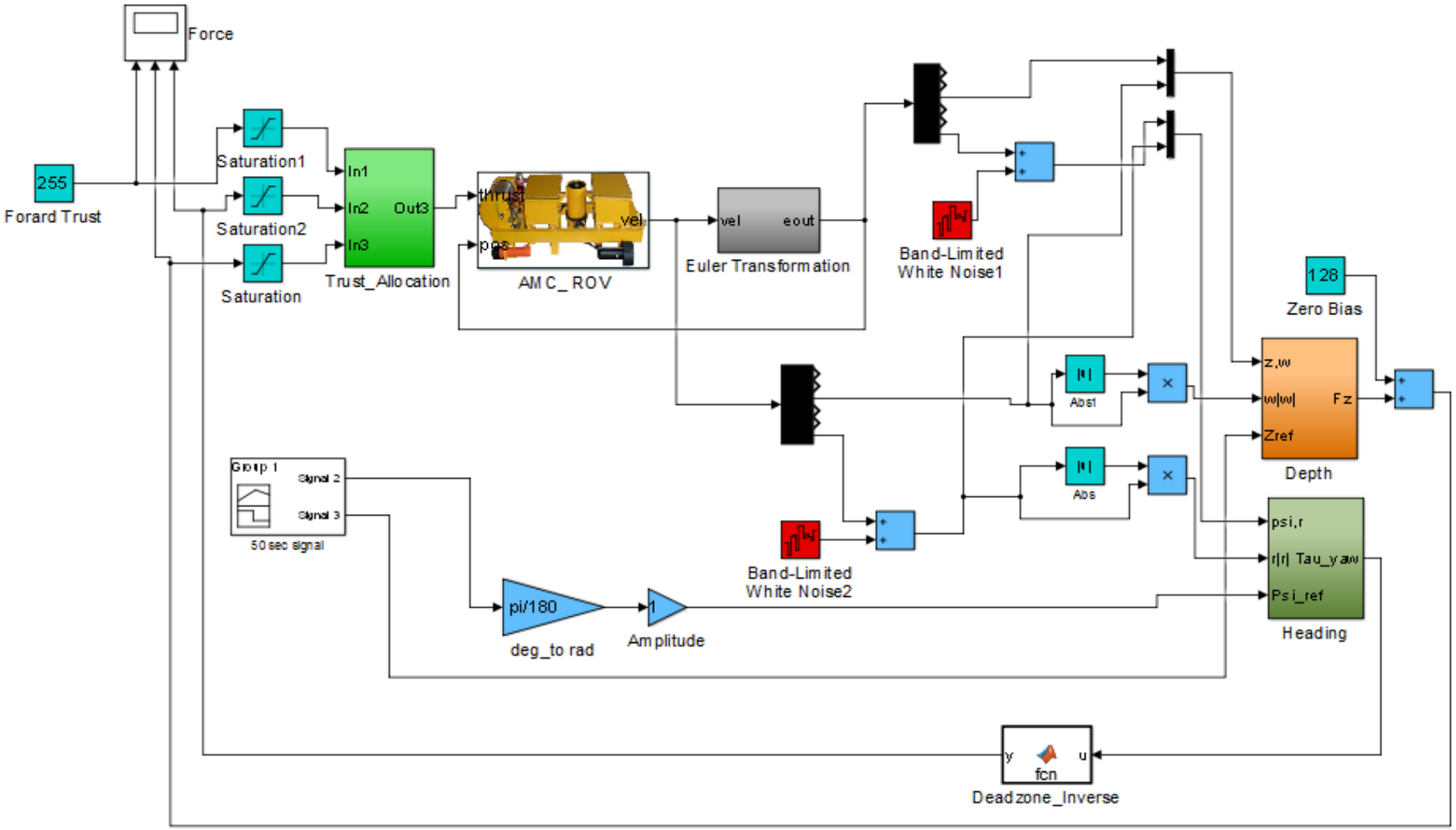

Figure AII. 1: The complete MATLAB/Simulink simulation model

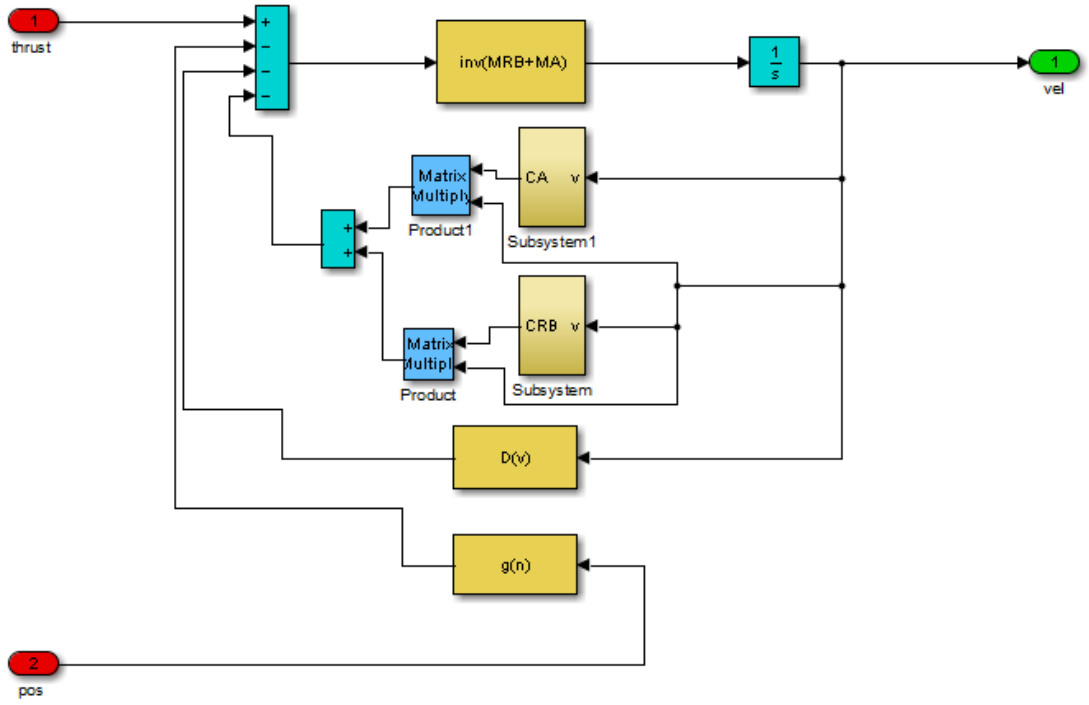

Figure AII. 2: Internal structure of "AMC ROV" block.

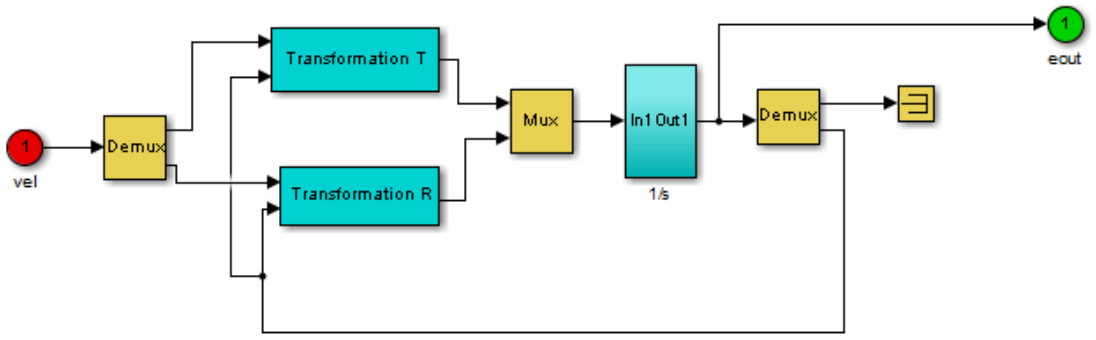

Figure AII. 3: Internal structure of "Euler Transformation" block.

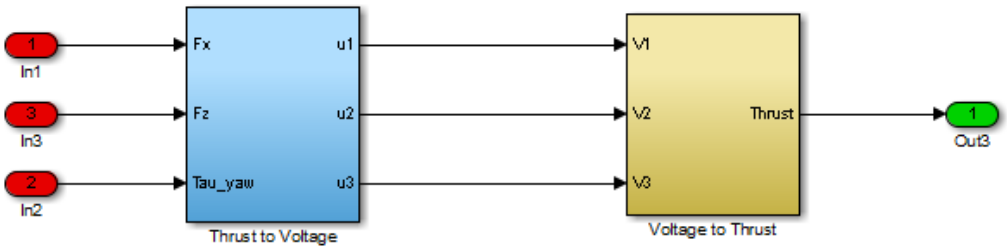

Figure AII. 4: Internal structure of "Thruster Allocation" block.

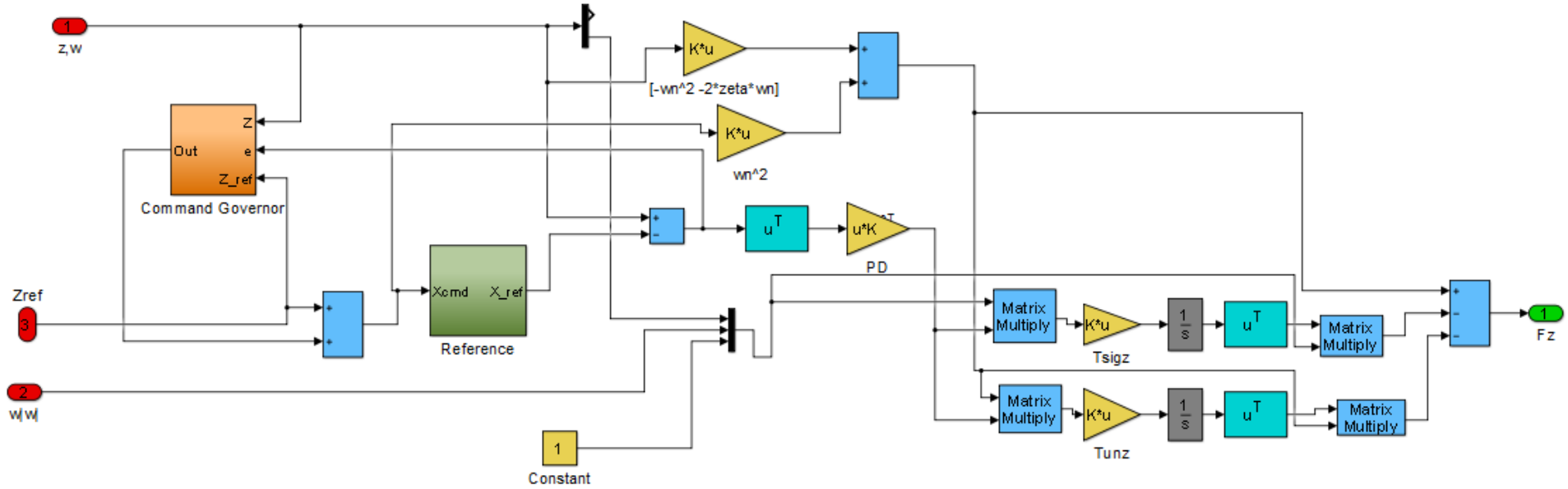

Figure AII. 5: Internal structure of the "Depth" block for CGAC controller.

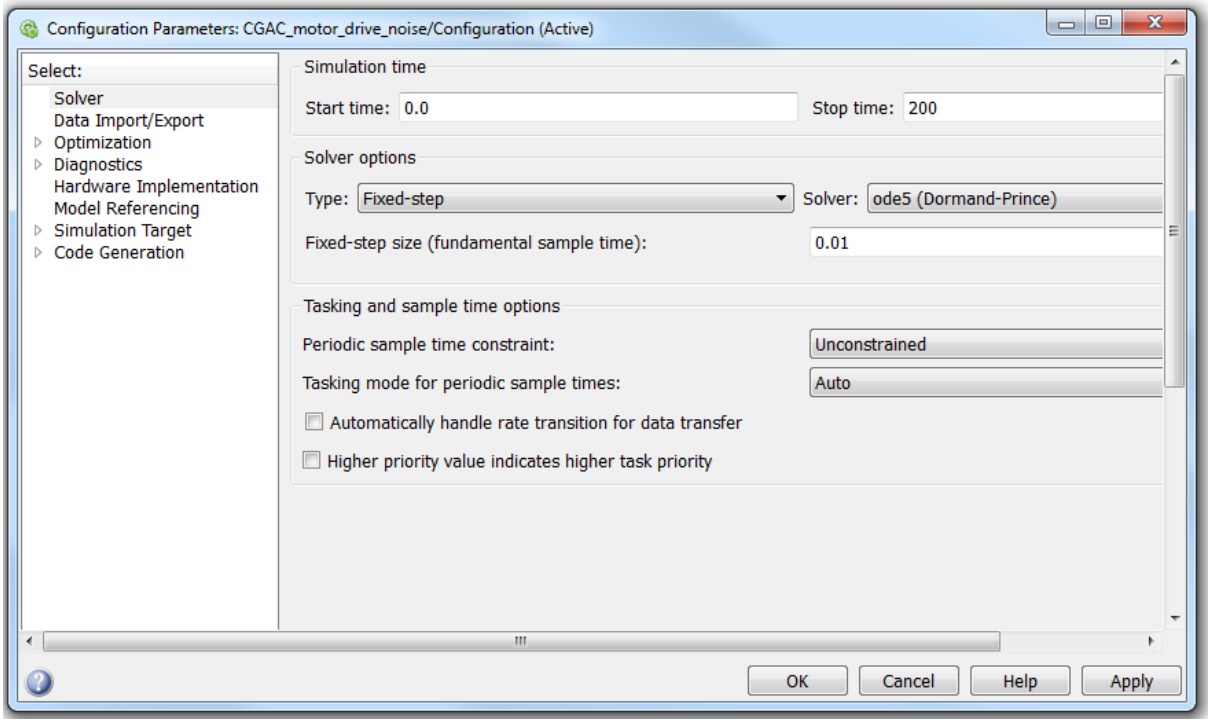

Figure AII. 6: Configuration parameters for simulations.

Appendix III:

Experimental Setup

This appendix describes the experimental setup used in all the experimental work in this thesis.

AIII.1 Configuration of the UUV

The unmanned underwater vehicle used for testing is the AMC ROV/AUV. The main components of this vehicle can be categorized into input unit (sensors), output unit (thrusters), processing unit (microcontroller), power unit and communications unit. The sensors measure the position and velocity which is processed by the processing unit and communicated to the computer through the communications unit. The control signal generated by the control system is communicated from the computer to the vehicle and then provided to the thrusters through the power unit. These different sections consist of the following devices.

AIII.1.1 Input Unit

The input unit consist of three sensors to measure heading, heading rate and depth. The specifications of each are given in Table AIII.1.

Table AIII. 1: Specification of the input unit components

Device name	Purpose	Specification
Measurement Specialties MS5837-30BA pressure sensor	Depth measurement	• Maximum depth rating of 300 m • Depth accuracy of 50 cm • Depth resolution of 2 mm
Honeywell HMC6352 digital compass	Heading measurement	• Heading accuracy of 2.5 degRMS • Heading resolution of 0.5 deg
Invesense MPU-9250 Inertial measurement Unit (IMU)	Heading rate measurement	• 3-axis angular rate sensors with user programmable full scale range of ±250, ±500, ±1000 and $\pm 2000^0/s$ • Integrated 16 bit ADC

AIII.1.2 Output Unit

The output unit consisted of 3 Seabotix BTD-150 thrusters. Two horizontal thrusters control the forward motion and heading changes while a single vertical thruster provided depth changes. The specification of the thrusters is given in Table AIII.2.

Table AIII. 2: Specification of the output unit components

Device name	Purpose	Specification
Seabotix BTD-150 thrusters	Actuators	• Depth rating of 150 m • Voltage: 17 -21 V • Current: 4.25 A continuous and 5.8 A maximum • Thrust: 2.2 KGF continual and 2.9 KGF maximum

AIII.1.3 Processing Unit

The processing unit consist of two Atmega 2560 microcontrollers. The specification of this is given in Table AIII.3.

Table AIII. 3: Specification of processing unit components

Device name	Purpose	Specification
Atmega 2560 microcontrollers	Processing of sensor data	• 16 MHz clock • 54 digital input/output pins and16 analogue inputs • 4 hardware serial ports (UARTS) • 256 KB flash memory

AIII.1.4 Power Unit

The power unit mainly consist of three Li-Po 18.5 V batteries and two MD-22 motor controllers, for which the specifications are given in Table AIII.4. In addition some other basic electronic components such as a relay and a 12 V to 5 voltage regulator were also used.

Table AIII. 4: Specification of power unit components

Device name	Purpose	Specification
	DC power	•
MD-22 motor controller	Actuator control	• Drive two motors with independent control • 5v and 50 mA for control logic and up to 24 v and 5 A for each motor • I2C control of motors with 0 (full reverse) 128 (stop) 255 (full forward)

AIII.1.5 Communication Unit

The communication between the host computer and the on-board microcontroller was carried out using RS485 communication protocol. The host computer was connected through a USB to FTDI cable to the RS232 to RS485 converter and then the RS485 bus is conveyed through the tether to the RS485 to RS232 converter connected to ATMEGA2560 microcontroller. A depiction of this is given in Fig.

In the host computer the data is received and send through Simulink Stream Input block and Stream Output block. The block representations and the settings are given Figs. In Stream Input block the main settings are the sample time, the data type and format

string that determine the number of data values that are received and how they are formatted. In this examplethe sample time is 0.01 s and three floating point numbers of type double are expected. In Stream Output block the main settings are the sample time and format string that determine the number of data values that are transmitted and how they are formatted. In the example given the -1 for sample time represents that it is inherited from Simulink overall sample time and A%fB shows that one floating point value is transmitted woth initial chatrcter A and ending charater B.

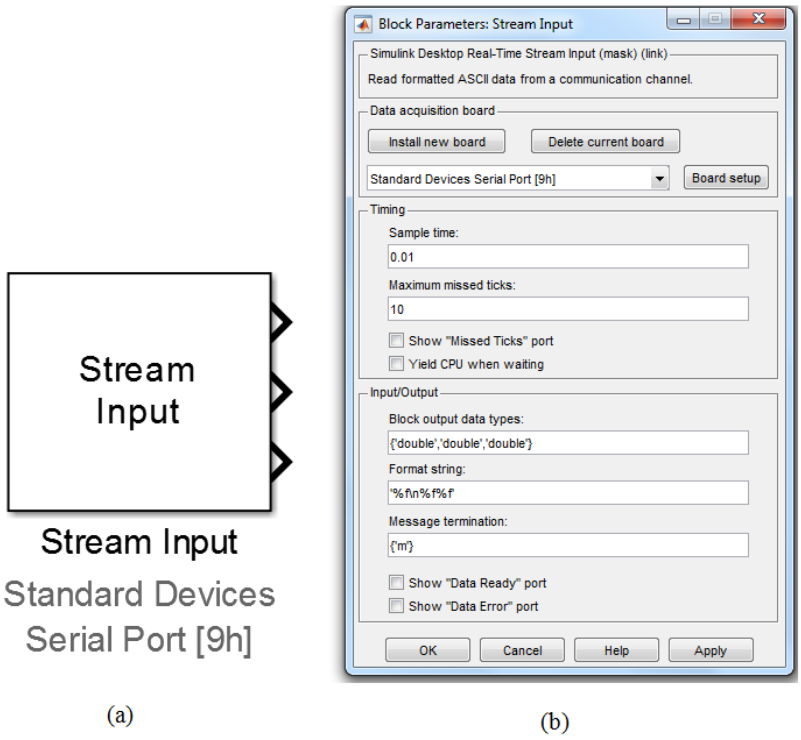

Figure AIII. 1: a) Block Diagram of Stream Input in Simulink and b) the settings panel of the stream input block

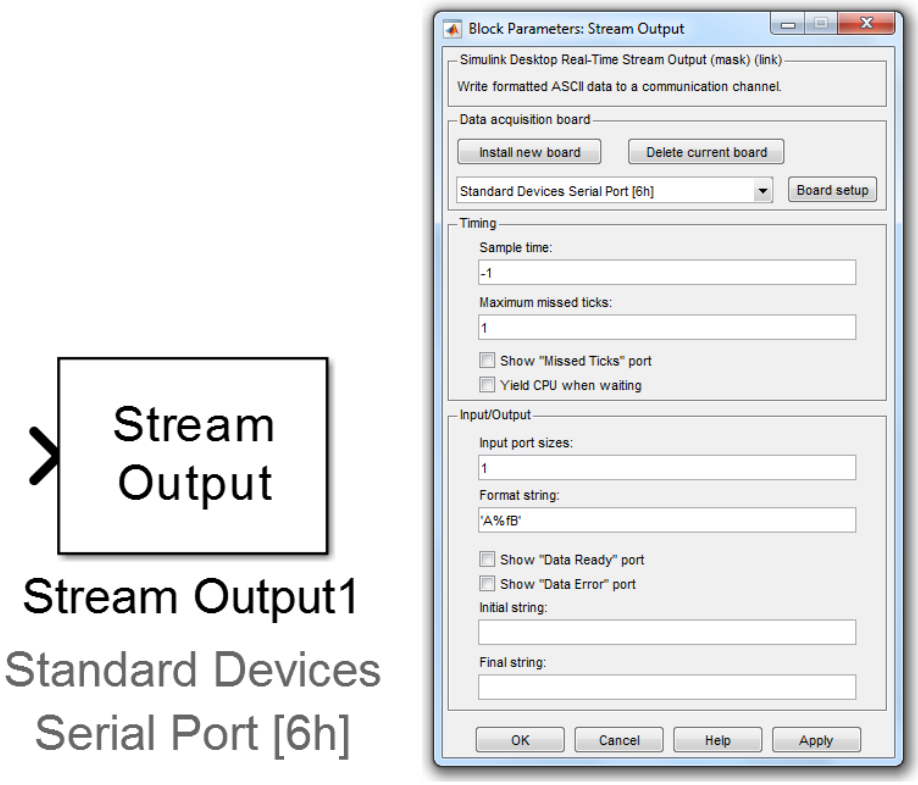

Figure AIII. 2: a) Block Diagram of Stream Input in Simulink and b) the settings panel of the stream input block

Appendix IV:

Stability Proof of ECGAC

This appendix gives the Lyapunov based stability analysis of the Extended Command Governor Adaptive Control (ECAGC) method which is proposed in Chapter 6.

In order to derive the stable adaptive laws, consider the following Lyapunov function candidate

$$V(\boldsymbol{e}_m, \hat{\boldsymbol{e}}, \tilde{\boldsymbol{W}}_{un}, \tilde{\boldsymbol{W}}_{\sigma}, \tilde{\boldsymbol{W}}_{un_f}, \tilde{\boldsymbol{W}}_{\sigma_f}) = \boldsymbol{e}_m^T \boldsymbol{P} \boldsymbol{e}_m + \hat{\boldsymbol{e}}^T \boldsymbol{P}_{prd} \hat{\boldsymbol{e}} + \text{trace}[(\tilde{\boldsymbol{W}}_{un} \Lambda^{\frac{1}{2}})^T \boldsymbol{\Gamma}_{un}^{-1} (\tilde{\boldsymbol{W}}_{un} \Lambda^{\frac{1}{2}}) + (\tilde{\boldsymbol{W}}_{\sigma} \Lambda^{\frac{1}{2}})^T \boldsymbol{\Gamma}_{\sigma}^{-1} (\tilde{\boldsymbol{W}}_{\sigma} \Lambda^{\frac{1}{2}})] +$$
$$\alpha \text{trace}[(\tilde{\boldsymbol{W}}_{un_f} \Lambda^{\frac{1}{2}})^T \boldsymbol{\Gamma}_{un_f}^{-1} (\tilde{\boldsymbol{W}}_{un_f} \Lambda^{\frac{1}{2}}) + (\tilde{\boldsymbol{W}}_{\sigma_f} \Lambda^{\frac{1}{2}})^T \boldsymbol{\Gamma}_{\sigma_f}^{-1} (\tilde{\boldsymbol{W}}_{\sigma_f} \Lambda^{\frac{1}{2}})]$$

Where $\boldsymbol{e}_m(t)$ is the system error, $\hat{\boldsymbol{e}}(t)$ is the prediction error, $\boldsymbol{P}$ and $\boldsymbol{P}_{prd}$ are positive definite matrices, $\tilde{\boldsymbol{W}}_{un}(t) \triangleq \hat{\boldsymbol{W}}_{un}(t) - \boldsymbol{W}_{un} \in \mathbb{R}^{q \times q}$ and $\tilde{\boldsymbol{W}}_{\sigma}(t) \triangleq \hat{\boldsymbol{W}}_{\sigma}(t) - \boldsymbol{W}_{\sigma} \in \mathbb{R}^{s \times q}$ are weight estimation errors, $\boldsymbol{\Gamma}_{un} \in \mathbb{R}^{q \times q}$ and $\boldsymbol{\Gamma}_{\sigma} \in \mathbb{R}^{s \times s}$ are learning rates, $\tilde{\boldsymbol{W}}_{un_f}(t) \triangleq \hat{\boldsymbol{W}}_{un_f}(t) - \boldsymbol{W}_{un} \in \mathbb{R}^{q \times q}$ and $\tilde{\boldsymbol{W}}_{\sigma_f}(t) \triangleq \hat{\boldsymbol{W}}_{\sigma}(t) - \boldsymbol{W}_{\sigma} \in \mathbb{R}^{s \times q}$ are low-pas filtered weights estimation errors, $\boldsymbol{\Gamma}_{un_f} \in \mathbb{R}^{q \times q}$ and $\boldsymbol{\Gamma}_{\sigma_f} \in \mathbb{R}^{s \times s}$ are positive definite filter gain matrices and $\boldsymbol{\Lambda} \in \mathbb{R}^{q \times q}$ is an unknown control effectiveness matrix with positive diagonal elements.

Note that $V(0, 0, 0, 0, 0, 0) = 0$ and $V(\boldsymbol{e}_m, \hat{\boldsymbol{e}}, \tilde{\boldsymbol{W}}_{un}, \tilde{\boldsymbol{W}}_{\sigma}, \tilde{\boldsymbol{W}}_{un_f}, \tilde{\boldsymbol{W}}_{\sigma_f}) > 0$ for all $(\boldsymbol{e}_m, \hat{\boldsymbol{e}}, \tilde{\boldsymbol{W}}_{un}, \tilde{\boldsymbol{W}}_{\sigma}, \tilde{\boldsymbol{W}}_{un_f}, \tilde{\boldsymbol{W}}_{\sigma_f}) \neq (0,0,0,0,0,0)$. In addition, $V(\boldsymbol{e}_m, \hat{\boldsymbol{e}}, \tilde{\boldsymbol{W}}_{un}, \tilde{\boldsymbol{W}}_{\sigma}, \tilde{\boldsymbol{W}}_{un_f}, \tilde{\boldsymbol{W}}_{\sigma_f})$ is radially unbounded.

Now, differentiating $V(\boldsymbol{e}_m, \hat{\boldsymbol{e}}, \tilde{\boldsymbol{W}}_{un}, \tilde{\boldsymbol{W}}_{\sigma}, \tilde{\boldsymbol{W}}_{un_f}, \tilde{\boldsymbol{W}}_{\sigma_f})$ yields

$$\begin{aligned}\dot{V}(\boldsymbol{e}_m, \hat{\boldsymbol{e}}, \tilde{\boldsymbol{W}}_{un}, \tilde{\boldsymbol{W}}_{\sigma}, \tilde{\boldsymbol{W}}_{un_f}, \tilde{\boldsymbol{W}}_{\sigma_f}) &= \dot{\boldsymbol{e}}_m^T \boldsymbol{P} \boldsymbol{e}_m + \boldsymbol{e}_m^T \boldsymbol{P} \dot{\boldsymbol{e}}_m + \dot{\hat{\boldsymbol{e}}}^T \boldsymbol{P}_{prd} \hat{\boldsymbol{e}} + \hat{\boldsymbol{e}}^T \boldsymbol{P}_{prd} \dot{\hat{\boldsymbol{e}}} \\ &+ 2\text{trace}[(\tilde{\boldsymbol{W}}_{un}{}^T \boldsymbol{\Gamma}_{un}^{-1} \dot{\hat{\boldsymbol{W}}}_{un} + \tilde{\boldsymbol{W}}_{\sigma}{}^T \boldsymbol{\Gamma}_{\sigma}^{-1} \dot{\hat{\boldsymbol{W}}}_{\sigma}) \Lambda] \\ &+ 2\alpha \text{trace}[(\tilde{\boldsymbol{W}}_{un_f}^T \boldsymbol{\Gamma}_{un_f}^{-1} \dot{\hat{\boldsymbol{W}}}_{un_f} + \tilde{\boldsymbol{W}}_{\sigma_f}^T \boldsymbol{\Gamma}_{\sigma_f}^{-1} \dot{\hat{\boldsymbol{W}}}_{\sigma_f}) \Lambda]\end{aligned}$$

Substituting from error dynamics of (6.11) and (6.29)

$$\dot{V}(\boldsymbol{e}_m, \hat{\boldsymbol{e}}, \tilde{\boldsymbol{W}}_{un}, \tilde{\boldsymbol{W}}_{\sigma}, \tilde{\boldsymbol{W}}_{un_f}, \tilde{\boldsymbol{W}}_{\sigma_f}) = \left(\boldsymbol{A}_m \boldsymbol{e}_m - \boldsymbol{H}\boldsymbol{\Lambda}\left[\tilde{\boldsymbol{W}}_{un}{}^T \boldsymbol{u}_n(t) + \tilde{\boldsymbol{W}}_{\sigma}{}^T \boldsymbol{\sigma}(\boldsymbol{x}) \right] \right)^T \boldsymbol{P}\boldsymbol{e}_m$$
$$+ \boldsymbol{e}_m^T \boldsymbol{P} \left(\boldsymbol{A}_m \boldsymbol{e}_m - \boldsymbol{H}\boldsymbol{\Lambda}\left[\tilde{\boldsymbol{W}}_{un}{}^T(t) \boldsymbol{u}_n(t) + \tilde{\boldsymbol{W}}_{\sigma}{}^T \boldsymbol{\sigma}(\boldsymbol{x}) \right] \right)$$
$$+ \left(\boldsymbol{A}_m \hat{\boldsymbol{e}} + \boldsymbol{H}\boldsymbol{\Lambda}\left[\tilde{\boldsymbol{W}}_{un}{}^T \boldsymbol{u}_n(t) + \tilde{\boldsymbol{W}}_{\sigma}{}^T \boldsymbol{\sigma}(\boldsymbol{x}) \right] \right)^T \boldsymbol{P}_{prd} \hat{\boldsymbol{e}}$$
$$+ \hat{\boldsymbol{e}}^T \boldsymbol{P}_{prd} \left(\boldsymbol{A}_m \hat{\boldsymbol{e}} + \boldsymbol{H}\boldsymbol{\Lambda}\left[\tilde{\boldsymbol{W}}_{un}{}^T \boldsymbol{u}_n(t) + \tilde{\boldsymbol{W}}_{\sigma}{}^T \boldsymbol{\sigma}(\boldsymbol{x}) \right] \right)$$
$$+ 2\mathrm{trace}[(\tilde{\boldsymbol{W}}_{un}{}^T \boldsymbol{\Gamma}_{un}^{-1} \dot{\hat{\boldsymbol{W}}}_{un} + \tilde{\boldsymbol{W}}_{\sigma}{}^T \boldsymbol{\Gamma}_{\sigma}^{-1} \dot{\hat{\boldsymbol{W}}}_{\sigma})\Lambda]$$
$$+ 2\alpha\,\mathrm{trace}[(\tilde{\boldsymbol{W}}_{un_f}^T \boldsymbol{\Gamma}_{un_f}^{-1} \dot{\hat{\boldsymbol{W}}}_{un_f} + \tilde{\boldsymbol{W}}_{\sigma_f}^T \boldsymbol{\Gamma}_{\sigma_f}^{-1} \dot{\hat{\boldsymbol{W}}}_{\sigma_f})\Lambda]$$

$$\dot{V}(\boldsymbol{e}_m, \hat{\boldsymbol{e}}, \tilde{\boldsymbol{W}}_{un}, \tilde{\boldsymbol{W}}_{\sigma}, \tilde{\boldsymbol{W}}_{un_f}, \tilde{\boldsymbol{W}}_{\sigma_f}) = \boldsymbol{e}_m^T \left[\boldsymbol{A}_m^T \boldsymbol{P} + \boldsymbol{P}\boldsymbol{A}_m \right] \boldsymbol{e}_m + \hat{\boldsymbol{e}}^T \left[\boldsymbol{A}_{prd}^T \boldsymbol{P}_{prd} + \boldsymbol{A}_{prd} \boldsymbol{P}_{prd} \right] \boldsymbol{e}$$
$$- 2\boldsymbol{e}_m^T \boldsymbol{P}\boldsymbol{H}\boldsymbol{\Lambda}\left[\tilde{\boldsymbol{W}}_{un}{}^T \boldsymbol{u}_n(t) + \tilde{\boldsymbol{W}}_{\sigma}{}^T \boldsymbol{\sigma}(\boldsymbol{x}) \right]$$
$$+ 2\hat{\boldsymbol{e}}^T \boldsymbol{P}_{prd} \boldsymbol{H}\boldsymbol{\Lambda}\left[\tilde{\boldsymbol{W}}_{un}{}^T \boldsymbol{u}_n(t) + \tilde{\boldsymbol{W}}_{\sigma}{}^T \boldsymbol{\sigma}(\boldsymbol{x}) \right]$$
$$+ 2\mathrm{trace}[(\tilde{\boldsymbol{W}}_{un}{}^T \boldsymbol{\Gamma}_{un}^{-1} \dot{\hat{\boldsymbol{W}}}_{un} + \tilde{\boldsymbol{W}}_{\sigma}{}^T \boldsymbol{\Gamma}_{\sigma}^{-1} \dot{\hat{\boldsymbol{W}}}_{\sigma})\Lambda]$$
$$+ 2\alpha\,\mathrm{trace}[(\tilde{\boldsymbol{W}}_{un_f}^T \boldsymbol{\Gamma}_{un_f}^{-1} \dot{\hat{\boldsymbol{W}}}_{un_f} + \tilde{\boldsymbol{W}}_{\sigma_f}^T \boldsymbol{\Gamma}_{\sigma_f}^{-1} \dot{\hat{\boldsymbol{W}}}_{\sigma_f})\Lambda]$$

Substituting from the Lyapunov equations $\boldsymbol{0} = \boldsymbol{A}_m^T \boldsymbol{P} + \boldsymbol{P}\boldsymbol{A}_m + \boldsymbol{Q}$ for some $\boldsymbol{Q} = \boldsymbol{Q}^T > 0$ and $\boldsymbol{0} = \boldsymbol{A}_{prd}{}^T \boldsymbol{P}_{prd} + \boldsymbol{P}_{prd} \boldsymbol{A}_{prd} + \boldsymbol{Q}_{prd}$ for some $\boldsymbol{Q}_{prd} = \boldsymbol{Q}_{prd}{}^T > 0$.

$$\dot{V}(\boldsymbol{e}_m, \hat{\boldsymbol{e}}, \tilde{\boldsymbol{W}}_{un}, \tilde{\boldsymbol{W}}_{\sigma}, \tilde{\boldsymbol{W}}_{un_f}, \tilde{\boldsymbol{W}}_{\sigma_f}) = -\boldsymbol{e}_m^T \boldsymbol{Q}\boldsymbol{e}_m - \hat{\boldsymbol{e}}^T \boldsymbol{Q}_{prd} \boldsymbol{e}$$
$$+ 2\left(\hat{\boldsymbol{e}}^T \boldsymbol{P}_{prd} - \boldsymbol{e}_m^T \boldsymbol{P} \right) \boldsymbol{H}\boldsymbol{\Lambda}\left[\tilde{\boldsymbol{W}}_{un}{}^T \boldsymbol{u}_n(t) + \tilde{\boldsymbol{W}}_{\sigma}{}^T \boldsymbol{\sigma}(\boldsymbol{x}) \right]$$
$$+ 2\mathrm{trace}[(\tilde{\boldsymbol{W}}_{un}{}^T \boldsymbol{\Gamma}_{un}^{-1} \dot{\hat{\boldsymbol{W}}}_{un} + \tilde{\boldsymbol{W}}_{\sigma}{}^T \boldsymbol{\Gamma}_{\sigma}^{-1} \dot{\hat{\boldsymbol{W}}}_{\sigma})\Lambda]$$
$$+ 2\alpha\,\mathrm{trace}[(\tilde{\boldsymbol{W}}_{un_f}^T \boldsymbol{\Gamma}_{un_f}^{-1} \dot{\hat{\boldsymbol{W}}}_{un_f} + \tilde{\boldsymbol{W}}_{\sigma_f}^T \boldsymbol{\Gamma}_{\sigma_f}^{-1} \dot{\hat{\boldsymbol{W}}}_{\sigma_f})\Lambda]$$

Defining $\bar{\boldsymbol{e}} = \left(\hat{\boldsymbol{e}}^T \boldsymbol{P}_{prd} - \boldsymbol{e}_m^T \boldsymbol{P} \right) \boldsymbol{H}$

$$\dot{V}(\boldsymbol{e}_m, \hat{\boldsymbol{e}}, \tilde{\boldsymbol{W}}_{un}, \tilde{\boldsymbol{W}}_{\sigma}, \tilde{\boldsymbol{W}}_{un_f}, \tilde{\boldsymbol{W}}_{\sigma_f}) = -\boldsymbol{e}_m^T \boldsymbol{Q}\boldsymbol{e}_m - \hat{\boldsymbol{e}}^T \boldsymbol{Q}_{prd} \boldsymbol{e}$$
$$- 2\bar{\boldsymbol{e}}^T \boldsymbol{\Lambda} \tilde{\boldsymbol{W}}_{un}{}^T \boldsymbol{u}_n(t) - 2\bar{\boldsymbol{e}}^T \boldsymbol{\Lambda} \tilde{\boldsymbol{W}}_{\sigma}{}^T \boldsymbol{\sigma}(\boldsymbol{x})$$
$$+ 2\mathrm{trace}[(\tilde{\boldsymbol{W}}_{un}{}^T \boldsymbol{\Gamma}_{un}^{-1} \dot{\hat{\boldsymbol{W}}}_{un} + \tilde{\boldsymbol{W}}_{\sigma}{}^T \boldsymbol{\Gamma}_{\sigma}^{-1} \dot{\hat{\boldsymbol{W}}}_{\sigma})\Lambda]$$
$$+ 2\alpha\,\mathrm{trace}[(\tilde{\boldsymbol{W}}_{un_f}^T \boldsymbol{\Gamma}_{un_f}^{-1} \dot{\hat{\boldsymbol{W}}}_{un_f} + \tilde{\boldsymbol{W}}_{\sigma_f}^T \boldsymbol{\Gamma}_{\sigma_f}^{-1} \dot{\hat{\boldsymbol{W}}}_{\sigma_f})\Lambda]$$

Using the trace identity $\mathrm{a}^T\mathrm{b} = \mathrm{trace}(\mathrm{b}\mathrm{a}^T)$

$$\dot{V}(\boldsymbol{e}_m, \hat{\boldsymbol{e}}, \tilde{\boldsymbol{W}}_{un}, \tilde{\boldsymbol{W}}_{\sigma}, \tilde{\boldsymbol{W}}_{un_f}, \tilde{\boldsymbol{W}}_{\sigma_f}) = -\boldsymbol{e}_m^T \boldsymbol{Q} \boldsymbol{e}_m - \hat{\boldsymbol{e}}^T \boldsymbol{Q}_{prd} \boldsymbol{e}$$
$$- 2\text{trace}\left[\tilde{\boldsymbol{W}}_{un}{}^T \boldsymbol{u}_n(t) \bar{\boldsymbol{e}}^T \boldsymbol{\Lambda}\right] - 2\text{trace}\left[\tilde{\boldsymbol{W}}_{\sigma}{}^T \boldsymbol{\sigma}(\boldsymbol{x}) \bar{\boldsymbol{e}}^T \boldsymbol{\Lambda}\right]$$
$$+ 2\text{trace}[(\tilde{\boldsymbol{W}}_{un}{}^T \boldsymbol{\Gamma}_{un}^{-1} \dot{\hat{\boldsymbol{W}}}_{un} + \tilde{\boldsymbol{W}}_{\sigma}{}^T \boldsymbol{\Gamma}_{\sigma}^{-1} \dot{\hat{\boldsymbol{W}}}_{\sigma}) \Lambda]$$
$$+ 2\alpha\text{trace}[(\tilde{\boldsymbol{W}}_{un_f}^T \boldsymbol{\Gamma}_{un_f}^{-1} \dot{\hat{\boldsymbol{W}}}_{un_f} + \tilde{\boldsymbol{W}}_{\sigma_f}^T \boldsymbol{\Gamma}_{\sigma_f}^{-1} \dot{\hat{\boldsymbol{W}}}_{\sigma_f}) \Lambda]$$

Substituting from the filtered weights equation (6.21) and proposed ECGAC weight update laws given by (6.33) and (6.34)

$$\dot{V}(\boldsymbol{e}_m, \hat{\boldsymbol{e}}, \tilde{\boldsymbol{W}}_{un}, \tilde{\boldsymbol{W}}_{\sigma}, \tilde{\boldsymbol{W}}_{un_f}, \tilde{\boldsymbol{W}}_{\sigma_f}) = -\boldsymbol{e}_m^T \boldsymbol{Q} \boldsymbol{e}_m - \hat{\boldsymbol{e}}^T \boldsymbol{Q}_{prd} \boldsymbol{e}$$
$$- 2\text{trace}\left[\tilde{\boldsymbol{W}}_{un}{}^T \boldsymbol{u}_n(t) \bar{\boldsymbol{e}}^T \boldsymbol{\Lambda}\right] - 2\text{trace}\left[\tilde{\boldsymbol{W}}_{\sigma}{}^T \boldsymbol{\sigma}(\boldsymbol{x}) \bar{\boldsymbol{e}}^T \boldsymbol{\Lambda}\right]$$
$$+ 2\text{trace}\left[\left(\tilde{\boldsymbol{W}}_{un}{}^T \left(\boldsymbol{u}_n(t) \bar{\boldsymbol{e}}^T - \alpha\left(\hat{\boldsymbol{W}}_{un} - \hat{\boldsymbol{W}}_{un_f}\right)\right) + \tilde{\boldsymbol{W}}_{\sigma}{}^T \left(\boldsymbol{\sigma}(\boldsymbol{x}(t)) \bar{\boldsymbol{e}}^T - \alpha\left(\hat{\boldsymbol{W}}_{\sigma} - \hat{\boldsymbol{W}}_{\sigma_f}\right)\right)\right) \Lambda\right]$$
$$+ 2\alpha\text{trace}\left[\left(\tilde{\boldsymbol{W}}_{un_f}^T \left(\hat{\boldsymbol{W}}_{un} - \hat{\boldsymbol{W}}_{un_f}\right) + \tilde{\boldsymbol{W}}_{\sigma_f}^T \left(\hat{\boldsymbol{W}}_{\sigma} - \hat{\boldsymbol{W}}_{\sigma f}\right)\right) \Lambda\right]$$

$$\dot{V}(\boldsymbol{e}_m, \hat{\boldsymbol{e}}, \tilde{\boldsymbol{W}}_{un}, \tilde{\boldsymbol{W}}_{\sigma}, \tilde{\boldsymbol{W}}_{un_f}, \tilde{\boldsymbol{W}}_{\sigma_f}) = -\boldsymbol{e}_m^T \boldsymbol{Q} \boldsymbol{e}_m - \hat{\boldsymbol{e}}^T \boldsymbol{Q}_{prd} \boldsymbol{e}$$
$$- 2\alpha\text{trace}\left[\left(\tilde{\boldsymbol{W}}_{un}{}^T \left(\hat{\boldsymbol{W}}_{un} - \hat{\boldsymbol{W}}_{un_f}\right) + \tilde{\boldsymbol{W}}_{\sigma}{}^T \left(\hat{\boldsymbol{W}}_{\sigma} - \hat{\boldsymbol{W}}_{\sigma_f}\right)\right) \Lambda\right]$$
$$+ 2\alpha\text{trace}\left[\left(\tilde{\boldsymbol{W}}_{un_f}^T \left(\hat{\boldsymbol{W}}_{un} - \hat{\boldsymbol{W}}_{un_f}\right) + \tilde{\boldsymbol{W}}_{\sigma_f}^T \left(\hat{\boldsymbol{W}}_{\sigma} - \hat{\boldsymbol{W}}_{\sigma f}\right)\right) \Lambda\right]$$

$$\dot{V}(\boldsymbol{e}_m, \hat{\boldsymbol{e}}, \tilde{\boldsymbol{W}}_{un}, \tilde{\boldsymbol{W}}_{\sigma}, \tilde{\boldsymbol{W}}_{un_f}, \tilde{\boldsymbol{W}}_{\sigma_f}) = -\boldsymbol{e}_m^T \boldsymbol{Q} \boldsymbol{e}_m - \hat{\boldsymbol{e}}^T \boldsymbol{Q}_{prd} \boldsymbol{e}$$
$$- 2\alpha\text{trace}\left[\left(\left(\tilde{\boldsymbol{W}}_{un} - \tilde{\boldsymbol{W}}_{un_f}\right)^T \left(\tilde{\boldsymbol{W}}_{un} - \tilde{\boldsymbol{W}}_{un_f}\right)\right) \Lambda\right]$$
$$- 2\alpha\text{trace}\left[\left(\left(\tilde{\boldsymbol{W}}_{\sigma}{}^T - \tilde{\boldsymbol{W}}_{\sigma_f}^T\right)^T \left(\tilde{\boldsymbol{W}}_{\sigma} - \tilde{\boldsymbol{W}}_{\sigma_f}\right)\right) \Lambda\right]$$

By definition

$$\text{trace}\left[\left(\left(\tilde{\boldsymbol{W}}_{un} - \tilde{\boldsymbol{W}}_{un_f}\right)^T \left(\tilde{\boldsymbol{W}}_{un} - \tilde{\boldsymbol{W}}_{un_f}\right)\right) \Lambda\right] = \sum_{i=1}^{N} \sum_{j=1}^{M} \left(\tilde{\boldsymbol{W}}_{un} - \tilde{\boldsymbol{W}}_{un_f}\right)_{ij}^2 \Lambda_{ii} \geq \left\|\tilde{\boldsymbol{W}}_{un} - \tilde{\boldsymbol{W}}_{un_f}\right\|_F^2 \Lambda_{\min}$$ where

$\left\|\tilde{\boldsymbol{W}}_{un} - \tilde{\boldsymbol{W}}_{un_f}\right\|_F^2 = \sum_{i=1}^{N} \sum_{j=1}^{M} \left(\tilde{\boldsymbol{W}}_{un} - \tilde{\boldsymbol{W}}_{un_f}\right)_{ij}^2$ is the Forbenius norm of $\left(\tilde{\boldsymbol{W}}_{un} - \tilde{\boldsymbol{W}}_{un_f}\right)$ and $\Lambda_{\min}$ is the minimum diagonal element of Λ. A similar definition is applicable to $\text{trace}\left[\left(\left(\tilde{\boldsymbol{W}}_{\sigma}{}^T - \tilde{\boldsymbol{W}}_{\sigma_f}^T\right)^T \left(\tilde{\boldsymbol{W}}_{\sigma} - \tilde{\boldsymbol{W}}_{\sigma_f}\right)\right) \Lambda\right]$. Thus,

$$\dot{V}(\boldsymbol{e}_m, \hat{\boldsymbol{e}}, \tilde{\boldsymbol{W}}_{un}, \tilde{\boldsymbol{W}}_{\sigma}, \tilde{\boldsymbol{W}}_{un_f}, \tilde{\boldsymbol{W}}_{\sigma_f}) \leq -\boldsymbol{e}_m^T \boldsymbol{Q} \boldsymbol{e}_m - \hat{\boldsymbol{e}}^T \boldsymbol{Q}_{prd} \boldsymbol{e} - 2\alpha \left\| \tilde{\boldsymbol{W}}_{un} - \tilde{\boldsymbol{W}}_{un_f} \right\|_F^2 \Lambda_{\min} - 2\alpha \left\| \tilde{\boldsymbol{W}}_{\sigma} - \tilde{\boldsymbol{W}}_{\sigma_f} \right\|_F^2 \Lambda_{\min}$$

Therefore, as $\Lambda_{\min}$ is positive and the Forbenius norm is positive

$$\dot{V}(\boldsymbol{e}_m, \hat{\boldsymbol{e}}, \tilde{\boldsymbol{W}}_{un}, \tilde{\boldsymbol{W}}_{\sigma}, \tilde{\boldsymbol{W}}_{un_f}, \tilde{\boldsymbol{W}}_{\sigma_f}) \leq -\boldsymbol{e}_m^T \boldsymbol{Q} \boldsymbol{e}_m - \hat{\boldsymbol{e}}^T \boldsymbol{Q}_{prd} \boldsymbol{e} \leq 0$$

Hence, this proves that the closed-loop system is Lyapunov stable and that $\boldsymbol{e}_m, \hat{\boldsymbol{e}}, \tilde{\boldsymbol{W}}_{un}, \tilde{\boldsymbol{W}}_{\sigma}, \tilde{\boldsymbol{W}}_{un_f}$, and $\tilde{\boldsymbol{W}}_{\sigma_f}$ are uniformly ultimately bounded.

Since $c(t)$ is bounded and $\boldsymbol{A}_m$ is Hurwitz, then $x_m(t)$ and $\dot{x}_m(t)$ are bounded. Hence, the system state $x(t)$ is bounded. This implies $\hat{\boldsymbol{x}}(t)$, $\boldsymbol{u}_n(t)$ and $\boldsymbol{\sigma}(x)$ are bounded. Since the weight estimation errors $\tilde{\boldsymbol{W}}_{un}, \tilde{\boldsymbol{W}}_{\sigma}$ are bounded and the ideal weights $\boldsymbol{W}_{un}, \boldsymbol{W}_{\sigma}$ are constant, the weight estimations $\hat{\boldsymbol{W}}_{un}, \hat{\boldsymbol{W}}_{\sigma}$ are also bounded. Thus, it follows from (6.11) and (6.29) that $\dot{\boldsymbol{e}}_m, \dot{\hat{\boldsymbol{e}}}$ are also bounded. Therefore, $\ddot{V}(\boldsymbol{e}_m, \hat{\boldsymbol{e}}, \tilde{\boldsymbol{W}}_{un}, \tilde{\boldsymbol{W}}_{\sigma}, \tilde{\boldsymbol{W}}_{un_f}, \tilde{\boldsymbol{W}}_{\sigma_f})$ is bounded.

Now, it follows from Barbalat's lemma (Ioannou & Fidan 2006) that $\lim_{t \to \infty} \dot{V}(\boldsymbol{e}_m, \hat{\boldsymbol{e}}, \tilde{\boldsymbol{W}}_{un}, \tilde{\boldsymbol{W}}_{\sigma}, \tilde{\boldsymbol{W}}_{un_f}, \tilde{\boldsymbol{W}}_{\sigma_f}) = 0$. Which consequently shows that $\boldsymbol{e}_m(t)$ and $\hat{\boldsymbol{e}}(t)$ asymptotically converge to zero as $t \to \infty$. Moreover, since the Lyapunov function V is radially unbounded this convergence is global.

Thus, the system error and prediction error are globally, uniformly asymptotically stable. i.e. $\lim_{t \to \infty} \|\boldsymbol{e}_m\| = 0$ and $\lim_{t \to \infty} \|\hat{\boldsymbol{e}}\| = 0$.

This completes the proof.